POLITECHNIKA LUBELSKA

MONOGRAFIE

Computational Intelligence, Information Technology and Systems Research

edited by
Małgorzata Charytanowicz
Paweł Karczmarek
Adam Kiersztyn

Lublin 2020

Computational Intelligence Information Technology and Systems Research

Monografie – Politechnika Lubelska

Politechnika Lubelska
Wydział Elektrotechniki i Informatyki
ul. Nadbystrzycka 38A
20-618 Lublin

Computational Intelligence Information Technology and Systems Research

edited by
Małgorzata Charytanowicz
Paweł Kaczmarek
Adam Kiersztyn

Wydawnictwo Politechniki Lubelskiej
Lublin 2020

Reviewers:
Jarosław Gocławski
Szymon Grabowski
Lidia Maria Jackowska-Strumiłło
Tomasz Jaworski
Paweł Kapusta
Jacek Kucharski
Maciej Kusy
Dorota Pylak
Krzysztof Strzecha
Krzysztof Ślot
Paweł Urbanek
Radosław Wajman

Publikacja wydana za zgodą Rektora Politechniki Lubelskiej

ISBN: 978-83-7947-438-7

Wydawca: Wydawnictwo Politechniki Lubelskiej
www.biblioteka.pollub.pl/wydawnictwa
ul. Nadbystrzycka 36C, 20-618 Lublin
tel. (81) 538-46-59

Contents

Part I: Computational Intelligence and Systems Research

Part II: Data Analysis and Information Technology

Preface

Department of Computer Science at the Lublin University of Technology focuses on research and education in computer science including software engineering, database systems, programming, numerical analysis, information security and computer vision. The monograph "Computational Intelligence, Information Technology and Systems Research" contains selected research works. The main aim of the monograph is an attempt to present the scientific investigations and research works that are being undertaken in the Department.

The list of topics spans all the areas of modern intelligent systems and computing such as: Artificial Intelligence, Computational Intelligence, data mining and knowledge discovery, medical imaging, computer methods in medicine, image processing, 2D and 3D reconstruction, discrete tomography, computer engineering, computational methods in applied physics, modelling and identification, decision support systems, statistics and quality control.

There is no doubt that the areas of computational intelligence, decision support systems, data mining and knowledge discovery have been enjoyed a rapid growth and has attracted a great deal of interest. Likewise, granular computing has demonstrated a remarkable progress. All these areas naturally exhibit a lot of synergistic connections leading to interesting conceptual and application-oriented developments.

We would like to express our gratitude to the authors who contributed their original research papers as well as to all reviewers for their valuable comments.

August 2020

Editors
Małgorzata Charytanowicz
Paweł Karczmarek
Adam Kiersztyn

Part I

Computational Intelligence and Systems Research

Jan W. Owsiński[1], Jarosław Stańczak[2], Karol Opara[3], Sławomir Zadrożny[4], Janusz Kacprzyk[5]

Contributing to spatial planning and policy debates through the reverse clustering approach

Abstract: The paper presents the reverse clustering approach, consisting in finding the parameters of the clustering technique, which approximates the best given partition P_A of the set of n objects, X. The closest partition of the same set thereby obtained, denoted P_B, can be interpreted in a variety of manners. In this study, sets of administrative units are analysed, with the formal administrative categorisation of municipalities (rural, urban and urban-rural) and the more refined typologies, proposed for planning purposes, being treated as the given partitions P_A. Some concrete examples for Poland and Polish provinces are shown and discussed.

Keywords: clustering, reverse clustering, administrative units, spatial typologies

1. Introduction

The present paper contains the results from a study, in which the approach of „reverse clustering" is applied to the data on Polish administrative units. The purpose of this study is to verify the applicability of the "reverse clustering" approach to issues related to territorial planning and management, and also to recognise the kind of insight that can be gained from such an exercise. Thus, we first outline the "reverse clustering approach", then present the considered issue and the way of treating it, the results obtained, and conclude with a discussion.

The "reverse clustering" approach consists in finding a set of parameters, defining a clustering procedure, which yields a partition P_B, being the closest one to some given partition P_A of a set of n objects, whose descriptions ("positions in space") are contained in the data set X.

In the particular case here considered, the objects are the administrative units (at the municipality level), described with their socio-economic and physical features, and their sets correspond to higher-level units (like provinces or the entire country). The objects (municipalities) are classified in Poland formally

[1] Jan Owsiński, Systems Research Institute, Polish Academy of Sciences, Warsaw, Poland
[2] Jarosław Stańczak, Systems Research Institute, Polish Academy of Sciences, Warsaw, Poland
[3] Karol Opara, Systems Research Institute, Polish Academy of Sciences, Warsaw, Poland
[4] Sławomir Zadrożny, Systems Research Institute, Polish Academy of Sciences, Warsaw, Poland
[5] Janusz Kacprzyk, Systems Research Institute, Polish Academy of Sciences, Warsaw, Poland

into three categories: urban, rural, and urban-rural municipalities (the latter being usually composed of a small town and the surrounding rural area). The urban status of a locality is the effect of tradition, historical and political circumstances, and a formal procedure. Thus, we have quite a formal partition P_A into three categories of the set of objects, these objects being, at the same time, characterised by definite socio-economic and physical variables. This gives rise to the question: is it possible to recreate this division into three formal categories on the basis of the "objective" data, and, since the obvious answer is: not fully (at best) – what are the differences, and how can they be interpreted?

Besides this tripartite formal division, there exist other divisions of municipalities, meant for pragmatic planning and management purposes, first of all. These divisions are obvious in view of the diversity of characteristics of municipalities, also within the three categories mentioned. We shall be considering one such proposal of municipality categorisation in this paper, also in the perspective of the potential reconstruction of this categorisation through clustering procedures.

2. The reverse clustering approach

The "reverse clustering" approach (see [6, 7, 8, 9]) can shortly be described as follows: we have n objects, indexed i, $i \in I = \{1,\ldots,n\}$, each of which is described by a vector of values, x_i, these vectors forming the data matrix X. At the same time, we are given a partition of this set of objects (i.e., in fact, a partition of the set I), denoted P_A. We are looking for some clustering procedure, specified by the vector of parameter values, denoted Z, which produces for the data set X the partition P_B that is as close to P_A as possible. The closeness between P_A and P_B is measured by some sort of Rand coefficient, i.e. a function of the count of pairs of objects in the same and in different clusters in the two partitions.

The vector Z, which is the subject of the search, is composed of the following elements: (i) the very clustering procedure (e.g. k-means, single link, subtractive, etc.); (ii) the key parameters of the procedure (e.g. the number of clusters for k-means, the neighbourhood parameters for the density-based clustering algorithms, the thresholds for some other etc.); (iii) the weights and/or the choice of variables accounted for; and (iv) the definition of distance (e.g. through the Minkowski exponent value).

Thus, the search for the "optimum" values of components of Z is quite cumbersome, so that the methodology of choice is constituted by evolutionary algorithms, capable of dealing with strange optimisation landscapes. The algorithms used are differential evolution from the R package and one of the present author's own algorithm ([11]). In the calculations performed, the algorithms used were k-means (see [14] and [5]), DBSCAN as a representative

of the density-based procedures (see [1]), and the general hierarchical aggregation technique, parameterised with the Lance-Williams formula ([3, 4]).

A short discussion on the interpretation of the reverse clustering approach is due at this point. At the first glance, it can be interpreted as another "classifier determination", this classifier being constituted by the procedure, defined by the best *Z*. This is definitely true, but there are at least two essential differences, which make the approach much more general than the classical "classifier search": These differences are: 1. The aim is to assign the whole set of objects to various classes, rather than to assign an object-by-object stream of incoming data; 2. The partition P_B, and hence the parameter vector Z can – and in practice often do – establish quite a different classification pattern from P_A, in particular a different number of classes (clusters). Hence, the reverse clustering approach does not simply lead to "another classifier", but brings much wider implications.

3. The case analysed: an outline

The administrative breakdown of Poland is composed of the following three tiers: provinces, counties and municipalities, namely some 2 500 municipalities, some 350 counties and 16 provinces. The municipalities are very significantly differentiated. The formal categorisation classifies them into urban (302 units), rural (1 537 units) and urban-rural (638 units, very small towns coupled with their rural surroundings). This formal categorisation reflects both the "objective reality" and the aspects, related to historical tradition, procedural intricacies and political processes.

Due to the way in which the municipalities are categorised, and in view of the internal diversity of the three formal categories numerous proposals are often forwarded of more refined categorisation, either for purely scientific, or for pragmatic purposes. The present paper will show the results for the following exercises, drawn out from a wider study: first, in a sort of verifying calculations, the partitions obtained from the reverse clustering approach will be compared to the formal categorisation of municipalities, assumed to constitute the given partition P_A; then, a definite concrete proposal for the categorisation of Polish municipalities for planning purposes will be used as another P_A, and the reverse clustering will be used to approximate it.

Let us indicate at this point that we have used the data set *X*, describing the municipalities, of our own design, with the variables as listed in Table 1. Naturally, neither of the two P_A's used here was based on this data set, but, definitely, such data as those defined in Table 1 ought to reflect the diversified reality of the Polish municipalities in an adequate manner. Note that only the first two variables are of absolute character, all the other ones are relative (shares and rates). These variables, along with variable no. 3, were not used in the first of the exercises here mentioned.

Table 1. List of variables, describing municipalities, used in calculations. The asterisked variables were not used in the calculations regarding formal categorisation of municipalities

1. Population number*	12. Average farm acreage indicator
2. Overbuilt area*	13. Registered employment indicator
3. Share of transport related areas*	14. Registered businesses per 1 000 inhabitants
4. Population density	15. Average business employment indicator
5. Share of agricultural land	16. Share of manufacturing and construction businesses
6. Share of overbuilt areas	17. Pupils per 1 000 inhabitants
7. Share of forest areas	18. Students of over-primary schools per 1 000 inhabitants
8. Share of population over 60 years of age	19. Own revenues of municipality per inhabitant
9. Share of population below 20 years of age	20. Share of revenues from personal income tax in own communal revenues
10. Birthrate for the last 3 years	21. Share of social care expenses in total communal budget
11. Migration balance for the last 3 years	

Source: own elaboration

4. The calculations and the results

4.1. The formal categorisation of municipalities

This exercise was primarily performed for the province of Masovia, with its capital in Warsaw, being also the capital of Poland. The attempts of finding the possibly closest partition to the one, defined by the formal categorisation into three municipality types, gave quite satisfactory results, especially when carried out with k-means and hierarchical aggregation techniques. The (best) results, obtained with DBSCAN were much worse in terms of similarity of the formal and the obtained partitions.

An instance of the best results is illustrated in Table 2, containing the contingency matrix for a result, produced with the k-means algorithm. In particular, it should be stressed that no error was committed as to the distinction of the urban and rural municipalities. The problem appears when the urban-rural category is considered, definitely much less clearly defined in terms of the variables used. Yet, quite astonishingly, the "total error" in terms of the number of units, assigned in the partition P_B to the third category, is very small indeed. In these terms, the most doubtful appears to be the category of "urban" municipalities.

Table 2. An instance of results for the formal categories of municipalities for the province of Masovia, obtained with the k-means algorithm

Clusters: Obtained→ Administrative ↓	1	2	3	Totals
1. Urban	27	0	8	35
2. Rural	0	216	12	228
3. Urban-rural	2	20	31	53
Totals	29	236	51	316

Source: own calculations

Let us add that in view of the limited space of this article, we shall not be providing the details of the results, encompassing more components of the parameter vector *Z*, such as e.g. the values of the Minkowski exponent.

A very important step in the study procedure consisted in the application of the vector *Z*, obtained for the province of Masovia, to another province. This is, indeed, a crucial step, for it might show the degree of applicability of the parameters, contained in $Z_{Masovia}$, to other, but essentially somewhat similar data sets (in purely statistical terms, the sets of municipalities, corresponding to different provinces, differ significantly). Thus, the *Z*, corresponding to the results of Table 2, was applied to the data on municipalities of the province of Wielkopolska, with the outcome shown in Table 3.

Table 3. Results for the formal categories of municipalities for the province of Wielkopolska, obtained with the clustering procedure, determined for the province of Masovia

Clusters: Obtained→ Administrative ↓	1	2	3	Totals
1. Urban	14	2	3	19
2. Rural	0	110	5	115
3. Urban-rural	2	70	22	94
Totals	16	182	30	228

Source: own calculations

Table 3 shows quite clearly that the vector *Z*, defining the clustering procedure, which was found as best for the province of Masovia, not only gave satisfactory results for this particular province, as illustrated in Table 2, but could also be applied, relatively successfully, to another province. Other analyses in the same series were oriented at the attempts of identifying provinces that distinctly differ from the other ones in terms of adequacy of the tri-partite formal categorisation.

4.2. The planning-oriented typology of municipalities

As said, the diversity of municipalities calls for their typologies that would be better fit for the study or pragmatic purposes than the formal tripartite categorisation. We do consider here the planning-oriented proposal of Śleszyński and Komornicki [12]. This proposal for typology is summarised in Table 4.

Table 4. A proposal for the functional typology of Polish municipalities

Functional types	Number of units		Population		Area		Population density
	No.	%	in '000	%	'000 km^2	%	Persons/sq. km
1. Urban cores of provincial capitals	33	1.3	9 557	24.8	4.72	1.5	2 025
2. Outer zones of urban areas of provincial capitals	266	10.7	4 625	12.0	27.87	8.9	166
3. Cores of urban areas of subregional centres	55	2.2	4 446	11.6	3.39	1.1	1 312
4. Outer zones of urban areas of subregional centres	201	8.1	2 409	6.3	21.38	6.8	113
5. Multifunctional urban centres	147	5.9	3 938	10.2	10.39	3.3	379
6. Communes with pronounced transport function	138	5.6	1 448	3.8	20.06	6.4	72
7. Communes with pronounced non-agricultural functions	222	9.0	1 840	4.8	33.75	10.8	55
8. Communes with intensive farming function	411	16.6	2 665	6.9	55.59	17.8	48
9. Communes with moderate farming function	749	30.2	5 688	14.8	93.83	30.0	61
10. Communes featuring extensive development	257	10.4	1 878	4.9	41.59	13.3	45
Totals for Poland	2479	100	38 495	100	312.59	100	123

Source: Śleszyński and Komornicki [12]

The reverse clustering calculations were performed for the whole of Poland. The results obtained, though, did not seem to be comparably good with those presented in the previous section. This fact is illustrated in Table 5, presenting one of the "best" results, obtained for this case with the use of the k-means algorithm (as before, k-means and hierarchical aggregation fared much better in the framework of this analysis than DBSCAN).

Table 5. The contingency table for the typology of Polish municipalities and the reverse clustering result obtained with k-means algorithm ("error": sum of municipality numbers off the diagonal along a row or column; "relative error": "error" divided by the respective total)

	Obtained clusters:										Error	Relative error
Typology clusters no.	***1***	***2***	***3***	***4***	***5***	***6***	***7***	***8***	***9***	***10***		
1	**16**	0	14	0	2	0	0	0	0	1	17	0.52
2	0	**88**	13	84	26	36	9	2	7	0	177	0.67
3	3	0	**45**	0	7	0	0	0	0	0	10	0.18
4	0	9	3	**76**	9	50	24	4	26	0	125	0.62
5	0	0	5	8	**126**	1	0	0	2	0	16	0.11
6	0	0	0	13	18	**34**	15	33	24	0	103	0.75
7	0	6	0	16	19	11	**98**	27	45	0	124	0.56
8	0	0	0	6	4	56	0	**384**	46	0	112	0.23
9	0	1	0	37	20	97	34	146	**330**	0	335	0.50
10	0	0	0	9	11	11	109	34	88	0	262	1
Error	3	16	35	173	116	262	191	246	238	0	1280	0.517

Source: own calculations

The result seems to be a complete failure: more municipalities are misclassified (1 280) than properly classified (remaining 1 199), yielding the overall "relative error" of 0.517! Yet, definitely, the qualitative character of the typology, partition P_A, is definitely largely preserved by the obtained partition P_B. Suffice it to look at the bolded diagonal of Table 5. Against this background a couple of telling observations can be made:

- the tenth cluster is a singleton: Warsaw, the capital of the country, at the expense of the extensive farming rural municipalities, which "disappeared";
- the (otherwise) highest error is observed for the typology cluster 6 ("transport-oriented municipalities");
- high errors are observed for the "suburban" types of municipalities;
- the lowest errors are noted for the "multifunctional urban centres" and for "intensive farming municipalities".

These observations give rise to a more substance-based discussion, which is presented in the following, final section of the paper.

5. A broader discussion

We shall divide this discussion into two parts. First, we shall consider the applicability of the reverse clustering approach to the issues of spatial and territorial analysis, planning and management. Then, we shall try to reach some conclusions, related to the particular spatial patterns.

Thus, let us emphasise that the data we used in both exercises illustrated here (Table 1) were in no way the basis for the two initial partitions analysed (the formal one and the proposed typology). These data reflect, of course, the characteristics of the particular municipalities in quite adequate manner, but their relation to the two partitions, used here as P_A, is solely hypothetical. While this is rather obvious for the formal categorisation of municipalities, a comment is due regarding the planning-oriented typology of municipalities. This typology, namely, was developed on the basis of data concerning the particular units, but also on the basis of other, formal and substantive aspects (e.g. some cities being provincial capitals). Actually, this also meant that not the very same set of data was used for all the municipalities. Hence, it can be said that the typology was compared with the clustering result, P_B, based on a uniform data set for all municipalities. Finally, the results for the formal categorisation (Tables 2 and 3) certainly demonstrate that both the data set that we used and the reverse clustering approach can be successfully used in the analysis of territorial systems at the level of municipalities.

Now concerning the substantive conclusions, the following ones can be formulated in a shorthand:

- of the formal categories, the urban and rural ones seem to be quite well defined, while there are serious doubts as to the urban-rural category; it appears that an "exchange" might be reasonable between this category and the other two;
- regarding the functional typology considered, the primary remark is that the typology proposed apparently features two important biases, which can be read out of the reverse clustering results, but which are also quite visible otherwise: a. limitation to exactly 10 categories (in either sense, upwards and downwards); b. inclusion of quite special or hybrid categories (nos. 6 and 7: the "transport-oriented municipalities" and the "non-agricultural activities", which put side by side tourism and large-scale mining);
- in deeper detail, concerning (not only) the functional typology, the following remarks are due: **i**. Warsaw (and its surroundings) ought to be treated separately rather than in the class of provincial capitals; to what extent this is an important issue could be observed about two years ago, when a proposal was coined of formal reshaping of the Warsaw Metropolitan Area, with a following furious debate, both political and scientific; a significant contribution to the debate is constituted by the report for the Parliament and

the corresponding paper [13][6]; **ii**. the results from the reverse clustering (also in the first of the exercises considered here) show very clearly the urban areas with their hinterlands (however defined), and these entities ("urban functional areas") are much more pronounced that most of other distinctions in space; here, the reverse clustering can definitely serve as a constructive tool; **iii**. it ought to be considered whether distinction of "intensive" and "extensive" farming municipalities is well justified – are we not dealing rather with categories of farms, while at the level of municipalities there is quite a continuum of "intensity"? **iv**. it can be proposed that the category or categories of rural municipalities, in which an important role is played by the non-agricultural activities, be rather considered in the perspective of local wealth, entrepreneurship and employment structure than through external, add-on variables, which may distort the actual image of the local socio-economic system.

All in all, reverse clustering provided quite interesting results, which may be deepened through additional analyses, oriented at more detailed aspects of territorial-administrative spatial systems. Some such analyses will, in fact, yet be conducted in the framework of work on reverse clustering.

Bibliography

[1] Ester M., Kriegel H.-P., Sander J., Xu X., 1996. A density-based algorithm for discovering clusters in large spatial databases with noise. In: E. Simondis, J. Han and U. M. Fayyad, eds., Proc. of the Second International Conference on Knowledge Discovery and Data Mining (KDD-96). AAAI Press, 226–231.

[2] Hubert L., Arabie Ph., 1985. Comparing partitions. Journal of Classification. 2 (1): 193–218.

[3] Lance G.N., Williams W.T., 1966. A generalized sorting strategy for computer classifications. Nature, 212: 218.

[4] Lance G.N., Williams W.T., 1967. A general theory of classification sorting strategies. 1. Hierarchical Systems. Computer Journal, 9: 373–380.

[5] Lloyd S. P., 1957. Least squares quantization in PCM. Bell Telephone Labs Memorandum, Murray Hill, NJ; reprinted in IEEE Trans. Information Theory, IT-28 (1982), 2: 129–137.

[6] Owsiński J.W., 2017. Is there any 'Law of requisite variety' in construction of indices for complex systems? Social Indicators Research, 136 (3): 1125–1137. DOI: 10.1007/s11205-016-1545-5.

[7] Owsiński J.W., Kacprzyk J., Opara K., Stańczak J., Zadrożny S., 2017. Using a reverse engineering type paradigm in clustering: An evolutionary

[6] This discussion has recently returned, and hence the importance of this and similar studies, despite the prevalence of the political arguments.

programming based approach. In: V. Torra, A. Dalbom, Y. Narukawa, eds., Fuzzy Sets, Rough Sets, Multisets and Clustering. Dedicated to Prof. Sadaaki Miyamoto. Studies in Computational Intelligence 671, Springer.

[8] Owsiński J.W., Opara K., Stańczak J., Kacprzyk J., Zadrożny S., 2017. Reverse clustering. An outline for a concept and its use. Toxicological & Environmental Chemistry, DOI: 10.1080/02772248.2017.1333614.

[9] Owsiński J. W., Stańczak J., Zadrożny S., 2018. Designing the municipality typology for planning purposes: The use of reverse clustering and evolutionary algorithms. In: P. Daniele, L. Scrimali, eds., New Trends in Emerging Complex Real Life Problems. ODS, Taormina, Italy, September 10-13, 2018. AIRO Springer Series, vol. 1. Springer, Cham.

[10] Rand W.M., 1971. Objective criteria for the evaluation of clustering methods. Journal of the American Statistical Association. American Statistical Association, 66 (336): 846–850. DOI:10.2307/2284239.

[11] Stańczak J., 2003. Biologically inspired methods for control of evolutionary algorithms. Control and Cybernetics, 32(2): 411–433.

[12] Śleszyński P., Komornicki T., 2016. Functional classification of Poland's communes (gminas) for the needs of the monitoring of spatial planning (in Polish with English summary). Przegląd Geograficzny, 88: 469–488.

[13] Śleszyński P., 2018. The problem of territorial division of the Warsaw Metropolitan Area and its implications for Poland. Studia Regionalne i Lokalne, 2 (72): 29–47.

[14] Steinhaus H., 1956. Sur la division des corps matériels en parties. Bulletin de l'Academie Polonaise des Sciences, IV (C1.III): 801–804.

Jarosław Protasiewicz[1], Daniel Jankowski[2]

A neuro-fuzzy framework for spam filtering: a basic concept and preliminary experiments

Abstract: In this study, we propose a neuro-fuzzy framework for spam filtering. Since spammers are introducing increasingly more sophisticated methods, we must improve anti-spam techniques continually. Relations amongst features indicating spam may be nonlinear, and boundaries between spam and regular emails could be blurry. Therefore, we propose the concept of a complex neuro-fuzzy system for spam filtering, in which the neural part models nonlinearity of features, and the fuzzy part models the uncertain boundary between spam and regular emails. The simplified application of this idea is validated in an empirical case study. The novelty of this study consists in incorporating techniques modelling nonlinearity and uncertainty in a single framework for spam filtering. We have to note that this study includes the preliminary experiments of the basic concept, which should be expanded significantly in further studies.

Keywords: spam filtering, self-organising map, fuzzy logic

1. Introduction

Myriads of messages travel through the global network every day. Some of them are unsolicited, unwanted, with no current relationship between the sender and the recipient. In the general concept, we call them spam, junk or bulk emails. According to [3], such emails are distinguished by three features, namely: (i) they could be sent to many addressees because an individual recipient cannot be clearly inferred from the message; (ii) the recipient has not given the permission to receive such messages; and (ii) the sender obtains far more benefits than the receiver.

It is estimated that spam represents roughly 45% of all emails sent in 2018, which cost $257 billion annually. This loss comes mainly from the increase of network load and storage occupancy, time consumed, damages, frauds, anti-spam infrastructure, etc. Consequently, spam filtering is an important and relevant issue. There are a variety of approaches for defending people against spam, such as reputation-based methods, rule-based filters, or machine learning models [2, 4].

Since spammers are introducing ever more sophisticated methods, we must improve anti-spam techniques continually. Amongst many ways of blocking spam, fuzzy logic seems to be an exciting proposition. As the boundary between

[1] Jarosław Protasiewicz, National Information Processing Institute, Poland
[2] Daniel Jankowski, University of Applied Computer Science and Management under the auspices of the Polish Academy of Sciences, Poland

spam and ham[3] is blurry, fuzzy logic allows us to model this uncertainty. Amongst several studies worth mentioning are: the application of fuzzy rules [15], clustering by a fuzzy C-Mean algorithm [1] or hybrid approaches involving fuzzy logic in some way [14]. These studies proved the usefulness of fuzzy logic in spam filtering. However, we believe that there is room for proposing a more complex system providing better quality based on two assumptions, namely: (i) nonlinear relations may exist in emails amongst features indicating spam, and (ii) boundaries between classes of spam and ham are blurry.

According to the above-mentioned reasons, the main objectives of this study are as follows: (1) to propose a complex neuro-fuzzy system for spam filtering, where the neural part models nonlinearity of features, and the fuzzy part models uncertain boundary between spam and regular emails; and (2) to provide a case study empirically demonstrating the usefulness of the proposed system. The novelty of this study relies on incorporating techniques modelling nonlinearity and uncertainty in a single framework for spam filtering.

The remainder of the paper is structured as follows: Section 2 shows some spam background and discusses related works; Section 3 overviews the concept of a neuro-fuzzy system for spam filtering; and Section 4 presents an experimental case study.

2. Spam background and related works

2.1. Terminology

It is not precisely known when exactly people began to use the word ‘spam’ in the context of receiving unsolicited information. Please note that ‘spam’ should be written in lowercase because ‘SPAM’ in uppercase is a trademark of Hormel Spiced Ham company. This is the name of luncheon meat which has been manufactured for over thirty years. There is a sketch produced by Monty Python and associated with the Hormel company, where the Vikings shout the word S-P-A-M. Additionally, we must note that the opposite term, ‘ham’, is commonly used to refer to wanted messages.

2.2. Reason

The main reason why spam is distributed over the world is the desire for making money, mainly by sending unwanted advertisements via mail. It is a very cheap way of spreading information about products and services. Spam can include dangerous attachments, which are able to install spyware in order to steal passwords, for example, to bank accounts, private e-mail accounts, etc. Such programs could also steal essential documents or perform industrial

[3] The term, ham is commonly used to name regular, standard messages. It is the antonym of spam.

espionage. Spam with an attachment can also change a computer into a zombie. Such an infected computer becomes a slave which executes spammer's orders; for instance, it may send unwanted emails. A more sophisticated method of making profits by spam is to manipulate stock prices. Spammers buy shares of cheap small companies. Afterwards, they send fake messages to encourage investors to buy these shares. Finally, they sell shares at the highest possible price. There are many other ways of making profits via spam. Notably, people sometimes send spam because they want to spread their ideas around, or they could be driven by malignant intentions, wishing to harm others.

2.3. Protection

Companies provide users with sophisticated software which protects both data and equipment. They utilise a variety of anti-spam methods, which may be applied depending on circumstances. The first group comprises reputation-based approaches based on the trust level associated with senders. This group covers: various heuristic filters; blacklists of e-mail or IP addresses which are banned; whitelists of trusted sources which are welcome; greylisting which relies on the temporary refusal by a recipient to check the response of thesender; challenge-response systems requiring additional confirmation from the sender; traffic analysis of the simple mail transfer protocol (SMTP); and even collaborative spam filtering involving social networks [2, 4]. The second group includes various rule-based approaches, honeypots, signature or checksum schemes, and machine learning models. Anti-spam models are usually trained by such algorithms as naive Bayes, support vector machines, or decision trees. The models may also utilise unsupervised clustering methods, or they can be ensembles of different models [2, 4, 12, 16].

2.4. Fuzzy logic

New techniques employed by spammers require a proper response. Fuzzy logic seems to be a technique which may sufficiently model uncertainty appearing in the classification of emails into spam or ham. Several patents utilising this approach to spam filtering confirm its practical usefulness. To name some of them, Jensen [7] patented a way to identify similar email messages and creating their groups using fuzzy logic; in [19] discussed an algorithm of fuzzy word matching to deal with word obfuscation, which is a well-known spammer tactic; In [8] fuzzy rules were applied to combine outputs of several classifiers.

Current research on fuzzy logic in spam filtering focuses on the application of fuzzy rules or fuzzy clustering. The rules are often based on Mamdani fuzzy inference, which classifies incoming emails [5, 15]. Particular studies analyse emails differently. Authors of [15] look for predefined spam words in entire emails. Words are ranked at six levels of threats, which corresponds to six fuzzy

sets. In turn, in [5] emails are split into two parts, and they apply two fuzzy sets (low, high) for each header, and three (low, mid, high) fuzzy sets for each body. In contrast, in [17] the authors construct are several fuzzy rules on context and attributes of email, and finally, they sum up the rule outputs.

Another powerful fuzzy technique of spam filtering is the Fuzzy C-Mean Clustering Algorithm. This algorithm may be applied as in [11, 18], or with some variations. In [1] Fuzzy C-Mean is applied after classical clustering to identify the overlapping entities in spam and ham clusters. In [14] a hybrid approach involving Particle Swarm Optimisation and Fuzzy C-Mean is proposed; whereas in [20] fuzzy clustering combined is with semantic information from the email body.

We have to note that data sets are usually imbalanced because ordinary messages outnumber spam emails. To circumvent this problem, in [9] proposed is a fuzzy-based oversampling method and validates it on Twitter data.

3. Concept of a neuro-fuzzy system for spam filtering

We propose a theoretical system for spam filtering, with its assumptions coming from the analysis of the nature of spam and solutions available in the literature. The system is composed of a preprocessing layer, neural networks performing clustering, and a fuzzy interface system making the final decision on emails under consideration (Figure 1).

3.1. Preprocessing

An email is composed of several parts such as the header, the subject, the content, and attachments. Since these sections cover information of varying importance and purpose, each component of an email message may unequally affect spam classification. Thus, the first layer of the system splits an email into parts. Moreover, it preprocesses textual and other data, which include: transformation graphics to text; language detection; stop-words removal; lemmatisation; transformation text to numerical representation; and feature projection. Amongst these typical natural language processing tasks, representation of features and their projection are especially crucial. Typically, text is represented as terms frequency and inverse document frequency (TF-IDF). However, modern pre-trained word embeddings, such as Word2vec [10] or GloVe [13], may be more useful as they infer semantic similarity of words.

3.2. Neural clustering

In the next layer, a group of self-organising maps (SOM) tries to group data into clusters corresponding to spam and ham. Each map corresponds to one email component. Our intuition is that features of a spam email may relate to each other nonlinearly since spammers are employing ever more sophisticated

techniques. Thus, we propose the use of SOMs because they are very efficient and flexible clustering tools, which allow us to infer nonlinear relations between features. We must note that an SOM may aggregate a particular email component into several clusters during self-organisation. The groups are represented by winning neurons. It is necessary to force this process by labelling neurons corresponding to spam and ham. Then, we can select a central neuron for each group. It this way, we get two superclusters (spam and ham) in each SOM.

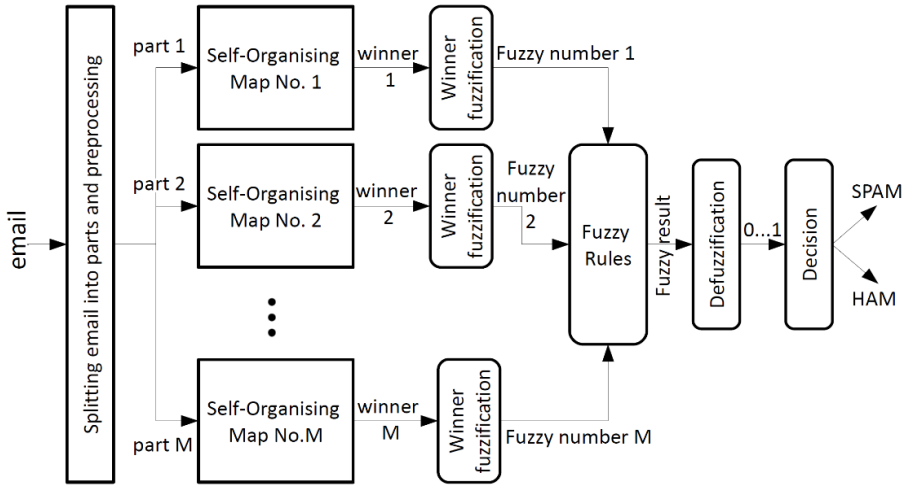

Fig. 1. Neuro-fuzzy system for spam filtering

3.3. Fuzzy interface system and final decision

During the classification of an incoming email message, each SOM selects precisely one winner. Moreover, each winner belongs to one of two possible superclusters. Assuming that the centre of the supercluster is also the centre of a fuzzy membership function, and knowing a topological position of the winner, we can easily read a fuzzy number. This idea is illustrated in Figure 2. Then, the fuzzy numbers are integrated by fuzzy rules. As a result, the system produces one fuzzy number, which, after defuzzification, is a number in the range from 0 to 1. Finally, a decision component, e.g. a logistics function, assigns the email under consideration to either the spam or the ham class.

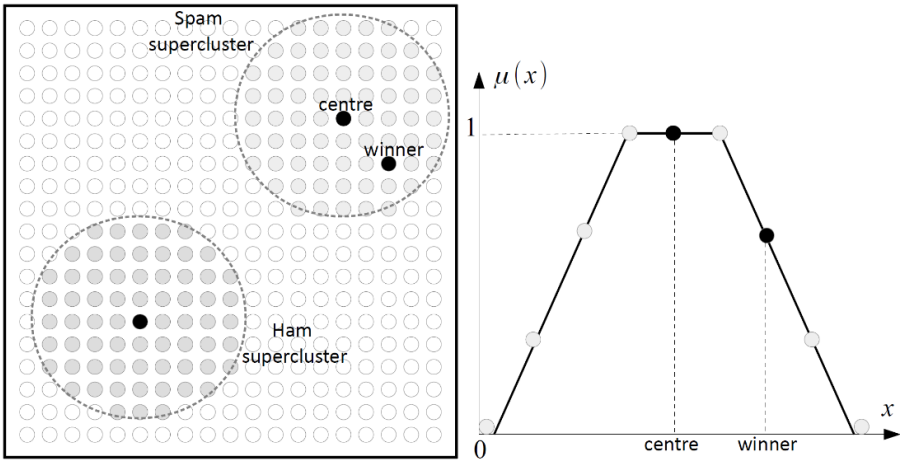

Fig. 2. Reading fuzzy numbers from a SOM

4. Simple experimental case study

The proposed idea of the neuro-fuzzy framework for spam filtering was roughly implemented as a master's thesis [6]. The thesis significantly simplified the original idea to make it feasible for the student. Below, we depict the experiments, results, and simplifications.

4.1. Experiments

4.1.1. Dataset and preprocessing

A data set contains 2,498 emails which originate from our sources. Half of the emails are labelled as spam and the rest as ham. Each email is split into four parts, namely: the header, the subject, the content, and attachments. This case study excludes data other than text. Each character has its own numerical representation based on ASCI numbers. These values are normalised to the range of $(0, 1)$ and transformed into a matrix of vectors containing eight elements each. Thus, only eight neighbouring characters are considered at once during clustering. The size of the vectors was selected experimentally.

4.1.2. Self-organising maps

Each part of an email is meant to be analysed by a separate SOM. The preliminary experiments showed that a country the email comes from has a significant effect on clustering. Thus, a separate SOM is created for each component type of emails and for each country. Based on the pre-experiments, we selected the following parameters for each map. Each map contains 30×30

neurons. They are trained by 300 epochs by using the Winner Takes Most algorithm with Gaussian neighbourhood and Euclidean metric of distance.

4.1.3. Decision component

Instead of reading a fuzzy number from each SOM and applying a fuzzy interface system, the following simple decision formula is used:

$$L = w_h N_h + w_t N_t + w_c N_c + w_a N_a + w_s \ . \tag{1}$$

In formula (1), N_h, N_t, N_c, N_a are normalised distances from inputs to the winner in each map. They represent winners for the header, the subject, the content, and attachments, respectively. As the inputs and neuron weights are normalised to the range of $(0, 1)$, the distances are also within this range. The parameters, w_h, w_t, w_c, w_a are weighting factors of winners allowing to pay more or less attention to particular email components. Their values are fixed and were selected either experimentally or based on our experience, as follows: $w_h = 0.05$, $w_t = 0.2, w_c = 0.7$, $w_a = 0.05$; their sum is equal to 1. Please note that $w_s = 0.1$ is an additional component which is active when typical spammers' tricks are detected. The final decision is based on a simple formula:

$$if \ \ L > T \ \ then \ email \ is \ spam; \ \ else \ email \ is \ ham, \tag{2}$$

where T is a decision threshold.

Table 1. Results of spam detection by the simplified neural system

Decision threshold	% of spam correctly detected	% of ham classified as spam
0.85	53.40	0.00
0.75	85.13	0.24
0.70	85.43	4.23

4.2. Results and discussion

Half of the dataset was used for training and the other half for testing. Spam and ham examples were equally distributed. Table 1 covers the results of spam detection by the simplified neural system, which was presented in subsection 4.1. The classification quality varies depending on the value of the decision threshold (2). T = 0.75 ensures roughly 85% efficiency in spam detection and merely 0.2% of regular mails classified as spam. These results are satisfactory but rather unacceptable in a real application. To show this, we trained a typical naive Bayes model on the same data. Its efficiency reached almost 92% of correctly detected spam emails, and none of the regular emails was misclassified

as spam. Based on these outcomes, we believe that the proposed method may be a valuable alternative for spam filtering; however, it requires further substantial improvement.

5. Conclusions

In this study, we discussed the issue of spam filtering in the face of continuous development of spamming techniques. As a result, we proposed a neuro-fuzzy framework for spam filtering, which addresses potential nonlinearity amongst features indicating spam and an unclear boundary between spam and ham classes. The framework, though substantially simplified by omitting the fuzzy part, was validated on our dataset. Although the outcomes are promising, they cannot compete with well-established methods, e.g. naive Bayes.

Based on that, we believe that the proposed framework is worth developing further. More specifically, the following research may be carried out:

1. Detailed analysis of features connected with spam is warranted. It may reveal hidden or nonlinear relations between them, which should help to select a proper tool for clustering.
2. Various approaches to features representation, including modern words embedding, must be tested. The text representation proposed for the experiments was naive and may have decreased the filtering quality considerably.
3. Boundaries between spam and ham should be truthfully investigated to justify the necessity to apply a fuzzy inference system. Moreover, detailed experiments including this system should be carried out.
4. All improvements mentioned above must be validated experimentally on well-known and well-established datasets for assessment methods of spam filtering.

Quite obviously, this paper represents a fairly preliminary study on the proposed idea for spam filtering. Despite that, we believe that the current status of this work is worth sharing.

Bibliography

[1] Aswani R., Kar A.K., Ilavarasan P.V., 2018. Detection of spammers in twitter marketing: a hybrid approach using social media analytics and bio-inspired computing. Information Systems Frontiers. 20: 515–530.

[2] Bhowmick A., Hazarika S.M., 2016. Machine learning for e-mail spam filtering: Review, techniques and trends. arXiv:1606.01042.

[3] Carpinter J., Hunt, R., 2006. Tightening the net: A review of current and next generation spam filtering tools. Computers & Security, 25: 566–578.

[4] Caruana G., Li M., 2012. A survey of emerging approaches to spam filtering. ACM Computing Surveys (CSUR), 44: 9.
[5] Fuad M.M., Deb D., Hossain M.S., 2004. A trainable fuzzy spam detection system. In: Proc. of the 7th Int. Conf. on Computer and Information Technology.
[6] Jankowski D., 2009. Neuronowo-rozmyty system antyspamowy. Master's thesis. Wyższa Szkoła Informatyki Stosowanej i Zarządzania. Warszawa.
[7] Jensen S., 2010. Method and apparatus for grouping spam email messages. US Patent 7,739,337.
[8] Lin W., 2006. Fuzzy logic voting method and system for classifying e-mail using inputs from multiple spam classifiers. US Patent 7,051,077.
[9] Liu S., Wang Y., Zhang J., Chen C., Xiang Y., 2017. Addressing the class imbalance problem in Twitter spam detection using ensemble learning. Computers & Security 69: 35–49.
[10] Mikolov T., Chen K., Corrado G., Dean J., 2013. Efficient estimation of word representations in vector space. arXiv:1301.3781.
[11] Mohammad N., 2011. A fuzzy clustering approach to filter spam e-mail. In: Proceedings of World Congress on Engineering, Citeseer.
[12] Pandey U., Chakraverty S., 2011. A review of text classification approaches for e-mail management. International Journal of Engineering and Technology, 3: 137.
[13] Pennington J., Socher R., Manning C., 2014. Glove: Global vectors for word representation. In: Proceedings of the 2014 conference on empirical methods in natural language processing (EMNLP), 1532–1543.
[14] Salehi S., Selamat A., Kuca K., Krejcar O., Sabbah, T., 2017. Fuzzy granular classifier approach for spam detection. Journal of Intelligent & Fuzzy Systems, 32, 1355–1363.
[15] Santhi G., Wenisch S.M., Sengutuvan P., 2013. A content-based classification of spam emails with fuzzy word ranking. International Journal of Computer Science Issues (IJCSI), 10: 48.
[16] Subramaniam T., Jalab H.A., Taqa A.Y., 2010. Overview of textual anti-spam filtering techniques. International Journal of Physical Sciences, 5: 1869–1882.
[17] Sudhakar P., Poonkuzhali G., Thiagarajan K., Keshav R.K., Sarukesi K., 2011. Fuzzy logic for e-mail spam deduction. In: Proceedings of the 10th WSEAS International Conference on Applied Computer and Applied Computational Science, 83–88.
[18] Wijayanto A.W., Takdir T., 2014. Fighting cybercrime in email spamming: An evaluation of fuzzy clustering approach to classify spam messages. In: 2014 International Conference on Information Technology Systems and Innovation (ICITSI), IEEE, 19–24.
[19] Yu T., 2010. Email analysis using fuzzy matching of text. US Patent 7, 644, 127.

[20] Zhang, Q.Y., Yang, H., Wang, P., Ma, W., 2011. Fuzzy clustering based on semantic body and its application in Chinese spam filtering. JDCTA: International Journal of Digital Content Technology and its Applications, 5 (4): 1–11.

Tomasz Rybotycki[1]

Simple boundary behaviours for optimisation of metaheuristic performance in closed search space

Abstract: In this paper two boundary behaviours for restricted domains are proposed in the context of training an artificial neural network (ANN) to solve an exemplary differential equation (Wessinger's equation) using metaheuristics. Benefits of using search space reduction (SSR) are discussed. The results obtained by application of proposed boundary behaviours in reduced search space are then compared with the results acquired by unbounded approach.

Keywords: evolutionary algorithm, firefly algorithm, neural network, reduced search domain, Wessinger's equation, metaheuristics

1. Introduction

Metaheuristics can be used to solve a numerous class of problems – from the travelling salesman [17] or knapsack problem [3] to ANN training [1, 7, 22] – and are usually used in situations where explicit solutions are not known or are computationally complex. This finding has enormous implications as it provides an alternative method of equipping an ANN with the proper weight set using as little as a target function, which in some cases may be easier to obtain than large amounts of training data required for other teaching algorithms. Moreover, metaheuristics and more standard training algorithms, such as back propagation, have several different drawbacks and merits that were thoroughly discussed in comparison work [5] and should be considered before selecting a training algorithm.

It comes as no surprise that being given prior knowledge of a problem can possibly help in finding a solution [19]. It is also a well-known fact, noted in [4], that metaheuristics, in theory working on unbounded domains, must be adjusted to closed ones due to computational reasons. Moreover, in [22], it has been found that these domains can be reduced even further since the scope of optimal solutions provided by metaheuristics (at least when considering the ANN training problem) was limited to values within a definable range. SSR, however, requires defining algorithms behaviour at boundaries. This problem has not been properly addressed (see section 5.2) yet, therefore the motivation behind this work is to provide simple algorithm behaviours that would enable one to apply SSR to these algorithms. In this work we present two approaches – bouncing and rolling boundaries – and compare them with solutions obtained without using search space reduction. We believe that this approach will result in the reduction

[1] Tomasz Rybotycki, Systems Research Institute, Polish Academy of Sciences, Warsaw, Poland; University of Warsaw, Departament of Physics, Poland

of bad solutions while at least maintaining accuracy of good ones, and thus improving the algorithm's performance.

The work is organised as follows. The next section introduces an exemplary problem. Wessinger's equation and its properties are presented and SSR is discussed as a potential method of accuracy enhancement. Sections 3 and 4 contain brief description of tools used in the work; more specifically, descriptions of ANNs and selected metaheuristics are provided in the context of acquiring a solution to the problem from section 2. Further on, we provide descriptions of the experiments with focus on methodology and the obtained results. Finally, the paper is closed with a discussion of the results provided.

2. Research problem

This paper discusses SSR with proposed boundary behaviours as a method of improving the accuracy of approximation in differential equations. Wessinger's equation, described further in section 2.1, was selected as an exemplary differential equation and its solutions were approximated via an artificial network taught using two selected metaheuristics – Firefly (FA) and Evolutionary (EA) Algorithms – with the application of SSR. The new results obtained in those experiments were then compared with the ones from [22].

2.1. Wessinger's equation

Wessinger's equation is an ordinary, first order, differential equation given by formulas (1)-(3):

$$tx^2x'^2 - x^3x'^2 + \big(t(t^2+1)\big)x' - t^2x = 0,\ 1 \le t \le 4, \tag{1}$$

$$x(1) = \sqrt{\frac{3}{2}} \tag{2}$$

$$x(4) = \sqrt{\frac{33}{2}} \tag{3}$$

where $x \equiv x(t)$ is an unknown function, t is the argument of x and x' is its first derivative with respect to x. A fully implicit solution to that equation is given by formula (4):

$$x_{imp}(t) = \sqrt{\frac{1}{2} + t^2}. \tag{4}$$

Wessinger's equation was selected for several reasons. Popular, well-known methods, such as Runge-Kutta [18] or improved Euler (or iterative methods in general) are inefficient in dealing with equations with fully implicit solutions

(such as Wessinger's equation, see [1, 7]), therefore it is necessary to use more complex methods when dealing with these kinds of equations. Moreover, Wessinger's equation is generally used when considering problems with the approximation of differential equations (see e.g. [1, 7, 10]), and thus, for comparison purposes, it was reasonable to use the same equation.

2.2. Search-space reduction

Another relatively well-known concept is search space reduction. In terms of metaheuristics it aims to improve the algorithm accuracy by excluding formally acceptable solutions which have very little possibility of being optimal. It has been shown that proper SSR is possible without losing optimal solutions [23].

SSR has various usages in optimisation problems, but in the context of this work one is exceptionally important. It has been successfully used in improving the accuracy of ANN training via a genetic algorithm [24]. Moreover, it has been shown to benefit the performance of particle swarm optimisation (PSO) algorithm [20], which is quite similar to the FA used in this work and thus generates a high possibility of its positively affecting the FA as well. SSR, with proposed boundary behaviours, discussed in section 5, was applied to both selected metaheuristics.

3. Artifcial neural networks

Neural networks, though old, are recently in the centre of research interest due to novel deep learning algorithms. It is, however, a fact that one does not have to use convolutional neural networks (CNNs) to achieve interesting results. Simpler tasks, such as the approximation of equations, require simpler solutions. The least complex kind of artificial neural networks are feedforward ANNs (FFNNs). These kinds of networks are significantly smaller than their deep learning counterparts and are characterised by the fact that the connections between their neurons (connections inside their structure) are only forward – from input to output. Moreover, being well known in the literature, FFNNs were already successfully trained using metaheuristics – thus having several defined metaheuristic operators (see [16]) – and are capable of providing good approximations for differential equations (see [1, 7]). The last reason as to why an FFNN was used in this work, is that the application of SSR requires a prior knowledge of the problem. Given that the application of FFNNs in the context of ANN training using metaheuristics has been a subject of extensive research [15, 16, 21] particularly in the context of approximating Wessinger's equation [1, 7, 22], it is safe to say that this requirement is satisfied when using the same tools (FFNNs) as in the aforementioned works.

A special type of FFNN is called multilayer perceptron (MLP). ANNs can be divided into layers and these consist of artificial neurons [14] which are linked with other neurons. In the case of MLPs, each neuron from layer i is connected

to each neuron in layer $i+1$ up until the output layer. Aside from the connections, each neuron also has an activation function (and it is common to have the same activation function throughout the whole net [6]), whose purpose is to smooth out the signal from the neurons. In this work a standard sigmoid (s-shaped) function was used. The output of i-th neuron n_i is given by the formula (5):

$$n_i = A\left(\sum_{j=1}^{n} w_{ij} n_j + b_i\right), \tag{5}$$

where A is the selected activation function, n is the number of neurons from lower layer connected to neuron i, n_j is the j-th neuron output value, b_i is i-th neuron bias and w_{ij} is the weight of the connection between *i*-th and j-th neuron.

The target of ANN training is to properly set w_{ij} for all connections. The number of connections in a multilayer perceptron is related only to the number of neurons in each layer. Kolmogorov's existence theorem states that every n parameter function can be approximated via a three-layer perceptron with $2n+1$ nodes in the hidden layer. Although there can be more than 1 hidden layer, it has been shown that it is the number of neurons in a hidden layer, not the number of layers, which affects an ANN's performance (see [8, 12, 13]). The MLP used consisted of one hidden layer, an input layer and an output layer. It had one output, one input and four hidden neurons. It was trained using a metaheuristics algorithm, described in more detail in the following section.

4. Metaheuristics

A set of stochastic techniques that can be used to find sub-optimal solutions for optimisation problems are called metaheuristics. They are often used when deterministic approaches are unavailable for a given problem, or when the problem domain is too large for using brute force (see [25]). Various groups of metaheuristics were classified. This research focused only on population-based techniques, which are well-known in the literature and will not be discussed in detail (see [4] for more information). Initial selection was dictated by the fact that population-based metaheuristics were successfully used in ANN teaching in the past (see [1, 2, 7, 15, 16]). The follow-up nature of this paper requires the same methods to be used. The usage of population-based metaheuristics requires addressing several general issues, such as population initialisation, agent structure or target function (which will be discussed in section 5.1).

In the presented research an initialisation approach proposed by Montana in [15] – using two-sided exponential distribution – was used, as it proved to provide satisfying results for both metaheuristics in initial researches (see [21]). Similarly, the population size was set to a fixed arbitrary number of 50.

Another problem was agent structure. It must store weights for all the inter-neuron connections in an ANN. Although in [16] and [15] a single dimensional

vector of real numbers was used, experiments in [22] proved that a multidimensional vector can also be successfully applied. Moreover, due to its more intuitive construction and additional ease in implementing reproduction operators, briefly discussed in [21], this strategy was used when creating agents.

4.1. Evolutionary algorithm

Being quite old in terms of computer science, evolutionary algorithms are already very well-known in the literature (e.g. [4]). These metaheuristics has been used in various optimisation problems due to their elasticity. Applying the EA to a problem requires only (besides general requirements mentioned in 4) describing the reproduction operators – mutation operator and crossover operator in particular – and a selection operator. It has previously been shown that EAs can be successfully used as a tool for teaching ANN. Moreover, crossover and mutation operators for ANNs teaching have already been discovered and described in detail. In initial experiments, as well as these experiments *node mutation* and *crossover weights* operators from [16] were used as they proved to work best for a given task. For the selection operator *roulette wheel selection* was used, as its selective pressure allows it to leave local extrema in search for better solutions (see [4]).

4.2. Firefly algorithm

The other selected metaheuristic is a nature-inspired variation of the well-known Particle Swarm Optimisation (PSO) algorithm named the Firefly algorithm (see [25] and [9]). It aims to find the solution to a given problem by imitating the movement of a firefly. Each firefly's position in the i-th iteration is given by the equation (6)

$$x_{i+1} = x_{i,k} + \sum_{j \neq i}^{*} \beta_0 e^{-\gamma r_{ij}^2} (x_{i,j} - x_{i,k}) , + \alpha \epsilon, \tag{6}$$

where $x_{i,k}$ denotes k-th firefly position in i-th iteration, α is step size, β_0 is base attraction of the firefly, e is the base of natural logarithm, r_{ij} is distance between i-th and j-th firefly, ϵ is a pseudo-random vector and γ is light absorption coefficient. The asterisk above the sum means that only brighter fireflies are meant to be included into the sum.

In this work the Euclidean distance was measured. Each firefly's position is based on the location of the others. In every iteration each agent is moved towards brighter ones that represents better solutions. One should note that if so, then the brightest firefly will only move in a random direction given by the statement $\alpha\epsilon$. Brightness – and thus attractiveness – of a given agent should be understood as the value of the fitness function in this case (see [25]).

The main reason behind initially selecting this algorithm was that similar technique (to the one presented) was previously used to solve Wessinger's

equation (see [1]) and that the FA was also successfully used to train an ANN (see [2]). Moreover, the FA in terms of SSR has not yet been thoroughly explored, and so it is additionally an interesting issue for research.

5. Experiments

This section describes the used methods and the results of the experiments. We present the general approach for approximating differential equations using ANNs, reduced to the problem of Wessinger's equation approximation, and a description of boundary behaviours for SSR. Then, the results are discussed.

5.1 Wessinger's equation approximation

Approximating differential equations using ANN has already been presented in many papers [1, 7]. The idea is to divide the solution into two parts – one satisfying boundary conditions and second, approximated by the ANN, which would approximate every value in between. This approach proved to work well in many works and was therefore selected as valid. The approximation s is given by the formula (7).

$$s(t,w) = \frac{\sqrt{66}}{6}(t-1) - \frac{\sqrt{6}}{6}(t-4) + (t-1)(t-4)N(t,w), \tag{7}$$

where $t \in R$ is the point in which s is evaluated, N is ANN output and w is the weights set.

ANN training was performed by two metaheuristics. For comparison purposes, the same algorithm parameters as in [22] were used. The number of agents was equal to 50, but the similarities between the two metaheuristics parameters ended there. As for the specific values of the algorithm, EA mutation chance was set to standard 5% [16] and the FA parameters, selected numerically from several sets of values [22], were as follows: $\beta_0 = 0.5$, $\alpha = 0.01$ and $\gamma = 1$. Fitness function f is given by the formula (8):

$$f(a) = 1 - \frac{E(a)}{E_{max}}, \tag{8}$$

where a denotes the solution represented by a given agent, E denotes error and E_{max} is maximal error that occurred during the search. The error function $E(a)$ can be expressed by equation (9)

$$E(a) = \sum_{t \in T} f^2\big(t, s(t,a), s_t'(t,a)\big), \tag{9}$$

where T denotes a discrete test set (for computational purposes)

$$T = \{t_i : 1 \leq t_i \leq 4, t_{i+1} = t_i + 0.1\}, \quad (10)$$

f is a general form of first order differential equation

$$f(t, s, s'_t) = 0 \quad (11)$$

and s'_t denotes s's first derivative with respect to parameter t.

It is worth noting that the present approach is not limited to Wessinger's equation and in [11] a more general method has been shown, presented with multiple kinds of differential equations.

5.2 Search space reduction

In [21] it has been noted that optimal sets of weights found via metaheuristics are always in a closed range. Given that knowledge one may expect that by reducing the search space to the whereabouts of these optima, one may possibly acquire better solutions. In this work a symmetrical domain in the form $(-\epsilon, \epsilon)$, where $\epsilon > 0$, was used.

SSR requires defining boundary behaviours. In [4], this issue is discussed along population initialisation and it is simply proposed to randomly select the solutions that are within the domain, but it fails to address situations wherein solutions evolve by adjusting their position in the search space in a movement-simulating manner (like in the case of FA). Another approach is search space resizing [19], however this is not a desirable method in the discussed scenario. Therefore, different boundary behaviours must be defined.

In this work two methods of handling reduced domain boundaries are proposed – boundary bounce and boundary roll. The first one is the less severe of the two. It simulates a situation wherein the value which exceeds the boundary condition is being bounced in the other direction. Formally it can be expressed by formula (12)

$$val = \begin{cases} upperBound - (val - upperBound) \text{ when } val > upperBound \\ lowerBound - (val - lowerBound) \text{ when } val < lowerBound \end{cases}. \quad (12)$$

Following the above expression is repeated if any boundary condition is being exceeded.

Another method used in this work simulates a situation where the domain boundaries relate to each other and thus the value exceeding a boundary begins at the other end of the domain. Formally it is expressed by formula (13).

$$val = \begin{cases} lowerBound + (val - upperBound) \text{ when } val > upperBound \\ upperBound - (lowerBound - val) \text{ when } val < lowerBound \end{cases}, \quad (13)$$

which, again, is repeated as long, as value exceeds any boundary.

5.3. Results

For algorithm parameters that were discovered during tuning in [21], search space reduction was applied. It is important to note that the focus of the research was on providing better approximations, not on finding sub-optimal ANN parameters, therefore the best set of weights obtained during the experiment is not provided (but can possibly be discovered using the proposed approach). In this work $\epsilon = 5$ was selected for reduced domain description, as this configuration contained previously found sub-optimal solutions, but covered greater area for algorithms to search than its small proximity. For each algorithm-behaviour configuration 30 experiments were conducted (as in the original work) and then the data gathered that way were compared with the research results from [22]. These results were the most recent, and the most up-to-date, since a comparison with other works, like [1, 7, 10], was performed in [21] and the results obtained there were favourable. Numerical data were presented in tables 1 and 2.

One may immediately notice that time variations for both algorithms are insignificant and thus their further analysis was omitted.

Errors presented in tables 1 and 2 have been calculated according to formula (9) described in section 5.1. Their analysis shows some interesting results. First, in most cases a better overall solution was found with the use of SSR. Only for the EA with a boundary bounce method the solution provided was worse by about 10 percentage points. One should note, however, that the consistency of solutions has greatly improved and the probability of the occurrence of a bad solution has been drastically reduced, which can be seen by comparing the max errors for each algorithm. One of the most interesting results is that the best and worst solutions overall for the FA occurred for the same boundary handling method.

Table 1. Comparison of EA performance with and without SSR for both boundary handling methods

Name \ Value	Min	1st quartile	2nd quartile	3rd quartile	Max
Error No SSR	0.93	1.48	3.58	12.85	131.46
Time No SSR [s]	47.50	48.58	48.87	49.22	50.46
Error Bounce	1.02	1.99	4.47	6.03	22.41
No SRR / Bounce Error Ratio [%]	109.19	134.88	124.91	46.93	17.05
Time Bounce [s]	47.74	47.92	35.08	48.75	49.80
No SRR / Bounce Time Ratio [%]	100.52	98.63	71.77	99.03	98.68
Error Roll	0.89	1.97	3.44	5.73	14.68
No SRR / Roll Error Ratio [%]	95.44	133.40	96.17	44.59	11.17
Time Roll [s]	48.38	48.38	48.38	48.38	50.55
No SRR / Roll Time Ratio [%]	101.86	99.58	99.00	98.29	100.17

Table 2. Comparison of FA performance with and without SSR for both boundary handling methods

Name \ Value	Min	1st quartile	2nd quartile	3rd quartile	Max
Error No SSR	0.80	1.30	2.05	4.71	12.74
Time No SSR [s]	112.64	113.18	113.83	114.62	116.10
Error Bounce	0.69	1.14	1.66	3.30	14.15
Bounce / No SRR Error Ratio [%]	86.42	87.67	80.85	70.05	111.02
Time Bounce [s]	113.59	114.02	63.87	115.28	115.88
Bounce / No SRR Time Ratio [%]	100.84	100.74	56.11	100.57	99.81
Error Roll	0.80	1.13	2.15	3.85	8.54
Roll / No SRR Error Ratio [%]	99.91	87.12	104.74	81.88	67.02
Time Roll [s]	112.96	113.26	115.50	115.89	117.07
Roll / No SRR Time Ratio [%]	100.28	100.07	101.46	101.11	100.83

6. Discussion

The topic of this work was improving ANN accuracy of approximating differential equations (using Wessinger's equation with implicit solutions as an example), using metaheuristics with reduced search spaces and defined boundary behaviours as training tools. It was expected that reducing the search space would have a beneficial influence on the results. Two boundary behaviours have been proposed as a means of successfully applying SSR to metaheuristics.

The conducted experiments have shown that search space reduction improves algorithm approximation results (in most cases) without having significant impact on their performance (e.g. training time stayed nearly unchanged). It can be seen that the application of SSR had a beneficial influence not only on reducing the number of bad solutions, but has also been shown to be able to generate a better solution (EA + SSR Roll, FA + SSR Bounce). Moreover, SSR greatly improved result consistency which can be seen by a quartiles analysis (especially higher ones).

During the research, the problems with normalising the evaluation of agents mentioned in [22] were still present. The reason for that were, again, large error values occurring during the search. Search space reduction, although successful in improving the algorithm performance, did not manage to eliminate large agent errors. That means that the error has little to do with neuron connection weights (at least in this case) and is bound to other issues. This problem should be tackled in another study.

Bibliography

[1] Biglari M., Ghoddosian A., Poultangari I., Assareh E., Nedaei M., 2013. Using evolutionary algorithms for solving a dierential equation. Global Journal of Science, Engineering and Technology, 14: 25–32.

[2] Brajevic I., Tuba M., 2013. Training feed-forward neural networks using firefly algorithms. In: Proceedings of the 12th International Conference on Artificial Intelligence, Knowledge Engineering and Data Bases, 156–161.

[3] Chu P.C., Beasley J.E., 1998. A genetic algorithm for the multidimensional knapsack problem. https://doi.org/10.1023/A: 1009642405419.

[4] Engelbrecht A.P, 2007. Computational intelligence: An introduction. Second edition. John Wiley & Sons Ltd, Chichester.

[5] Farag W.A., Quintana V.H., Lambert-Torres G., 1998. Genetic algorithms and backpropagation: a comparative study. In: IEEE Canadian Conference on Electrical and Computer Engineering, 93–96.

[6] Fausett L., 1994. Fundamentals of neural networks: Architectures, algorithms and applications. Prentice-Hall Inc., Upper Saddle River, NY, USA.

[7] Ghalambaz M., Noghrehabdi A. R., Behrang M. A., Assareh E., Ghanbarzadeh A., Hedayat N., 2011. A hybrid neural network and gravitational search algorithm (hnngsa) method to solve well-known Wessinger's equation. International Journal of Mechanical Aerospace, Industrial, Mechatronic and Manufacturing Engineering, 5(1):147–151.

[8] Hornick K., Stinchcombe M., White H., 1989. Multilayer feedforward networks are universal approximators. Neural Networks, 2(5): 359–366.

[9] Kennedy J., Eberhart R., 1995. Particle swarm optimization. In: Proceedings of IEEE International Conference on Neural Networks, 1942–1948.

[10] Khan J., Raja M., Qureshi I., 2009. Swarm intelligence for the problems of nonlinear ordinary differential equations and its application to well-known Wessinger's equation. European Journal of Scientific Research, 34: 514–525.

[11] Lagaris I.E., Likas A., Fotiadis D.I., 1998. Artificial neural networks for solving ordinary and partial differential equations. IEEE Transactions on Neural Networks, 9: 987–1000.

[12] Lippman R.P., 1987. An introduction to computing with neural nets. IEEE ASSP Magazine, 4: 4–22.

[13] Malek A., Beidokhti R.S., 2006. Numerical solution for high order differential equations using a hybrid neural network optimization method. Applied Mathematics and Computation, 183: 260–271.

[14] McCulloch W.S., Pitts W., 1943. A logical calculus of the ideas immanent in nervous activity. Bulletin of Mathematical Biophysics, 5: 115–133.

[15] Montana D. J., 1995. Neural network weight selection using genetic algorithms. Intelligent Hybrid Systems, 8(6): 12–19.
[16] Montana D.J., Davis L., 1989. Training feedforward neural networks using genetic algorithm. In: Proceedings of the International Joint Conference on Artificial Intelligence, 762–767.
[17] Potvin J., 1996. Genetic algorithms for the traveling salesman problem. https://doi.org/10.1007/BF02125403.
[18] Press W.H., Teukolski S.A.,Vetterling W.T., Flannery B.P, 1992. Numerical recipes in C. The art of scientific computing. Second Edition. Press Syndicate of the University Press.
[19] Rajarathinam K., J. Gomm B., Yu D., Abdelhadi A. S., 2017. An improved search space resizing method for model identification by standard genetic algorithm. https://www.tandfonline.com/doi/full/ 10.1080/21642583.2017. 1289130.
[20] Reungsinkonkarn A., Apirukvorapinit P., 2014. Search space reduction of particle swarm optimization for hierarchical similarity measurement model. In: 11th International Joint Conference on Computer Science and Software Engineering (JCSSE), 23–27.
[21] Rybotycki T., 2016. Nowoczesne metaheurystyki w optymalizacji procesów fizycznych. Master's Thesis, University of Silesia, Sosnowiec.
[22] Rybotycki T., 2018. Metaheuristics in physical processes optimization. In: Mesiar R., Kóczy L., Wisniewski R. Kacprzyk J., Kulczycki P., eds., Information Technology, Systems Research, and Computational Physics, Springer Nature Switzerland AH, Cham, 132–148.
[23] Siklóssy L., Tulp E., 1991. The space reduction method: a method to reduce size of search spaces. Information Processing Letters, 38: 187–192.
[24] Srinivas M., Patnaik L., M., 1991. Learning neural network weights using generic algorithms improving performance by search-space reduction. In: 1991 IEEE International Joint Conference on Neural Networks, 2331–2336.
[25] Yang X, 2010. Nature-inspired metaheuristic algorithms. 2nd Edition. Luniver Press.

Part II

Data Analysis and Information Technology

Dariusz Czerwiński[1], Małgorzata Charytanowicz[2], Tomasz Zientarski[3]

Soil structure analysis using 3D reconstructed model from CT images

Abstract: Recent advances in computed tomography and digital image processing algorithms provide technologically advanced tools for studying the internal structures of soil aggregates. Once scanned, the computed tomography information allows the non-destructive visualisation of slices, arbitrary sectional views and pseudo-colour representations. In this paper we propose a novel algorithm for 3D soil reconstruction with the use of CT images. The article presents a survey on this 3D reconstruction approach and draws conclusions for analysing the pore volume distribution and total porosity. The presented methodology is illustrated with a soil aggregate sample. The approach is expected to be more objective than traditional methods, very often limited in applicably due to their destructive character and inadequate pore characteristic reports.

Keywords: 3D reconstruction, image processing, matching, soil structure, pore size distribution, pore volume, CT-images

1. Introduction

Pore size distribution is one of many physical measurements characterising soil structure as far as plant growth is concerned. A number of scientists have reported studies of pore space as a general method for defining the soil structure [9, 13, 18, 21]. Pore spaces location within the soil impacts the majority of physical and physicochemical soil parameters, such as water retention, water conductivity, aeration, erosion susceptibility and gas diffusivity. They vary significantly due to several factors, including mutual interactions between soil fauna, soil macro-organisms, roots, inorganic agents and environment factors. Weather conditions, vegetation, fertilisation and soil tillage operations can also cause either soil loosening or compaction.

Among all measurements characterising the various aspects of a particular soil, total porosity provides a more useful physical description that is relevant to plant growth. Porosity determines the air and water relationships in the soil. This is defined by the ratio:

[1] Dariusz Czerwiński, Institute of Computer Science, Lublin University of Technology, Poland

[2] Małgorzata Charytanowicz, Institute of Computer Science, Lublin University of Technology, Poland; Systems Research Institute, Polish Academy of Sciences, Warsaw, Poland

[3] Tomasz Zientarski, Institute of Computer Science, Lublin University of Technology, Poland

$$\varphi = \frac{V_P}{V_T}$$

where V_P is the volume of void-space and V_T is the total volume of soil material, including the solid and void components. The total porosity is a dimensionless quantity and can be reported either as a decimal fraction or as a percentage. Being simply a fraction of total volume, it can range between 0 and 1, typically falling between 0.3 and 0.7 for most soils. The porosity of mineral soils is 30–60% and is the highest in the humus level, while the porosity of organic soils ranges from 41% to over 90%, and in the case of peats is 80–90% by volume.

General soil porosity is determined by indirect methods – based on the results of density determination of the solid soil phase and soil volume density; and direct ones – a Loebell porometer, i.e. an apparatus for measuring the pore volume occupied by air. Soils may be nearly uniform in the same total porosity but differ in pore size distribution. A more detailed analysis can be obtained by developing a pore-size distribution curve. This is often determined by mercury intrusion porosimetry or low temperature nitrogen adsorption. However, these conventional techniques have often been unsatisfactory due to being inadequate in truly describing pore characteristics. Moreover, they are limited in applicability as far as pore size and shape or preferential flow is concerned.

Recent advances in computed tomography and digital image processing algorithms provide technologically advanced measurement tools for studying the internal structures of soil aggregates [2, 5 , 12, 13]. The computed tomography image analysis belongs to indirect method of determining the soil porosity. CT images are usually obtained as greyscale images and to calculate the porosity several operations have to be taken. The type and number of operations performed on the 2D images should be reduced to the minimum necessary to avoid distortion of the boundary line between the pores and the solid phase. In such case only thresholding and segmentation are executed, thanks to which binary images are obtained from multishade images, on which the free spaces were assigned to the black colour, while the solid phase was white. Then, using the hole-fill operator, the openings visible on aggregate cross-sections (inter-aggregate pore sections) were filled, which could affect the surface and circumferences of aggregate cross-sections. For each aggregate section, its cross-section area is determined. In this way in each 2D slice the soil porosity can be obtained. Thus, image processing methods applied for 2D images provide suitable tools for characterising the pore volume distribution and in quantifying the differences in soil aggregate structures. Moreover, the non-destructive nature of computed tomography scanning allows the same object to be scanned multiple times, and provides an opportunity to investigate internal attributes at any location within a sample.

However, porosity is a 3D rather than a 2D property of soil aggregates. Therefore, the problem of obtaining information about the 3D structure of soil by analysis of its 2D cross-sections is very important. The solution is relatively simple if the 2D cross-sections are regularly distanced within a soil sample and the sample has morphologically homogeneous structure. If this is not so, more sophisticated and advanced computer-based methods should be used. The more complicated approach to this problem is to generate a 3D reconstruction of the soil structure, after which the exact information on diameter of pores can be obtained. Fortunately, the image processing operations applied for 2D images can be used successfully for characterising pore volume distribution and constructing 3D models.

In this paper, we proposed a novel algorithm for 3D soil reconstruction with the use of CT images. Herein, volumes are created with 2D images by rendering the pixels that the threshold is in the desired range. At this stage the Otsu method is applied. Next, the Marching Cubes algorithm is used to extract isosurfaces from series CT scan. Meshes of triangles described by a set of vertices become the isosurfaces and volumes. With the use of the aforementioned steps, it is possible to reconstruct the soil structure into 3D images.

The article presents a survey on this 3D reconstruction approach and draws conclusions for analysing the pore volume distribution and total porosity. It should be noted that a number of scientists have reported that studies of pore volume distribution are useful as a general method for defining the soil structure. The present methodology is illustrated with a sample of soil aggregate. The approach is expected to be more objective than classical methods, where arbitrary assumptions concerning the shape of pores are required.

2. Material and methods

The proposed methodology to elaborate an innovative image processing approach for detection pore space, based on computed tomography and the image processing methods, is summarised as follows:

1. soil sample prepared;
2. soil tomography slices captured;
3. 2D image preprocessing techniques applied;
4. 3D reconstruction produced;
5. porosity characterised.

2.1. Soil sample preparation

The investigated material was sampled from a cultivated soil layer, classified as silty loam (WRB Mollic Gleysols), explored at the Institute of Agrophysics, of the Polish Academy of Sciences in Lublin. The proportion of each particle size group in the soil was as follows: sand – 46%, silt – 28%, clay – 26%. Furthermore, the pH was: H_2O – 5.9, while KCl was 5.4. On the experimental

fields, a long-term fertilisation trial had been executed. The adopted crop rotation from 1955 to 1989 was a cycle of potato-barley-rye, and from 1990 – a cycle of sugar beat-barley-rape-wheat. Three treatments concerning fertilisation: control group – plant residues only, mineral fertilisation – according to plant needs, and pig manure – 80 ton per ha, were studied. Aggregate soil organic matter was measured by the Multi N/C 3100 Autoanalyser (Analitic Jena, Germany). The total organic carbon and total nitrogen contents for three fertilisations (pig manure, mineral fertilisers, control) were respectively: 21.50, 14.89, 13.54 g/kg, and 2.10, 1.51, 1.35 g/kg. The total organic carbon shows the same tendency as total nitrogen, i.e. increasing in the same order: the lowest – control, middle – mineral fertilisation, the highest – pig manure. The soil samples were air dried in normal room conditions, divided into smaller amounts, and gently sieved through 2 and 10 mm sieves. Soil aggregates remaining at 2 mm sieve and ranging from 2 to 10 mm, were then detected by means of X-ray computational tomography, using a GE Nanotom S device, with the voxel-resolution of 2.5 microns per volume pixel. Three 2D sections uniformly located within each aggregate were performed to characterise the aggregate structure.

2.2. Image 2D preprocessing

Tomography sections were processed by means of standard image processing techniques, using the Aphelion 4.0.1 package. In the initial step, the region of interest (ROI) selection from the original greyscale image was performed. All of the ROI's were selected by hand, around the aggregate, removing the ring artefacts, and next they were saved in bitmap format. Otsu's automatic thresholding method was then employed to separate pores within the sampled aggregate. The Otsu threshold T minimizes the overall within-class variance of the two groups of pixels separated by the thresholding operator [7, 14]

Thus, consider an image with L gray levels and its normalised histogram, i.e., for each grey-level value i, $i = 0,1,\dots,L-1$, the normalised frequency $p_i = P(i)$ is calculated. Assuming that we have set the threshold at t, the fraction of pixels that will be classified as background and object will be:

$$P_B(t) = \sum_{i=0}^{t} p_i \,,$$

$$P_O(t) = \sum_{i=t+1}^{L-1} p_i \,.$$

The mean grey-level value of the background and the object pixels will be:

$$\mu_B(t) = \frac{1}{P_B(t)} \sum_{i=0}^{t} i\, p_i \,,$$

$$\mu_O(t) = \frac{1}{P_O(t)} \sum_{i=t+1}^{L-1} i\, p_i \,.$$

The mean grey-level value over the whole image is:

$$\mu = \sum_{i=0}^{L-1} i\, p_i \,.$$

The variance of the background and the object pixels will be:

$$\sigma_B^2(t) = \frac{1}{P_B(t)} \sum_{i=0}^{t} (i - \mu_B)^2\, p_i \,,$$

$$\sigma_O^2(t) = \frac{1}{P_O(t)} \sum_{i=t+1}^{L-1} (i - \mu_O)^2\, p_i \,.$$

The variance of the whole image is:

$$\sigma^2(t) = \sum_{i=0}^{L-1} (i - \mu)^2\, p_i \,.$$

As the variance σ^2 is equal to the sum of the within-class variance and the between-class variance, the Otsu threshold T minimises the overall within-class variance – which is the same as maximising between-class variance:

$$T = \arg\max_{0<t<L-1} \sigma^2_{between-class}(t),$$

where the between-class variance can be shown as:

$$\sigma^2_{between-class}(t) = P_B\, P_O (\mu_B - \mu_O)^2 \,.$$

The well-established Otsu technique is commonly implemented to separate the image into solid particles and pores.

2.3. Three-dimensional image processing methods

Many algorithms have been proposed in the literature to illustrate the three-dimensional scene based on many cross-sections images obtained from computed tomography [3, 9, 11, 16, 17, 20]. The marching cube algorithm is one of the most popular algorithms for isosurface triangulation [11].

Marching cubes is a computer graphics algorithm, described in 1987 by Lorensen and Cline [11], for extracting a polygonal mesh of an isosurface from a three-dimensional data. Marching cubes method is based on a division of the data volume into elementary cubes, followed by a standard triangulation inside each cube. The triangulation that must be performed inside each logical cube depends only on an eight bit binary number. The algorithm combines simplicity with high speed because it works almost entirely on look-up tables.

In summary, the algorithm proceeds through the following steps:

1. Load 4 slices in memory.
2. Loop on the two central slices, creating a logical cube from the eight neighboring voxels.
3. Calculate the scalar field gradient on the eight voxels by the finite differences method.
4. Evaluate the binary index associated with the cube by comparing the voxel contents against the isovalue.
5. Get the triangulation type from the look-up table.
6. Compute the triangle vertex positions by linear interpolation.
7. Compute the scalar field gradient on the triangle vertexes by linear interpolation.
8. Store the triangle vertex coordinates and the gradient components.

2.4. Three-dimensional reconstruction

The 3D reconstruction of CT images can bring additional informational on pores size and distribution. The similar parameters can be also obtained with the use of 2D images analysis, however the 3D model has an advantages of further analysis i.e. water flow with the use of computation fluid dynamics.

The 2D CT slices were combined in 3D object with the use of marching cubes algorithm described above. All images were analysed using the public domain software Fiji version Madison with June 2019 updates [15].

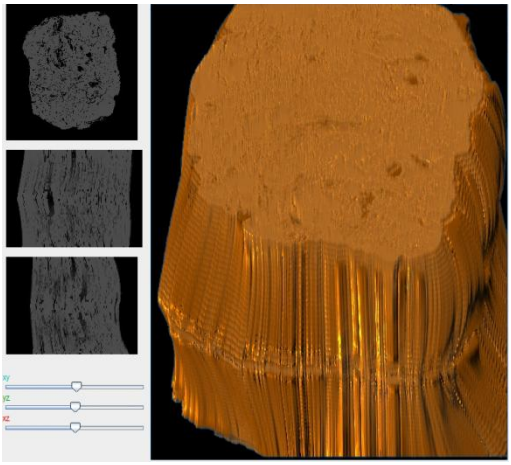

Fig. 1. The 3D volume obtained from the 2D images transformation

The triangle meshes described by a set of vertices become the iso-surfaces and volumes, which is shown in Figure 1.

Further analysis of the 3D reconstructed clod of soil can be performed with the use of region of interest selection. The ROI area and corresponding selection of the piece of soil was shown in Figure 2.

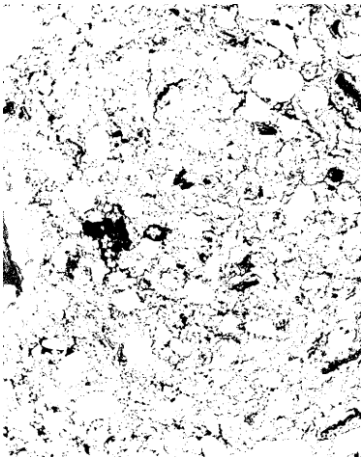

Fig. 2. ROI selection: inner area of the ROI which goes through all the slices

3. Results

The main aim of our research is to determine the total porosity of soil as well as to estimate fractions of micro-, meso- and macropores using 3D soil reconstruction. First, two-dimensional image analysis was performed by regarding binary soil sections. Next, 2D computed tomography images were imported as a sequence of slices and converted to the 3D volume as described in Section 2.4.

3.1. Porosity determination by two-dimensional image analysis

Pore size measurements of the examined soil aggregate were collected using a novel method of determining the pore size and its distribution described in the papers [3], [6]. Firstly, greyscale tomography sections were preprocessed by removing ring artefacts by means of the ROI method. After selecting the region of interest, the automatic Otsu binarisation method was then employed. The results are shown in Figure 3.

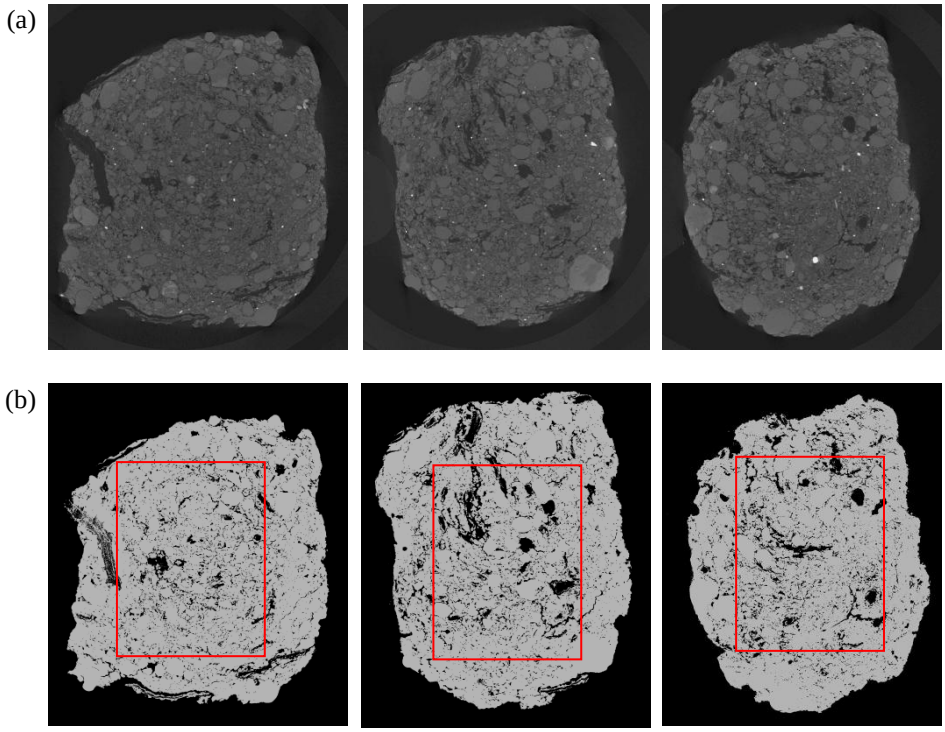

Fig. 3. Examined grey-scale soil aggregate sections (a); binary images of soil aggregate sections done by Otsu method, red lines indicate the boundary of the inner ROI (b)

Subsequently, binary morphological closing with increasing size of square structuring element, was processed. In each step, the source image was subtracted from the target image, and the result volumes were listed, giving soil aggregate pore distribution. The operation was repeated until all pores were filled. Subtraction of the transformed image from the original image gives the total pore volume.

To compare the 2D image analysis with 3D volume the porosity of the region of interest shown in Figure 3b was calculated. The values vary for different slices due to the different pores distribution and the average porosity is equal to 9.67%. In order to perform further analysis fractions of micro-, meso- and macropores were calculated. The limits of mesopores, taken arbitrarily, were between 30 and 75 μm. The results are shown in Table 1.

Table 1. Percentages of micro-, meso- and macropores of the examined aggregate

Fraction of micropores [%]	Fraction of mesopores [%]	Fraction of macropores [%]
52.69	32.48	14.83

This fraction of mesopores represents 32.48% of the total pore area. Moreover, the aggregate contains percentages of 14.83% of macropores and 52.69 of micropores. The fraction of micropores is the largest.

3.2. Porosity determination by three-dimensional image analysis

After the 3D extrusion process, void fraction (porosity) was calculated. The total volume of the clod of soil was worked out and compared with void volume. In this way the porosity was determined.

In this work the authors decided to calculate the average porosity in the region of interest area which is in cuboid shape with the basis shown in Figure 4. The ROI volume was chosen arbitrarily in such a way that it is going perpendicularly to the slices area and cannot cover external area of the soil. The ROI area and volume cover as large a quantity of soil as possible.

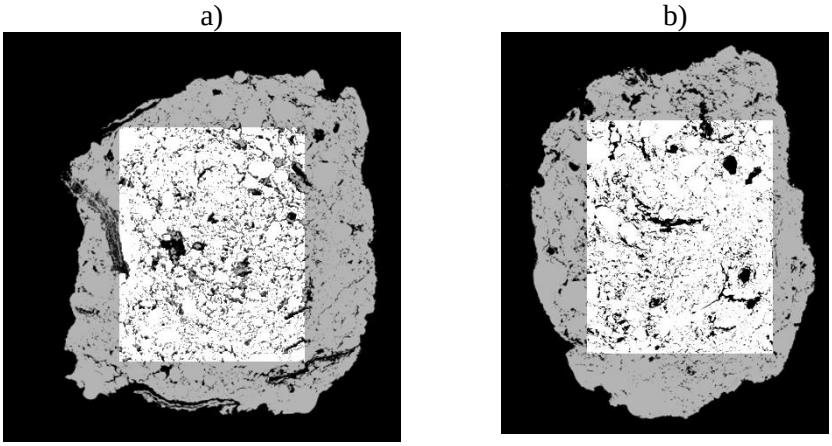

Fig. 4. Basis of ROI cuboid shown on the first a) and last b) slice of soil CT

The average porosity was calculated in both cases, i.e. the set of 2D images and reconstructed 3D volume. Soil volume fraction is the volume of soil fraction per unit volume of the sample. In the case of the calculations performed the number of foreground (soil) voxels divided by the total number of voxels in the image is the soil fraction. The calculations were performed in Fiji software with the use of the "Volume Fraction" plugin. The results for ROI analysis are

presented in Table 2. It can be noticed that the porosity value is slightly lower compared to the earlier results. It can be deduced that outer parts of the clod of soil are more dense and there are less pores in them.

Table 2. Void fraction (porosity) results for ROI volume

Property	Value
Void volume (μm^3)	$1.325 \cdot 10^9$
Total volume (μm^3)	$1.367 \cdot 10^{10}$
Average void fraction ratio calculated from 3D volume	0.09700
Average void fraction ratio calculated from 2D images	0.09676

Source: own study

The results of the 2D and 3D analysis show very good agreement. The difference between values is equal to 0.00024 (0.25%)

The idea presented by the authors in this article allows to calculate the pore properties in the 3D model of reconstructed soil. According to [1, 19] the classification of soil pores functional for water flowing is: 5–30 μm so called micropores – fully available for plant roots, 30–75 μm so called mesopores – available to a small extent for plant roots. For other pore sizes the water is not available or very hardly available for plants. Thus the interesting pore diameters are from 5 to 75 μm.

Table 3. Chosen pore number for ROI volume

Property	Value	Percentage (%)
Total number of pores	112	100.00
Total number of micropores	57	50.89
Total number of mesopores	36	32.14
Total number of macropores	19	16.96

Source: own study

It can be noticed that good quality pores, where the water is available for plants, are the majority in this soil and their number is more than 82% of the total pore number (see Table 3).

4. Conclusions

Total porosity of the investigated aggregate calculated as the mean of total porosities of 2D slices is equal to 0.09676, while in the case of 3D it is equal to 0.09700. The results are very consistent, thus the pore size and distribution could be calculated and compared. The following fractions of pores were determined:

micro-, meso- and macropores. In 2D analysis the percentage amounted to, accordingly: 52.69%, 32.48%, 14.83%, while in case of 3D the values were: 50.89%, 32.14%, 16.96%. One can notice that the results of 2D and 3D calculations are corresponding. The method described allows to reconstruct the soil aggregate in 3D space. Thanks to that, in future work the computation fluid analysis will be possible.

Acknowledgments. Our heartfelt thanks go to our colleague Professor Henryk Czachor, with whom we commenced the research presented here. This work has been supported by the national grant Frame No NN 310 307 639 of the Polish Ministry of Science and Higher Education.

Bibliography

[1] Brewer R., Fabric and Mineral analysis of soils, John Wiley & Sons, 1964.
[2] Charytanowicz M., 2013. Nonparametric Estimation for Soil Pore Size Distribution, Technical Transactions series Automatic Control (Czasopismo Techniczne seria Automatyka), 110, 4-AC (12): 17–27.
[3] Charytanowicz M., 2014. An Algorithm for the Pore Size Determination using Digital Image Analysis. Information Technologies in Biomedicine, E. Pietka, J. Kawa, W. Więcławek (red.), Advances in Intelligent Systems and Soft Computing, Springer, 3: 223–234.
[4] Charytanowicz M., Czachor H., Niewczas J., 2013. Nonparametric regression approach: applications in agricultural science. Technical Transactions series Automatic Control (Czasopismo Techniczne seria Automatyka), 1-AC/2013: 17–27.
[5] Charytanowicz M., Kulczycki P., 2015. An image analysis algorithm for soil structure identification, Intelligent Systems' 2014 Springer, Cham, 681–692.
[6] Czachor, H., Charytanowicz, M., Gonet, S., Niewczas, J., Józefaciuk, G., Lichner, L., 2015. Impact of long term mineral and organic fertilization on water stability, wettability and porosity of aggregates of two silt loamy soils. European Journal of Soil Science. 66(3): 577–588.
[7] Gonzalez R., Woods R., Digital Image Processing. Pearson Prentice Hall, 2009.
[8] Hallett P., Lichner L., Czachor H., Józefaciuk G., 2013. Pore shape and organic compounds drive major changes in the hydrological characteristics of agricultural soils, European Journal of Soil Science, 64: 334–344.
[9] Heiden W., Goetze T., Brickmann J., 1993. Fast generation of molecular surfaces from 3D data fields with an enhanced marching cube algorithm, Journal of Computational Chemistry, 14(2): 246–50.

[10] Król A., Niewczas J., Charytanowicz M., Gonet S., Lichner L., Czachor H., Lamorski K., 2012. Water-stable and non-stable soil aggregates and their pore size distributions, 20th International Poster Day and Institute of Hydrology Open Day "Transport of water, chemicals and energy in the soil – plant – atmosphere system", 870–871.
[11] Lorensen W., Cline H., 1987. Marching cubes: a high resolution 3D surface construction algorithm, Computer Graphics, 21(4): 163–169.
[12] Peth S., Nellesen J., Fischer G., Horn R., 2010. Non-invasive 3D analysis of local soil deformation under mechanical and hydraulic stresses by μCT and digital image correlation, Soil and Tillage Research, 111(1): 3–18.
[13] Pires de Silva A., Imhoff S., Kay B., 2004. Plant response to mechanical resistance and air-filled porosity of soils under conventional and no-tillage system, Scientia Agricola, 6: 451–456.
[14] Pratt W.K., Digital Image Processing, John Wiley and Sons, New York, 2001.
[15] Schindelin J., Arganda-Carreras I., Frise E., 2012. Fiji: an open-source platform for biological-image analysis, Nature methods 9(7): 676–682.
[16] Stein R., Shih A., Baker M., Cerco C., Noel M., 2000. Scientific visualisation of water quality in the Chesapeake Bay, Proceedings of visualisation, Salt Lake City, 509–12.
[17] Trembilski A., 2001. Two methods for cloud visualization from weather simulation data, Visual Computer, 179–84.
[18] Vogel, H.J., 2008. Morphological determination of pore connectivity as a function of pore size using serial sections. European Journal of Soil Science. 48(3): 365–377.
[19] Walczak R., Rovdan E., Witkowska-Walczak B., 2002. Water retention characteristics of peat and sand mixture,. International agrophysics, 16(2): 161–166.
[20] Yim P., Vasbinder G., Ho V., Choyke P., 2003. Isosurfaces as deformable models for magnetic resonance angiography, IEEE Transactions on Medical Imaging, 22(7): 875–81.
[21] Zdravkov B., Cermak J., Sefara M., Janku J., 2007. Pore classification in the characterization of porous materials. A perspective, Central European Journal of Chemistry, 5: 385–395.

Ryszard Knapiński[1], Róża Czabak-Garbacz[2]

Possibility of application of modern IT methods in cultural heritage on the example of the Płock Door

Abstract: Cultural heritage is a group of tangible and intangible resources inherited from the past which today's population considers to be worthy of being conveyed to the future. An outstanding example of Polish cultural heritage is the Płock Romanesque Door which was cast in the lost wax technique in the 12th century. The original artefact consisting of two wooden parts with 46 bronze quarters nailed to them was robbed in the 13th century and never returned to Poland. The door's panels were repeatedly dismantled and reassembled, and therefore lost their primary arrangement. The interpretative pictorial chaos present in the original door and next repeated in its copy hung in the Cathedral in Płock in the 20th century irritated Polish historians of sacral art. On the basis of their knowledge (derived from digital stocktaking of pictures taken in European churches) they proposed to rearrange the quarters properly. The new arrangement was done with the use of Photoshop and is available in printed form in books. Hopefully in future it can also be included into Internet resources and popularised to broader audience with the use of other modern IT-methods like GIS, CAD-programs, 3D-scanning, the hybrid system of voice acquisition, video clips, audio-guiding, geocaching or even virtual reality games.

Keywords: cultural heritage, lost wax technique, Płock Door, digitisation, modern IT-methods

1. Cultural heritage

The term cultural heritage primarily referred exclusively to monuments (mainly single buildings), but within the 20th century it evolved and changed its meaning. Nowadays it signifies e.g. 1) anything which has been inherited from the past generations [1]; 2) something that someone or a significant collective group in today's population considers to be worthy of being valued, admired, preserved, catalogued, exhibited and conveyed to the future [13]; 3) everything that the past generation has saved for the present purposes and bestowed for the benefit of future generations [4, 12]; 4) all that is good in history and culture [24]. According to Article 2 of the Faro Convention, cultural heritage is "a group of resources inherited from the past which people identify, independently of ownership, as a reflection and expression of their constantly evolving values, beliefs, knowledge and traditions. It includes all aspects of the environment resulting from the interaction between people and places through time" [7].

Cultural heritage is not limited to tangible (material) testimonies like historical and architectural places, buildings, monuments, underwater artefacts

[1] Ryszard Knapiński, Department of History of Sacral Art The John Paul II Catholic University of Lublin, Poland

[2] Róża Czabak-Garbacz, Institute of Rural Health, Lublin, Poland; Higher School of Economics, Law and Medical Sciences in Kielce, Poland

(shipwrecks and their freights, ruins and cities), museums with their collections of well-known or considered the most beautiful works (paintings, sculptures, coins, manuscripts) or other, often handmade objects, but also according to the definition provided by the UNESCO convention in 2003 includes intangible or immaterial (the term replaced historically familiar terms "traditional", "popular") forms such as beliefs, philosophical ideas, representations, expressions, practices concerning nature and the universe, knowledge, scientific achievements, educational systems, social practices and behaviour with often centuries-old traditions (folklore, rituals, customs, celebrations, festive events, music, oral expressions including language, tales and songs, folk medicine, craftsmanship, artistry, old professions, culinary arts, as well as hospitality) [4, 12, 28].

The word heritage has in many languages an overwhelmingly positive public connotation [19]. It can play an influential role in cultivating a sense of national identity [9], involving individuals and groups in social life, building new local ties and creating new social and cultural values that will be relevant in the future. Additionally it is integrated into everyday local life offering new jobs and business opportunities thus strengthening economies [5] and increasing quality of life of the community [4].

Cultural heritage also plays a big role in local and foreign tourism, which is an important element of the tourism strategy of the European Commission [8], because it cultivates culture, intensifies the traditional phenomena often of national importance, keeps traditions alive and attracts visitors wishing to experience history, however it can also be challenging and dangerous, especially if it is too strongly entertainment-oriented [12].

The growing UNESCO list of places of cultural heritage not only attracts them to the wider group of international tourists, but also increases the probability of invasion of unloaded crowds of visitors to the most popular objects. Modern consumer tourists require more and more convenience and high quality of service (including appropriate informational resources), but are often unaware of heritage values, therefore they can vandalise places and objects of historic importance causing a big challenge for heritage conservators and managers [12]. Additionally, border and ethnic conflicts [29], economic or religious wars and a growing number of ecological changes including climate change, especially in terms of flooding and erosion, may cause damage or complete loss of tangible heritage (e.g. destruction of salt sculptures in Wieliczka, Poland, sandstone buildings in Petra, Jordan [30] or opponent's buildings, structures and objects which became the target and an essential military goal [29] as in Warsaw during the second world war or in Mosul, Iraq and Tunis, Tunisia within the ISIS war), while urbanisation, globalisation and excessive commercialisation jeopardise several sectors of intangible cultural heritage (among others traditions of local handmade crafts that often cannot compete with the factory-produced cheap massive production [12]). The symbol

of the danger is also loss or decline in music, dances, rituals, performances, occupational and culinary traditions, craftsmanship, skills created over centuries, evidence of knowledge systems and the number of actively used languages. The loss of thousands of linguistic communities is combined with the loss of oral expressions like traditional stories.

Therefore protection and conservation of cultural heritage is an extremely important endeavour and requires specific technical, institutional and economic measures for consolidation, identification, documentation (e.g. collecting artefacts in museums and folk knowledge in manuscripts, recording speech, songs and music, videotaping celebrations), research, preservation, promotion, enhancement, transmission, particularly through formal and non-formal education as well as revitalisation [28]. The protection of cultural heritage includes development of national policies to strengthen the heritage preservation institutions, to establish qualified regional centres and create a network of professionals through online courses, e-magazines and forums as well as to carry out awareness campaigns [8] and introduce new users (like schools, administrations and other public services providing public access to artefacts) or alternative forms of uses (re-use) of tangible objects. However, in the case of economic re-use, buildings or ensembles can be improperly used, altered incompatibly with the typology and structure of their original asset or over-used, which can gradually reduce their cultural value and historic evidence [4]. Therefore it seems that nowadays the protection of cultural heritage needs more categorical actions, e.g. exclusion of objects from economic uses and their transformation in museums and protected areas, hiding originals and showing to tourists only copies of the most important attractions.

2. Romanesque Płock Door

One of the best examples of Polish material mediaeval Christian cultural heritage is the Romanesque Płock door (sometimes, for its place of origin, also called the Magdeburg door). Other, evidently erroneous, eponyms of the artefact include Korsun (in fact, another door in the Novgorod Cathedral, where the original Płock door can be found) and Sigtuna (a town in Sweden, a purported place of the door's origin). The door was ordered by the bishop Alexander of Malonne in the 12th century to the cathedral church in Płock, which at that time was a capital of Poland and the place where the Polish rulers were buried. The door consisted of two huge wooden parts of 3.6 m height and 2.4 m total width and 46 quarters cast by master Riquin and his helper Waismuth in bronze in the lost wax technique in 1152–1154 in a foundry in Magdeburg under the control of bishop Wichman from Wettin. The lost wax technique (also called cire perdue, lost wax or the method of smelting models) was known from ancient times. It included several steps following each other: 1) vaxing of the prototype of the intended object, 2) covering the prototype with a specially crafted gypsum, 3)

removal of the the wax (e.g. with hot water) and thus achieving the gypsum form, 4) pouring liquid metal into the gypsum form, 5) solidification of the the metal, 6) breaking the gypsum form, 7) eventual sanding of the the object. The bronze elements of different sizes cast in Magdeburg were next transported to Płock, where they were nailed with rivets to a wooden base and additionally covered in convex slats of a border with motifs of a diversified plant flagella.

Most of the scenes of of the quarters in of the Płock Door showed biblical motifs from the Old and New Testaments (Christ, Holy Mary, the Apostles, Angels, Satan and devils, numerous allegorical personifications and animations), but some of reliefs also presented historical figures of bishops (among them Bishop Alexander of Mallone and the archbishop Wichman of Seeburg and Magdeburg) and contractors (master Riquin and his young helper Waismuth), which was rare in the Middle Ages. Many quarters illustrated figures of lay people of various states and clergy of various degrees, and were additionally marked with Latin and Greek inscriptions. The unique character of iconological system of the Płock Door corresponded to the ideological programme of the Church in Mazovia, which was linked with an intensive Christianising mission.

The door was primarily situated in the northern side of the Romanesque cathedral church (as seen on the wax seal suspended at a document of 1239), which was the first brick church in Mazovia and in that time the largest in Poland. Certainly the monumental scale, valuable material and perfection of form (it may be discussed whether it is not more beautiful than the most famous Polish Gniezno Door) became the reason for plundering the door at the end of the 13th century, most likely as a spoil of the war of 1262, when Płock was invaded by warriors from Lithuania and Prussia [15]. Afterwards it was hidden for many years until the beginning of the 15th century, when it was hung as a "copper icon" in the Western portal of the Sofia cathedral church of Divine Wisdom in Novgorod the Great in Russia. The portal was accepted to the Orthodox Church and adapted to its new place by a Russian founder – Master Abraham, who added to the reliefs his own effigy and name at the foot of the fringe of the left leaf of the door and engraved into some quarters Cyrillic inscriptions translated into Russian from Latin (the type of letters allow to estimate they were engraved in 1430).

Within hundreds of years the door panels were many times repeatedly dismantled for easier transportation, hidden (even buried in the ground, e.g. during wars: Russian-Swedish, probably also Napoleonic and the second world war when it was transported to Siberia in 1941) and reassembled. The original in Great Novgorod indicates many places of carelessly carried out repairs of defects and cracks, reworking, flattening (even using modern screws that do not fit into the monument) and cutting the borders to refit the reliefs, which disturbed the original layout of the quarters.

(a) (b) (c)

Fig. 1. Cathedral church in Płock (a), wax seal of 1239 (b), Orthodox Sofia church in Great Novgorod (c)

Because of the political circumstances the original Płock door has never returned to Poland, therefore due to the efforts of the president of the Płock Scientific Society, dr inż. Jakub Chojnacki, the bronze copy of the door (a gift of the Government of the Republic of Poland) was cast according to its original in the years 1971–1981 in the Monument Preservation Workshops in Szczecin and Warsaw and mounted in the western vestibule of the Płock cathedral. However, the Polish founders introduced into the copy small changes like removal of some inscriptions, assuming them to be added in Ruthenia. Not being too well aware of the key to the panels' mutual association, they left an improper arrangement of the quarters, not connected logically together (neither the typological order was legible nor the full cycle of Vita Christi was realised; additionally St Peter appeared twice in the same scene). The chaos of pictorial narratives is also present in other copies of the Romanesque Płock Door (e.g. in two gypsum models from the second half of the 19th century present in Moscow and Nurnberg, and two plastic artefacts in Gniezno and Warsaw).

Such a state of affairs was not to the liking of many researchers, and at the end of the 20th century, when the scientists of the Department of History of Sacral Art at The John Paul II Catholic University of Lublin (Poland) established that the quarters did not illustrate the Life of Jesus, but the twelve tenets of the Christian faith, variously defined as, for example, the Apostolic Creed, Symobolum Apostolorum, Credo Apostolorum (such illustrations were extremely rare in Medieval Art). Therefore the original iconographic arrangement (reconstruction of the quarters) should be associated with articles of faith, referring to the ancient Christian tradition, according to which each of the Apostles, before everyone spread to the world on his mission of evangelisation, gave a single article of faith.

2.1. The modern IT methods and the Płock Door

The start-point for a statement about the Door's mistaken iconography was the top, three-part panel of the left Door leaf with a well visible improper quarter arrangement. The correct sequence there should be the College of Apostles, Christ's Ascension and the Descent of the Holy Ghost (a panel with this image is now in the lower part of the right leaf). The Polish scientists correctly arranged the scenes of the Płock Door by means of Photoshop, aided by their great experience and knowledge of the principles of typological or allegorical ways of thinking gained during their deep, long-lasting studies of other mediaeval artefacts like miniatures in the Utrecht Psalter (Reims ca 830) as well as monumental paintings from the 10th and 11th century in Reichenau, Oberzell and Niederzell.

(a) (b) (c)

Fig. 2. Original of the left leaf – in situ (a), the Płock Door – reconstruction (b), original of the right leaf – in situ (c)

The selected iconographic material related to the Credo theme in art also served them to create the Digital Photographical Archive of 2-D pictures stored on hard discs and additionally on external discs as an inventory file containing the basic data on specific works of sacral art as well as the relevant bibliography

in the form of scans of publications. The archive has an open character to allow its future enlargement. The historians from Lublin hope to introduce some data from their research into the database descriptions of cultural heritage (among others into the Scala Archives which acquires data about objects present in churches) and modern information systems addressed to tourists, including electronic applications, audioguides (also for blind or visually impaired people), interpretative guiding with the use of 3D-graphics (for the Door's 3-D scanning and next its 3-D printing), city walk systems, geocaching and augmented reality (to show the Door's changes over time).

The Płock Door is not a unique example of a wrong approach to cultural heritage. The British Museum possesses a work issued by Marcandio Raimondi and reproduced in the past under the title "The Sign of the Ram" or "Mars' picture" which in fact is an exemplification of John the Baptist. The correction of the false identification of the stored artefact was possible due to two methods of data organisation: 1) indexing and alphabetical ordering, 2) structural classification [25]. Classification systems which in the past mainly described works of arts (e.g. a pictures with words), the nature of their purpose, old and present forms and local varieties, were together with other ancillary tools like thesauri, the basic parts of databases which served as documention of cultural heritage [26].

Some tools used over the years for traditional cataloguing in cultural heritage institutions did not fulfil their function, because they widely differed (had variations in the field structure, depth, focus and vocabulary applied [21]), were present non-exclusively on several, often professional sites in the Web (thus being difficult to find without prior knowledge), additionally were complicated, inflexible, expensive and often also not user-friendly. Therefore a complex task of integration of huge amount of large digital data sets needed widely accepted metadata standards, possible for common use [10, 26]. The attempts of ordering the data necessary for cataloguing and exchange of information related to cultural heritage included implementation of various systems, e.g. classical Iconclass (which tried to discipline the language of the description [21, 25]), multilingual LIDO (Lightweight Information Describing Objects – an XML schema for delivering metadata [10]), MIDAS (A Manual and Data Standard for Monument Inventories – the basis of cataloguing and providing textual and pictorial material on buildings, archaeological sites, shipwrecks, parks and gardens, battlefields, areas of interest and artefacts [3]), MONA (modular system designed to collect information about museum exhibits in the form of huge amount of digital pictures in JPG format, acoustic files and animations [23]), MUS.NET (MUSeum NETwork which used a transparent and logical graphic system with simultaneously visible data, grouped in sets identifying the object, its acquisition, creation and administration, and displayed in full, sometimes with several photos or signalled partially by an appropriate definition in fields, developed in accordance with several copies of Windows [22]), CDWA

(Categories for Description of Works of Art – a meticulous set of elements, which became a common data structure for information about various types of collected objects and was used to manage private and commercial collections), Museumdat XML Schema [10] and many others.

Old systems were not perfect (many of them were accused of being incompatible in describing the world in all its complexity with the use of numeric and letter codes), hence they were often improved, e.g. difficulties in sharing many categories between systems by CDWA caused its supplementation/replacement by the CCO (Cataloguing Cultural Objects: A Guide to Describing Cultural Works and Their Images) standard, which was designed specifically for documenting and cataloguing of objects of cultural heritage and contained recommendations for improvement of structure, description and use of common data values found in relevant controlled vocabulary dictionaries (which facilitated precise and unambiguous description of objects) and thesauruses, such as TGM (Thesaurus for Graphic Materials), AAT (The Art and Archival Thesaurus), ULAN (The Union List of Artist Names), TGN (The Getty Thesaurus of Geographic Names) and others [10]. Ancillary tools like thesauri and dictionaries should ensure a uniformity of terms and protect against incorrect entries, however hierarchical dictionaries (including multilingual and polyhierarchical) often raised doubts when comparing different language versions, for example, methods of presenting proper names (which were added in brackets for this reason), dates and ordinal numbers [25]. Thus it was highly important to unify terminology by creating data sets with the use of ready thesauri and avoiding individual features or literacy figures in order to simplify a junction of different bases [22].

A CDWA Lite data format was also developed, which used the XML schema for storing metadata of tangible cultural heritage in the basic categories and exchanged descriptive information between data formats and systems, based on CCO and using a subset of the CDWA categories [10]. Nevertheless, the lack of a uniform standard in the field of file description hindered for years the synergy and exchange of information between institutions dealing with cultural heritage. Therefore, international projects were initiated (among them eEurope [14]) to solve the problem by implementation of the latest technologies, i.e. development of modern IT programs which could improve the documentation process, protection (against theft or destruction), maintenance, administration and sharing of cultural resources [14]. The cooperation of scientific institutions, especially museums in the exchange of information, is supervised by ICOM (International Council of Museums), operating under the auspices of UNESCO, bringing together international committees, among others CIDOC/ICOM (International Committee for Documentation) which developed a conceptual model of reference data for cultural goods – CIDOC-CRM (CIDOC Conceptual Reference Model), containing definitions and formal structure recommended in the description of the concepts and relationships used in the documentation of

cultural heritage in order to facilitate its unified understanding, to provide a common language for specialists and contractors, to be the basis for formulating requirements for information systems, and to serve as a guide to good practice in conceptual modelling. CIDOC CRM described tangible and intangible aspects of the artefact (how, where, by whom, for what purpose it was manufactured, whether it was transformed/renovated or transported, where and how it was stored, preserved and conserved) and expressed temporal dependence between time and various events in the artefact's life (the spatio-temporal information), by adding its geospatial data such as: topology, directions, distances and location [6]).

Requirements for all programs collecting information about cultural heritage included taxonomy of basic standards such as: data fields & data structure (metadata sets, diagrams), content & data values (controlled vocabulary, thesauri, lists and registers, records visible in the form of a table or a full description) as well as data exchange. Additionally electronic systems should allow to gather basic and detailed information about the object and its pictures, to perform semantic analysis and image comparison (including three-dimensional), to move the data (documents) easily, to put even longer descriptions into appropriate fields (which could be enlarged to large sizes, favouring reading comfort) and to allow junction of databases [22], moreover to become popular they must be well-described, easily accessible (possible to be browsed in several languages), expandible and preferably free [26]. System hierarchy with a multi-level breakdown – main groups, subgroups, etc., sometimes with the use of structural digits with proper descriptive code and index of keywords should allow at any level simple and quick search for needed information (based on the mechanism of so-called full-text search for a given word, string of words or phrases) in the entire database, or more precisely, limited to indicated fields in its selected part (without the need of using a key to formulate questions [22].

Improved programs became a great support in documentations of cultural heritage [21], facilitating the work of people who inserted the data, eliminating repetitive activities, allowing to copy whole items or their fragments (e.g. during cataloguing sets of identical or very similar artefacts), quick checking of many objects with little effort (limited to entering small proofreading), duplication of information, manipulation on a large number of objects, grouped for a specific purpose, transferring documents from other programs (for example MS Word text editor, and vice versa), reusing previously prepared text or creating any statements or graphic forms of the document and giving them unique names, as well as specifying private or public status (as required), deciding on widespread or limited availability [22].

In reducing the time of the collection process a hybrid system of voice acquisition can be useful, which is based on machine learning techniques (and thus can automate the acquisition of dictionaries and specialist grammars, as

well as the annotation of text) and on NLP (natural language processing) technology. It uses a voice interface (man-machine dialogue with signal processing, knowledge modelling and understanding of natural speech). The first step includes division of text into sentences and words and labelling elements based on external resources and grammars. Next, linguistic analysis is performed of the transcribed text and extraction of information with the use of advanced technology of the robust XIP (Xe-Incremental Parser) software, enriched by semantic lexicons and rules, specific to the large vocabulary of cultural heritage (therefore being guaranteed proper process also in the case of text malformation by errors which may occur within oral transcription). The resulting text depends on many parameters, such as the acoustic (quiet or noisy) environment, thus being also displayed to experts who validate linguistic correctness and eventually correct errors. Although the speech recognition (the identification of words or phrases with the use of their morphosyntactic analysis) is not easy, seeing that they can be used in different contexts and have multiple meanings, additionally the same object can have several names (this is caused by the richness of the vocabulary of cultural heritage and the complexity of the language itself), information extraction achieves high (90–98 %) concordance between the original content and the content of the automatically transcribed texts [6]. The end stages of the process include conversion into different formats of computer languages (RDF, DAML 4, OIL, OWL or XML, which allow to group the data according to needs and search for criteria in coding, which is not visible on websites and does not interfere with reading the text) and pasting into the Web (generation of a domain ontology can be semi-automatic), i.e. filling the coherent and well structured verbal descriptions into proper fields: mandatory (their content is defined by a lexicon) and sometimes also optional (their content remains free).

Today there is no alternative to digitisation of cultural heritage, which apart from good IT systems also needs support of the Internet – an excellent tool for rapid (much faster than in traditional institutions and independent of their working hours [3]) worldwide overview of stocks (cursory access to online visual materials). Improving the "discoverability" of resources of cultural heritage on the Web and avoiding the invisibility in information infrastructure is possible due to such devices as Google search engines, Alta Vista, Alexa Internet or Teoma, which conduct cross-cutting thematic searches through a wide spectrum of public and private domains, commercial and non-profit portals and personal opinions as well as all available (published and unpublished, formal and informal) sources of information, and then facilitate the transition to local resource databases, which can be integrated with topographic services (like Google Maps or with orthophotomaps), e.g. by using applications based on the Java2ee platform, which make it possible to work with any data bases and in any operating system as part of the user interface.

Via the Internet, whose role is increasingly growing, one can access online collections, e.g. Arcyclopedia (which contains an index of names of artists represented on hundreds of museum sites, photo archives and other resources, as well as avail oneself, apart from online art information and digital views of works of art, of the possibility to obtain them in the form of a digital record, poster or postcard), Foto Marburg (that together with the Digital Image Index of Art and Architecture has one of the most extensive databases), National Portrait Gallery's Picture Library (the most renowned specialised archive of British portraits), Scala Archives (virtual museum and database of European painting and sculpture from the period 1100–1850, also offering commentaries and bibliographies of artists and sightseeing options, music related to a specific historical period, postcards and illustrations of works present in churches), Olga's Gallery, Art Magis and many others [18]).

The extraordinary universal value of the very fast developing Internet (every year there appear new methods which set new standards in application development) is its openness to modifications, remaining in opposition to everything that has been completed, static and closed. It allows to correct and supplement the Web database, which contains a huge amount of records of cultural heritage from any location, at any time. Internet users who have equal opportunities of free access for everyone can decide about the time of their activity, skip viewing digital images and descriptions or effectively conduct more independent detailed searches to obtain results in the form of texts, iconography and topographic visualisations [2]. Therefore, it is extremely important for many Web users to be able to use data at the same time without the danger of system blockage (which can occur in the case of high pressure from eager users, as was the case with Europeana in 2008 [27]), to access information (including dictionaries) with ease from various platforms and operating systems, and achieve a high level of security also in terms of the unchangeability and durability of digital data. The ensuring of long-term availability, especially the life longevity of fast changing means and formats of recording and compression should avoid quick loss of access, as happened to the 1986 digital version of The Domesday Book (with the names of the nobility and local place names from the time of William the Conqueror), which at present cannot be read from the special discs operated only by no longer available computers (hence the electronic version served less than sixteen years, but the eleventh century book is still well preserved and available in one of the British archives [14]). Paper and wood can survive for ages, text engraved in stone thousands of years, while digital media a maximum of a decade [17]. Therefore documents concerning cultural heritage in some institutions, apart from their spreading in the Internet and saving in digital form, are additionally printed, because the best practice in collection management is a long-term preservation of data and artefacts.

The digitisation of collections' artefacts – converting their material physical forms into digital code (a point cloud or textured triangle grid for each object)

and then pasting the images into Web allows to "replace" and to "save" the originals in the form of digital copies (serving as a reliable source of knowledge [14]). It is extremely important in the case of an object's random loss or its poor technical condition (e.g. due to age). Among techniques which allow documentation of cultural heritage with very high precision is digital photography characterized by detailed recording of colours, textures and shapes, high image resolution and possibility to enlarge photography without loss of achieved quality. Constant improvement of technical parameters of digital cameras allows taking high-quality pictures, their multiple use and after proper compression sending via computer network to a wide audience (Web sharing).

Effective data compression techniques overcame the barrier of image file transfer. The IPlImage system (with image representation in TIFF format, saved in the tiled pyramid system of subsequent approximations) provides remote viewing and sending of large files with high resolution even via slow Internet connections [18], however it cannot exclude the danger of errors (caused by bad transmission or faulty conversion of data from older databases or perpetuations during data insertion by hand or machine) or the risk of losing or damaging some data, e.g. by changing the bitmap pixel layout (when processing photos or scans) and by repeated migration between forms. The IPlImage system allows operations which were previously impossible, i.e. to provide a fragment of the image needed at a given moment and then to view, move and zoom it (even very large size details that can be download and process on a home computer). Therefore zoomify has replaced the magnifying glass [20].

Thanks to easy access Internet optimises the chances of getting information, minimises the costs of describing the resources and allows greater data interoperability within cultural heritage, which, thanks to the presence in the Web, is subjected to convergence and virtual integration, ceases to be the property of specific institutions and becomes a global property in a shared network space, used for various processes, e.g. for teaching, learning, performing research, spending free time in important social networks or even travelling virtually). The Internet, apart from the mass aspect, offers a decentralised communication model, allowing interchangeability of data [3] and avoiding high costs and crowds of intermediaries.

Younger generations of Internet users, who participate in crowdsourcing, are ready and eager to take over the role of collaborators in remix and reuse of data and information, as well as in building virtual resources, e.g. by programming tools through Web 2.0, thus expanding the shared spaces in YouTube and Flickr, MSpace, Facebook and Linkedin. Such approach, by allowing to elaborate the Web sites by volunteers, helps different users (not only scientists or experienced connoisseurs but also ordinary people) to benefit from the Internet sources connected to cultural heritage [10]. The Internet guarantees access to an increasing flow of data offered by heritage institutions which in the Past were difficult to be found and used. Nowadays it is possible to successfully open up

multimedia-based multilingual data (e.g. records efficiently collected in the form of text, photos, sketches, maps and videos) from diverse Web sources (by keeping the formal and semantic standards) and to benefit from the standardised cataloguing of stocks [22], however the amount of gathered information about cultural heritage considered to be scientifically reliable is really huge and often heterogenic. Paradoxically, such a large amount of data is not a big choice, because when using search engines, most of the results are informational noise – many of them are duplicated and some institutions, thanks to the positioning technique, obtain first places on the results list, although their meaning and offer do not match the declared expectations of the user.

Another milestone in the development of IT methods implemented into cultural heritage was recording of spatial parameters and mapping the shape of three-dimensional objects with the use of a special 3-D techniques. 3D-graphics tools allow to visualise both existing and nonexistent (lost, threatened, dispersed or damaged) objects based on their text description or 2-D pictures. Due to the 3-D images it is possible to provide conservation works, e.g. to fill vast areas of damaged artefacts with incredible precision or to make simulacra (digital representations which in the whole are imitations of other objects [20]), e.g. created by the creator on the base of their imagination or based on the view of the scanned original object. Sometimes such methods may also help in protection and conservation of artefacts at risk, when conservators first try reconstruction works on model and then on the original artefact. Therefore the development of CAD (Computer Aided Design) software, which took place in the early 1990s and allowed with the help of digital technologies the generation of 3-D views of artefacts from different perspectives and their 3-D reconstruction significantly facilitated the introduction of changes in conservation works and to prepare 3-D models in plastics, resin, copper and other materials according to the needs of recipients, exhibition location, technological capabilities and financial resources of clients. A three-dimensional graphics enriched by printing of 3-D models or typographic printing of pictures is widely used in institutions of cultural heritage (especially in places where the touching of original objects is not possible or they are to big) in order to allow blind or visually disabled people to experience by touch the proportions, shapes and texture of artefacts [20]. The use of printed 3-D mockups in combination with dynamic projection and animation leads to a variety of visual information and facilitates its perception. 3-D modelling with appropriate expression and climate includes: analysis of the individual elements of the reconstructed work, appropriate reduction of details, spatial development, classification and fusion of objects, and the introduction of "atmosphere", which revives soulless geometry [17].

The first adopted standard in modelling three-dimensional objects was VRML (Virtual Reality Modelling Language), which was next replaced by eXtended 3D (X3D). Both standards allowed the creation of virtual worlds and

allowed real-time navigation. 3-D Modelling included the use of 1) the Level of Detail node for improvement of rendering performance, 2) DEF (Definition node) and USE (Instance node) to improve model display performance randomisation, 3) Cylinder Sensor node in enrichment with an interactive element 4) TouchSensor node to move elements, e.g. opening gates, 5) TimeSensor time node which enriched the scene in an animated sky, 6) textureTransform node in enrichment with additional elements, such as plants, 7) Transparency node for translucency, 8) the Point Light node for lighting and 8) Sound node in adding sounds. There were also elaborated hybrid technologies which combined manual input of the X3D language code into a text editor and a post-programming method with the use of existing programs (e.g. Cinema 4 D or Avatar Studio [30].

The concept of virtual cultural heritage includes virtual reconstructions of objects that cannot be reconstructed, e.g. building changes, hence the possibility of computer-generation of a non-existent object and pasting its image into real environments with the use of special application is an extremely attractive tourist product supporting cultural heritage. In the space of video games and virtual worlds, it is possible to use creation of images and interpretations for educational purposes as a method of explaining, commenting on or presenting circumstances of the creation process. Interpreting serves to understand the heritage, and thus to understand its meaning, to realise the need for its protection, as well as to build a tourist offer and popularise the object or place. There also exist applications which allow to virtually paste an image of a non-existent architecture into an early urban layout (a virtual image of the reconstructed architecture is "superimposed" on the image captured by the camera and displayed on the monitor). Thanks to the location using a GPS signal and a compass, when moving, the image adapts to the place in real time or with the use of special filters to an interesting historical era, giving the feeling of travelling into the Past (existing in 4-D, because the world is four-dimensional and changes over time).

In popularising cultural heritage on a wider scale, including offers for tourists one can also effectively use a form of geocaching game, which exists since 2000 when President Bill Clinton unblocked the availability of the GPS signal to all users. The game has many forms (traditional-cache, multi-cache, travel bugs, mystery cache, event-cache, virtual cache, night-cache) and includes hiding specially prepared treasure packages (geocaches), informing about their location by specifying geographical coordinates (longitude and latitude in WGS-84 format) with the use of the Internet, finding and taking the gift (a treasure) by the finder, who enters into the logbook and puts a new treasure in the package. The advantages of geocaching are the potential of presenting and assimilating information about cultural space, high universality, low cost, increasing accuracy of GPS receivers, easy communication and location of interesting boxes on websites using Google Maps, additionally the possibility of matching

the route with boxes according to the knowledge, interests, age and language of the players, who can be deliberately guided [16]. Gamification aimed to increase the recipient's involvement in the process of experiencing virtual reconstruction (by evoking emotions) provides viewers with a rich visual experience (immersing them in the visual and tactile space appropriate for a given environment, creating the impression of escaping physicality and experiencing telepresence). It uses a simple navigational system, offers easy access to information and is comparable to good maps, therefore can also be used as a new means of communication for presenting cultural heritage apart from classic forms (printed or shared in Internet documents, posters or postcards) or other "old" digital means like presentations, animated films (assembled from sequences generated from a 3-D scene and then combined into animations, simulations and interactive trips by materialisation of virtual reconstructions and visualisation with the use of mobile devices and games engine which allow network players to move in virtual reality in real time, coordinating their movements and ensuring their interaction and communication [17]).

Thanks to the use of many different multimedia techniques, including 3D modelling, digital photography, rendering and animation, creating Web presentations and using the Google Earth platform, attractive forms of protection, popularisation and promotion of cultural heritage have been developed. Especially important is the role of the Internet, which allows multiple, easy access, creative use and exchange of data between many users (interoperability, implementation and automatic sharing of digital documentation), therefore it is extremely important to control all Web resources in terms of protection of sensitive data and respect to inventory and intellectual property rights [10]. It is also necessary to use mechanisms for controlling computer graphics, used for spatial imaging of artefacts (suitable for particular scientific disciplines and consistent with the purpose of research), i.e. developing a reliable methodology that guarantees historical credibility of created virtual objects [2] because the computer image obtained as a result of visualisation may be unreliable or even falsified.

Available in Web metadata regarded to cultural heritage attract attention however they also may cause a threat of a decline in visiting of really existing institutions by replacing the direct view of the work of art by contact with its ever more faithful representation and drawing people away from contact with real exhibitions. The futuristic vision of the audience that admires cultural heritage on the screen of a home computer seems quite disturbing, however this way can also popularise it by bringing it closer to a potential viewer, including those temporary or permanently disabled [18], e.g. having problems with their motor system. Some tools available in the Web, like audio guides, can also be used directly by visiting objects connected to cultural heritage. The special audio guides use AD (so-called audio description) which is burdened with high autonomy and a dose of subjectivity of verbal description of visual content (thus

is something like translation between two languages) transmitted by auditory means to blind and visually impaired people, enabling them to perceive visual art. Such description is a big challenge because it needs adaptation of means of expression to the capabilities of respondents, often of different age, education, religion and nationality. Thus it requires fidelity of translation, appropriate length and degree of detail, as well as expression that builds the aesthetic tension of the blind or visually impaired recipient [20], who independently can move in museum due to transmitters attached to the walking sticks or limbs, headphones and audio guides. Special detectors located in appropriate places detect signal send by transmitters and then switch on audio-description by radio signals), however sometimes too close situated detectors can cause unexpected suspension of audio description [20].

The online tourist can obtain the latest information from the Internet (which is full of easy accessible information) in order to contact, admire, use and benefit the cultural heritage fruitfully, creatively, cognitively and relatively cheaply, even if trips and visiting of collections are performed only in the space of virtual reality. In the harassed world more and more people travel on Websites, even more than could ever fit in the museum, however it cannot be excluded that online audience can partly become real visitors whom the modern IT techniques may help to take decision about potential destinations and encourage online tourists to visit on-line collections in the real world [18], because it is obvious that even the most perfect mappings will not replace real objects.

In conclusion it can be stated that the introduction of modern IT techniques can guarantee that cultural heritage (including the famous Płock Door) which undergoes transformations over time not only had a past and has a present, but will also have a future.

Bibliography

[1] Aitchison C., MacLeod N.E., Shaw S.J., 2014. Leisure and tourism landscapes: Social and cultural geographies. London, Routledge.

[2] Bentkowska-Kafel A., 2008. Historyczna wiarygodność zabytku wirtualnego. Uwagi na marginesie postulatów Karty londyńskiej. In: Nowoczesne metody gromadzenia i udostępniania wiedzy o zabytkach. Eds. Seidel-Grzesińska A., Stanicka-Brzezicka K. Wrocław, Acta Universitas Wratislaviensis.

[3] Brandt T., 2008. MIDAS – New Developments in an Established Standard. In: Nowoczesne metody gromadzenia i udostępniania wiedzy o zabytkach. Eds. Seidel-Grzesińska A., Stanicka-Brzezicka K. Wrocław, Acta Universitas Wratislaviensis.

[4] Breil M., 2019. Cultural heritage. Available from http://www. coastalwiki.org /wiki/ Cultural_heritage [accessed on 22-08-2019].

[5] Devidze E., Gigauri L, 2015. Promotion of Cultural Heritage Tourism in Chokhatauri District in Georgia. In V. Katsoni, ed. Cultural Tourism in a Digital Era. First International Conference IACuDiT, Athens 2014. Switzerland, Springer International Publishing.
[6] du Chateau S., Boulanger D., Mercier-Laurent E., 2012. Advanced system for acquisition and knowledge management in cultural heritage. In: Dobra kultury w sieci. Eds. Herden E., Seidel-Grzesińska A., Stanicka-Brzezicka K. Wrocław, Acta Universitas Wratislaviensis.
[7] Framework Convention on the Value of Cultural Heritage for Society, adopted in Faro on 27 October 2005.
[8] Gwardzińska Z., 2018. Cultural Heritage Objectives of the Eastern Partnership of the European Union. Santander Art and Culture Law Review, 2(4): 71–88.
[9] Ireland T. and Schofield J., 2015. The Ethics of Cultural Heritage. in The Ethics of Cultural Heritage, edited by Tracy Ireland and John Schofield, Springer, New York.
[10] Kailus A., 2012. LIDO – the harvesting format for heritage collection data. In: Dobra kultury w sieci. Eds. Herden E., Seidel-Grzesińska A., Stanicka-Brzezicka K. Wrocław, Acta Universitas Wratislaviensis.
[11] Kamiński M., Ciasnocha R., 2008. Nowoczesne techniki informacyjne w działalności museum. In: Nowoczesne metody gromadzenia i udostępniania wiedzy o zabytkach. Eds. Seidel-Grzesińska A., Stanicka-Brzezicka K. Wrocław, Acta Universitas Wratislaviensis.
[12] Kavelashvili N., 2018. Protecting the Past for Today: Development of Georgia's Heritage Tourism. Turystyka Kulturowa, 2: 97–109.
[13] Kersel M.M., Luke C., 2015. Civil Societies? Heritage Diplomacy and Neo-Imperialism, in Global Heritage: A Reader, edited by Lynn Meskell. Chichester, John Wiley & Sons, Inc., https://works.bepress.com /morag_kersel/59/ [accessed on 22-08-2019].
[14] Kępczyńska-Walczak A., 2008 Technologie cyfrowe dla dziedzictwa kulturowego – model opracowania danych o zabytkach architektury. In: Nowoczesne metody gromadzenia i udostępniania wiedzy o zabytkach. Eds. Seidel-Grzesińska A., Stanicka-Brzezicka K. Wrocław, Acta Universitas Wratislaviensis.
[15] Knapiński R., 2013. Uniwersalny charakter sztuki średniowiecznej na przykładzie diecezji płockiej w czasach biskupa Aleksandra z Malonne (1129–1156). in Fundamenty średniowiecznej Europy, red. Sztylc Ż., Zagórski D., Radzimiński A., Biskup R. Pelplin, Wydawnictwo Bernardinum.
[16] Kuroczyński P., 2008. Z Breslau do Wrocławia – geocatching w promocji przestrzeni kulturowej miasta. In: Nowoczesne metody gromadzenia i udostępniania wiedzy o zabytkach. Eds. Seidel-Grzesińska A., Stanicka-Brzezicka K. Wrocław, Acta Universitas Wratislaviensis.

[17] Kuroczyński P., 2014. Z płaszczyzny obrazu w wirtualną przestrzeń komputerowej rekonstrukcji. In: Obraz i metoda. Eds. Seidel-Grzesińska A., Stanicka-Brzezicka K. Wrocław, Agencja Wydawnicza Argi.
[18] Kuśmidrowicz-Król, 2008. A. Odwzorowanie cyfrowe dzieła sztuki i techniki multimedialne – perspektywa rozwojowa czy konkurencja dla współczesnego muzealnictwa? In: Nowoczesne metody gromadzenia i udostępniania wiedzy o zabytkach. Eds. Seidel-Grzesińska A., Stanicka-Brzezicka K. Wrocław, Acta Universitas Wratislaviensis.
[19] Macdonald S., 2009. Difficult Heritage: Negotiating the Nazi Past in Nuremberg and Beyond. New York, Routledge.
Pawłowska A., Wendorff A., 2016. Usłyszeć obraz – koncepcja audiodeskrypcji Sali Neoplastycznej w Muzeum Sztuki w Łodzi. In: Dostrzec więcej. Eds. Seidel-Grzesińska A., Stanicka-Brzezicka K. Wrocław, Agencja Wydawnicza Argi.
[20] Seidel-Grzesińska A., 2008. Światowe standardy klasyfikacyjne i przykłady ich zastosowań w polskiej praktyce dokumentacji zabytków. Nowoczesne metody gromadzenia i udostępniania wiedzy o zabytkach. Eds. Seidel-Grzesińska A., Stanicka-Brzezicka K., Wrocław, Acta Universitas Wratislaviensis.
[21] Sieradzka-Malec B., 2008. Musnet – moduły systemu wpływające na zmianę jakości pracy muzealnika. In: Nowoczesne metody gromadzenia i udostępniania wiedzy o zabytkach. Eds. Seidel-Grzesińska A., Stanicka-Brzezicka K. Wrocław, Acta Universitas Wratislaviensis.
[22] Słomka H, 2008. Opis zabytku na podstawie systemu muzealnego MONA. In: Nowoczesne metody gromadzenia i udostępniania wiedzy o zabytkach. Eds. Seidel-Grzesińska A., Stanicka-Brzezicka K. Wrocław, Acta Universitas Wratislaviensis.
[23] Smith L., 2010. Ethics or Social Justice? Heritage and the Politics of Recognition. Australian Aboriginal Studies,2: 60–68.
[24] Stanicka-Brzezicka K., 2008. System klasyfikacji ikonograficznej Iconclass: charakterystyka, przykłady zastosowania, problemy. In: Nowoczesne metody gromadzenia i udostępniania wiedzy o zabytkach. Eds. Seidel-Grzesińska A., Stanicka-Brzezicka S. Wrocław, Acta Universitas Wratislaviensis.
[25] Stanicka-Brzezicka K., 2012. Tradycyjny a bazodanowy opis zabytku. Próba porównania i artykulacji. In: Dobra kultury w sieci. Eds. Herden E., Seidel-Grzesińska A., Stanicka-Brzezicka S. Wrocław, Acta Universitas Wratislaviensis.
[26] Śliwińska M., Kożurno P., 2014. Wirtualne Muzeum Europejskie. In: Obraz i metoda. Eds. Seidel-Grzesińska A., Stanicka-Brzezicka K., Wrocław, Agencja Wydawnicza Argi.

[27] UNESCO, 2003. Convention for the Safeguarding of Intangible Cultural Heritage. Paris, 17 October http://portal.unesco.org/en/ev.php-url_id 17716&url_do do_topic&url_section 201.html [accessed on 26.08.2019].
[28] Zagato L., 2015. The Notion of "Heritage Community" in the Council of Europe's Faro Convention. Its Impact on the European Legal Framework. In: Between Imagined Communities of Practice Participation, Territory and the Making of Heritage, eds. Adell N., Bendix R.F., Bortolotto C. and Tauschek M. Göttingen, Göttingen University Press.
[29] Zawadzki T., Filipczuk P., 2014. Modelowanie 3D w rekonstrukcji nieistniejących obszarów zabytkowych. In: Obraz i metoda. Eds. Seidel-Grzesińska A., Stanicka-Brzezicka K. Wrocław, Agencja Wydawnicza Argi.

Adam Kiersztyn[1], Paweł Karczmarek[2], Witold Pedrycz[3], Ebru Al[4]

The concept of a supply chain management system using intermodal transport: a case study

Abstract: In this paper we present an outline of the supply chain management model using intermodal transport. The starting point is cooperation with a large logistics company using various forms of transport. The work presents assumptions of the model, which, thanks to the use of real data from the transport management systems used by the company so far, will be able to use a wide range of factors affecting the cost and transport time. The aim of the planned model is the optimisation of costs and transport time as well as reducing the impact on the natural environment.

Keywords: fuzzy sets, Particle Swarm Optimization, intermodal transport, sustainable supply chain management

1. Introduction

The activities of enterprises, in particular transport companies, have a huge impact on the natural and social environment. Research on sustainable supply chain management (SSCM) remains still of interest to scientists, as evidenced by the number of publications on this subject (see [10, 22]). A lot of work has been devoted to literature review on the subject [1, 18, 21, 43]) and meetings [9], a compilation [37] and a comparison of different solutions [16]. The literature considers four main approaches to the definition of SSCM, namely quantitative methods [2, 17, 38, 42, 49] qualitative methods [14, 25, 31, 47], mixed methods [29, 28], and conceptual papers [7, 8, 40, 44].

The issue of Intermodal Transport is very closely related to the supply chain considered at work in a logistics company. One should properly build a model describing the transport of goods by means of various means of transport. The literature on the subject considers the proper location of terminals [3, 4, 23], [27, 30, 34, 39], location of factories [13, 35, 49], goods distribution planning [5, 20, 35, 46] and intermodal planning [6, 11, 12, 15, 19, 26, 32, 41, 45].

[1] Adam Kiersztyn, Institute of Computer Science, Lublin University of Technology, Poland
[2] Paweł Karczmarek, Institute of Computer Science, Lublin University of Technology, Poland
[3] Witold Pedrycz, Department of Electrical & Computer Engineering, University of Alberta, Edmonton T6R 2V4 AB, Canada; Department of Electrical and Computer Engineering, King Abdulaziz University, Saudi Arabia; Systems Research Institute, Polish Academy of Sciences, Warsaw, Poland
[4] Ebru Al, Ekol Lojistik Inc., Turkey

However, there is a lack of a model that, based on real data from a logistics company, would take into account many transport modes and optimise at the same time such factors as time, cost and impact of transport on the environment.

The purpose of the work is to present the assumptions of the system being developed. The starting point is to present the concept of the system, not its exact form.

The work is organised in the following way: Section 2 presents the assumptions of the model created, Section 3 describes the method of using empirical data to determine the membership function. The last, 4th section presents the model assumptions defined in the project.

2. Model assumptions

Managing the supply network with the use of intermodal transport is a very complex problem if one ultimately wishes to develop a model that allows to optimise transport costs, transport time and reduce the negative impact on the environment. A simplified model of intermodal transport is presented in Fig. 1.

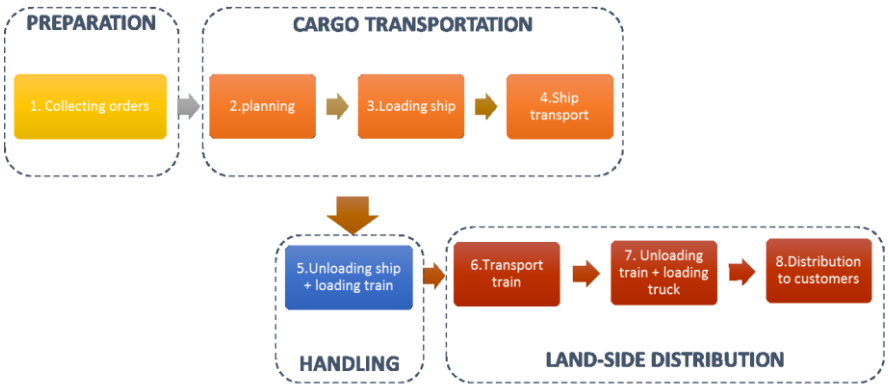

Fig. 1. Supply chain diagram using intermodal transport. Source: Chist-Era demonstration materials

The starting point for the construction of a system supporting supply chain management is to learn about the strengths and weaknesses of the currently applied solution and an in-depth analysis of available historical data.

During the data analysis, the membership functions corresponding to the time of realisation of individual transport stages should be determined. Then, based on fuzzy values of individual transport stages, it will be possible to determine the transport route ensuring the shortest implementation. In addition, it will be

possible to identify places of potential downtime and congestion. It is worth noting that instead of fuzzy numbers, one can use random variables describing the stages of transport. However, using the expected value of a random variable, being the sum of variables corresponding to particular stages is not the best solution. It seems reasonable to determine the extremely favourable and extremely unfavourable course of the goods transport process.

3. Defining the membership function based on empirical data

In order to increase the transparency of considerations in the first stage of the construction of the supply chain management model, it is assumed that the membership functions have a trapezoidal (in particular, triangular) form. With empirical values of the duration of individual stages of the supply chain, membership functions can be determined.

Let us assume that we have N real values of the duration of the k-th stage of the supply chain implementation. Let us denote these values by $X_1^k, X_2^k, \dots, X_N^k$. Let us also introduce the variables Y_i^k specifying the number of occurrences of each value

$$Y_i^k = \sum_{j=1}^{N} \mathbf{1}\left(X_i^k = X_j^k\right),$$

where $\mathbf{1}\left(X_i^k = X_j^k\right)$ denotes a characteristic function. It is therefore necessary to specify the function $f_k(x)$ in such a way as to minimise the value of the expression

$$\sum_{i=1}^{N} \left| f\left(X_i^k\right) - \frac{Y_i^k}{\tau} \right|,$$

where $\tau \leq \max_{1 \leq i \leq N} Y_i^k$ is a normative constant.

The optimisation issue put in this way amounts to determining 5 constants $a, b, c, d, \tau \in R$ such that $a < b \leq c < d$. A graphic representation of this issue is presented in Fig. 2.

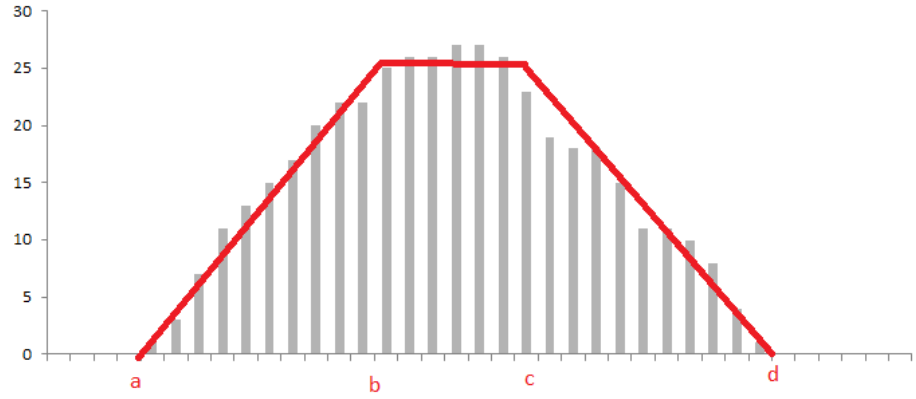

Fig. 2. Visualisation of the problem of determining the membership function based on empirical data

One of the simplest and immediately very effective methods of solving this type of issues is the use of the Particle Swarm Optimisation PSO [24] method. The PSO algorithm employs a swarm of people which is a multidimensional search space to seek out optima. Each of them is neighbour as well as itself (see reviews [36, 48, 51] for more detail). In this particular issue, the elements of the five-dimensional space $\theta^j = (\theta_1, \theta_2, \theta_3, \theta_4, \theta_5) \in R^5$ are considered. In *i*th iteration (*i*>0) a new direction of motion for each *j*th of the object is determined in accordance with the formula

$$\Delta_i = \Delta_{i-1} + \rho_1 \cdot \left(\theta_{lbest} - \theta^j\right) + \rho_2 \cdot \left(\theta_{gbest} - \theta^j\right)$$

where θ_{lbest} means the best position of the *j*th element in the previous history, and θ_{gbest} means the best position so far determined by the entire swarm. The new position of the object is determined by moving the object in accordance with the designated direction. Having empirical fuzzy values of individual stages, one can model the transport time of goods on the basis of additional data from the data warehouse. It is possible to specify different variants of the duration of transport of goods from the most optimistic to the most pessimistic at different levels of α-cutting. In addition, one can determine the impact of weather, social and economic conditions on the time and cost of transporting goods.

4. The concept of the model

The project will develop a model supporting the management a fleet of cars, trains and ships. The network of existing and planned sea and rail connections is presented in Fig. 3.

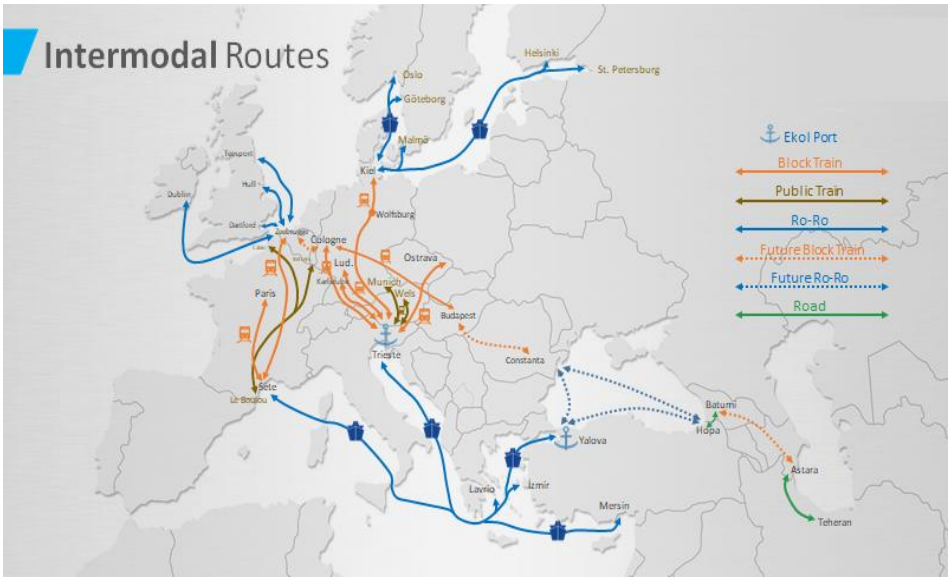

Fig. 3. A transport base used by a business partner. In the drawing, currently used as well as planned transport channels are marked. Source: Chist-Era demonstration materials

During the development of the model, a number of factors (Fig. 4) will be taken into account that affect the time and cost of transport. It is necessary to take into account the variability of physical factors, the human factor and other components.

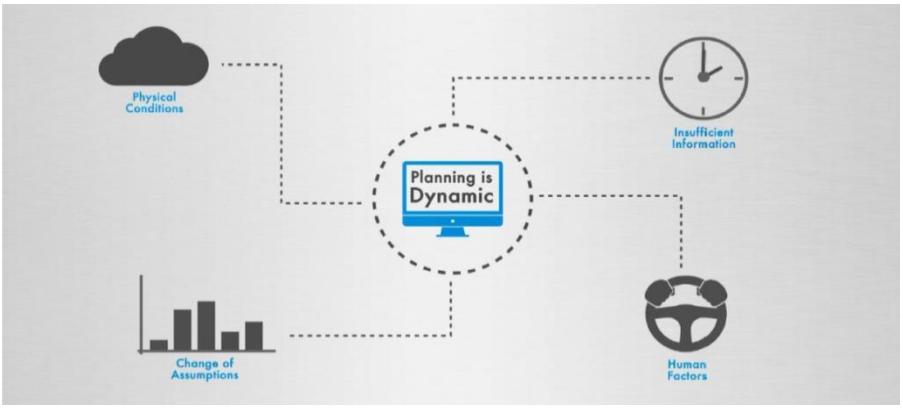

Fig. 4. Factors dynamically affecting the model. Source: Chist-Era demonstration materials

The developed model will use many sources of information to be able to react quickly to any changes and tune in to the needs. Thanks to access to various sources of information, from data warehouses, through the transport management system to the possibilities offered by continuous GPS and mobile telephony supervision (see Fig. 5), it will be possible to develop a theoretical model that the company will be able to implement in the future.

Fig. 5. Planned data sources used during the construction of the model. Source: Chist-Era demonstration materials

Acknowledgments. Funded by the National Science Centre, Poland under CHIST-ERA programme, grant no. 2018/28/Z/ST6/00563.

Bibliography

[1] Ahi P., Searcy C., 2013. A comparative literature analysis of definitions for green and sustainable supply chain management. Journal of cleaner production, 52: 329–341.

[2] Akhtar P., Tse Y. K., Khan Z., Rao-Nicholson R., 2016. Data-Driven and Adaptive Leadership Contributing to Sustainability: Global Agri-Food Supply Chains Connected with Emerging Markets. International Journal of Production Economics, 181: 392–401.

[3] Alumur S. A., Yaman H., Kara B. Y., 2012. Hierarchical multimodal hub location problem with time-definite deliveries. Transportation Research Part E: Logistics and Transportation Review, 48(6): 1107–1120.

[4] Arnold P., Peeters D., Thomas I., 2004. Modelling a rail/road intermodal transportation system. Transportation Research Part E: Logistics and Transportation Review, 40(3): 255–270.

[5] Arntzen B. C., Brown G. G., Harrison T. P., Trafton L. L., 1995. Global supply chain management at Digital Equipment Corporation. Interfaces, 25(1): 69–93.

[6] Bierwirth C., Kirschstein T., Meisel F., 2012. On transport service selection in intermodal rail/road distribution networks. Business Research, 5(2): 198–219.

[7] Birasnav M., 2013. Implementation of Supply Chain Management Practices: The Role of Transformational Leadership. Global Business Review, 14(2): 329–342.

[8] Birasnav M., Mittal R., Loughlin S., 2015. Linking Leadership Behaviors and Information Exchange to Improve Supply Chain Performance: A Conceptual Model. Global Journal of Flexible Systems Management, 16(2): 205–217.

[9] Brandenburg M., Govindan K., Sarkis J., Seuring S., 2014. Quantitative models for sustainable supply chain management: Developments and directions. European Journal of Operational Research, 233(2): 299–312.

[10] Carter C. R., Liane Easton P., 2011. Sustainable supply chain management: evolution and future directions. International Journal of Physical Distribution and Logistics Management, 41(1): 46–62.

[11] Chang T. S., 2008. Best routes selection in international intermodal networks. Computers and Operations Research, 35(9): 2877–2891.

[12] Choong S. T., Cole M. H., Kutanoglu E., 2002. Empty container management for intermodal transportation networks. Transportation Research Part E: Logistics and Transportation Review, 38(6): 423–438.

[13] Cordeau J. F., Pasin F., Solomon M. M., 2006. An integrated model for logistics network design. Annals of operations research, 144(1): 59–82.

[14] Da Cruz V. de J. S., Paulillo L. F., 2016. Hybrid Governance Complementary to Contract Manufacturing: A Study Case. Gestão and Produção, 23(4): 842–852.
[15] Erera A. L., Morales J. C., Savelsbergh M., 2005. Global intermodal tank container management for the chemical industry. Transportation Research Part E: Logistics and Transportation Review, 41(6): 551–566.
[16] Feng Y., Zhu Q., Lai K. H., 2017. Corporate social responsibility for supply chain management: A literature review and bibliometric analysis. Journal of Cleaner Production, 158: 296–307.
[17] Goffnett S. P., Goswami A., 2016. Supply Chain Transformational Leadership, Supply Chain Innovation Performance, and Satisfaction with Relationships and Results: Moderating Role of Supply Chain Innovativeness. International Journal of Logistics Systems and Management, 24(3): 356–382.
[18] Gold S., Seuring S., Beske P., 2010. Sustainable supply chain management and inter-organizational resources: a literature review. Corporate Social Responsibility and Environmental Management, 17(4): 230–245.
[19] Groothedde B., Ruijgrok C., Tavasszy L., 2005. Towards collaborative, intermodal hub networks: A case study in the fast moving consumer goods market. Transportation Research Part E: Logistics and Transportation Review, 41(6): 567–583.
[20] Hammami R., Frein Y., Hadj-Alouane A. B., 2012. An international supplier selection model with inventory and transportation management decisions. Flexible Services and Manufacturing Journal, 24(1): 4–27.
[21] Hartmann J., Moeller S., 2014. Chain liability in multitier supply chains? Responsibility attributions for unsustainable supplier behavior. Journal of Operations Management, 32(5): 281–294.
[22] Hong J., Zhang Y., Ding M., 2018. Sustainable supply chain management practices, supply chain dynamic capabilities, and enterprise performance. Journal of Cleaner Production, 172: 3508–3519.
[23] Ishfaq R., Sox C. R., 2010. Intermodal logistics: The interplay of financial, operational and service issues. Transportation Research Part E: Logistics and Transportation Review, 46(6): 926–949.
[24] Kennedy J., 2010. Particle swarm optimization. Encyclopedia of Machine Learning, 760–766.
[25] L'Hermitte C., Tatham P., Bowles M., Brooks B., 2016. Developing Organisational Capabilities to Support Agility in Humanitarian Logistics. Journal of Humanitarian Logistics and Supply Chain Management, 6(1): 72–99.
[26] Lawley M., Parmeshwaran V., Richard J. P., Turkcan A., Dalal M., Ramcharan D., 2008. A time-space scheduling model for optimizing recurring bulk railcar deliveries. Transportation Research Part B: Methodological, 42(5): 438–454.

[27] Limbourg S., Jourquin B., 2009. Optimal rail-road container terminal locations on the European network. Transportation Research Part E: Logistics and Transportation Review, 45(4): 551–563.
[28] McAdam R., Brown L., 2001. Strategic Alignment and the Supply Chain for the Steel Stockholder Sector: An Exploratory Case Study Analysis. Supply Chain Management: An International Journal, 6(2): 83–95.
[29] Melnyk S. A., Lummus R. R., Vokurka R. J., Burns L. J., Sandor J., 2009. Mapping the Future of Supply Chain Management: A Delphi Study. International Journal of Production Research, 47(16): 4629–4653.
[30] Meng Q., Wang X., 2011. Intermodal hub-and-spoke network design: incorporating multiple stakeholders and multi-type containers. Transportation Research Part B: Methodological, 45(4): 724–742.
[31] Mzembe A. N., Lindgreen A., Maon F., Vanhamme J., 2016. Investigating the Drivers of Corporate Social Responsibility in the Global Tea Supply Chain: A Case Study of Eastern Produce Limited in Malawi. Corporate Social Responsibility and Environmental Management, 23(3): 165–178.
[32] Newman A. M., Yano C. A., 2000. Scheduling direct and indirect trains and containers in an intermodal setting. Transportation Science, 34(3): 256–270.
[33] Perron S., Hansen P., Le Digabel S., Mladenović N., 2010. Exact and heuristic solutions of the global supply chain problem with transfer pricing. European Journal of Operational Research, 202(3): 864–879.
[34] Racunica I., Wynter L., 2005. Optimal location of intermodal freight hubs. Transportation Research Part B: Methodological, 39(5): 453–477.
[35] Robinson A. G., Bookbinder J. H., 2007. NAFTA supply chains: facilities location and logistics. International Transactions in Operational Research, 14(2): 179–199.
[36] Sengupta S., Basak S., Peters R., 2018. Particle Swarm Optimization: A survey of historical and recent developments with hybridization perspectives. Machine Learning and Knowledge Extraction, 1(1): 157–191.
[37] Seuring S., Gold S., 2012. Conducting content-analysis based literature reviews in supply chain management. Supply Chain Management: An International Journal, 17(5): 544–555.
[38] Sinha N., Garg A. K., Dhall N., 2016. Effect of TQM Principles on Performance of Indian SMEs: The Case of Automotive Supply Chain. The TQM Journal, 28(3): 338–359.
[39] Sörensen K., Vanovermeire C., Busschaert S., 2012. Efficient metaheuristics to solve the intermodal terminal location problem. Computers and Operations Research, 39(9): 2079–2090.
[40] Szekely F., Strebel H., 2013. Incremental, Radical and Game-Changing: Strategic Innovation for Sustainability. Lenssen G., Painter M., and Ion A., eds., Corporate Governance: The International Journal of Business in Society, 13(5): 467–481.

[41] Taylor G. D., Broadstreet F., Meinert T. S., Usher J. S., 2002. An analysis of intermodal ramp selection methods. Transportation Research Part E: Logistics and Transportation Review, 38(2): 117–134.
[42] Thornton L. D. M., Esper T. L., Autry C. W., 2016. Leader or Lobbyist? How Organizational Politics and Top Supply Chain Manager Political Skill Impacts Supply Chain Orientation and Internal Integration. Journal of Supply Chain Management, 52(4): 42–62.
[43] Touboulic A., Walker H., 2015. Theories in sustainable supply chain management: a structured literature review. International Journal of Physical Distribution and Logistics Management, 45(1/2): 16–42.
[44] Tuomikangas N., Kaipia R., 2014. A Coordination Framework for Sales and Operations Planning (SandOP): Synthesis from the Literature. International Journal of Production Economics, 154: 243–262.
[45] Verma M., Verter V., Zufferey N., 2012. A bi-objective model for planning and managing rail-truck intermodal transportation of hazardous materials. Transportation Research Part E: Logistics and Transportation Review, 48(1): 132–149.
[46] Vidal C. J., Goetschalckx M., 2001. A global supply chain model with transfer pricing and transportation cost allocation. European Journal of Operational Research, 129(1): 134–158.
[47] Vivaldini M., Pires S. R. I., 2016. Sustainable Logistical Operations: The Case of McDonald's Biodiesel in Brazil. International Journal of Logistics Systems and Management, 23(1): 125.
[48] Wei Y., Qiqiang L., 2004. Survey on Particle Swarm Optimization Algorithm, Engineering Science, 5(5): 87–94.
[49] Wilhelm W., Liang D., Rao B., Warrier D., Zhu X., Bulusu S., 2005. Design of international assembly systems and their supply chains under NAFTA. Transportation Research Part E: Logistics and Transportation Review, 41(6): 467–493.
[50] Yuen K. F., Thai V., 2017. Barriers to Supply Chain Integration in the Maritime Logistics Industry Oa. Maritime Economics and Logistics, 19(3): 551–572.
[51] Zhang Y., Wang S., Ji G., 2015. A comprehensive survey on particle swarm optimization algorithm and its applications. Mathematical Problems in Engineering.

Edyta Łukasik[1], Maria Skublewska-Paszkowska[2], Małgorzata Charytanowicz[3]

Nonparametric density estimation for human motion tracking

Abstract: In today's world, human motion tracking has truly emerged as a vivid research area. This relates to the task of analyzing the movement of a person over time, using the data obtained by a motion capture device. The results obtained via a motion capture system allow clear identification of the degree of training of the subjects studied, their technique and level of movement efficiency. In our study, a motion capture system (Vicon, Oxford Metrics Ltd., UK) was used to register the three-dimensional movement of rowers. The study was performed on the Concept II Indoor Rower ergometer. The sample population was a group of ten non-rowers and a professional rower. The main aim of the study was to construct a mathematical model for analysing the speed and accuracy of the rowing technique. The method presented here is based on the theory of kernel density estimation. The approach is universal, and it can be successfully applied for many tasks in human motion tracking where arbitrary assumptions concerning the form of regression function are not recommended.

Keywords: mathematical modelling, nonparametric regression, kernel estimators, kernel regression, ergometer rowing, motion capture

1. Introduction

Today, modern technologies are an important element supporting effective training of athletes. Three-dimensional analysis systems provide the opportunities for a global quantitative assessment of rowers' performance. Motion capture systems are very precise and, therefore, widely used in medicine, sport (athlete performance) and entertainment. Such systems are convenient for studying body movements and forces. Analysis of recorded and post-processed 3D data provides information about the many biomechanical parameters of athletic performance. One possibility is applying a motion capture system to capture the movement of competitive rowers. Precise analysis of the trajectories of individual body parts, by defining qualitative and quantitative measures, permits the assessment of the rower's fitness level from the point of view of the correctness of the motor technique [20].

[1] Edyta Łukasik, Institute of Computer Science, Lublin University of Technology, Poland
[2] Maria Skublewska-Paszkowska, Institute of Computer Science, Lublin University of Technology, Poland
[3] Małgorzata Charytanowicz, Institute of Computer Science, Lublin University of Technology, Poland; Systems Research Institute, Polish Academy of Sciences, Warsaw, Poland

Indoor rowing is a sport discipline developed in the academic environment. Water rowers use ergometers off season to maintain the correct body condition. The biomechanical parameters and the movement effectiveness and efficiency of rowers' legs, hands and spine have been widely researched. In this study, a motion capture system (Vicon, Oxford Metrics Ltd., UK) was used to register the three-dimensional movement of rowers. The study was performed on the Concept II Indoor Rower ergometer. The Plug-in Gait biomechanical model was used to calculate a number of various parameters, including angles, moments and forces in the joints of a subject. The use of motion capture systems allows for a quantitative analysis that cannot be noticed by a trainer and setting the level of a rower's technique, which is important for achieving better results and performance [26], and is done on the basis of analysis of parameter changes measured in successive phases of physical activity. The basic biomechanical parameters that characterise the ergometer rowing technique are the stroke length, the duration and ratio of the stroke phases, the forces of the stroke on the handle and foot stretcher, the power of the stroke, the trajectory of the handle motion and the body posture and the body joint loads [6, 19, 20].

Movement patterns are important factors in sport [7, 22]. Specific kinetic variables that influence technique are worth investigating from the coach's perspective. The use of mathematical modelling aims at creating a pattern for a selected athlete's movement or parameter. Cyclic activities in rowing strokes where technique affects performance output are worth knowing and being described mathematically.

Modern up-to date equipment allows to obtain detailed kinematics and kinetics analysis, but it is very hard to interpret such vast amounts of raw data [2]. Applying nonparametric regression may simplify this process.

Mathematical modelling was used to describe the changes in the rowing technique and to determine the participant's abilities with and without back pain [21]. Hence, a hypothesis was posed that the rowing stroke technique is associated with the incidence of low back pain. Thus, the authors applied the multivariate logistic regression analysis to examine the relationship between the linear stroke model parameters for healthy participants and those suffering from low back pain. For the purpose of the research, four phases of the ergometer were used: load, forward motion, torsion contrast and roll contrast. A two-variable model was created for assessing the relationship between the low back pain history and the mean of the stroke parameters concerning the skewness of the load profile and forward motion position variable. The obtained results showed a significant difference between the stroke characteristics for two groups of participants. The hypothesis, therefore, was proved correct.

The mathematical model with regression may also be applied to assess the prediction of young people for a specified sport discipline, including indoor rowing. The model of regression of multiple variables of the 2nd degree to determine correlations between selected somatic traits and indoor rowing test

results over a distance of 500 m was proposed in [8]. It described the effects of the decisive variables on the dependent variable. The correlation concerned time required to cover the ergometer distance of 500 m, body height and body weight.

The second degree polynomial regression model was also applied to verify factors such as the subjects' mass and height, CPI value (height/body mass ratio), BMI index and the female students' slenderness ratios and their influence into the time of covering the 500 m distance [23]. The results of the research stated that repetition of the exercise lowered the mean time of covering the 500 m distance on a rowing ergometer (based on the results obtained between the 1st and the 10th trial). This decreased by ca. 15-20s.

Prediction of the rowing performance has been the subject of much research. Five various prediction models of 200 m ergometer rowing which used anthropometric measurement results, strength test results, anaerobic power test results, combination of the strength and anaerobic power and combination of all measurement categories were applied in [1]. Reliability of the regression models was expressed by R^2 and the standard error of estimate (SEE). The multiple regression model to predict 2000 m indoor rowing performance time from sprint performance, maximal oxygen uptake and the blood lactate response to submaximal rowing is presented in [25]. 30 seconds of female rowing spring test data was used, while maximal and minimal powers, percent fatigue in the sprint test and maximal oxygen uptake were taken into consideration to define the model. The prediction of the performance speed expressed as meters by seconds, for 200 m ergometer rowing is presented in [28]. The model included power at VO2max, VO2 at the blood lactate threshold, concentration of blood lactate and maximal power. Together, this explained 98% of the variance in the rowing performance over 2000 m on an ergometer. The model was validated by 18 elite rowers.

The research concerning the selection of the correct formula to evaluate anthropometric characteristics as determinants for 500 m ergometer rowing is described in [24]. In it, stepwise multiple regression analysis was performed for the purpose of the research. The study population consisted of 196 female student-athletes. The students' year of studies, body height and mass, and upper and lower limb length were taken into consideration.

The study concerning the examination of lower limb kinematic asymmetries and their consequent impact on lumbar-pelvic kinematics during varying intensities of ergometer rowing and between rowers of varying standards is presented in [3]. For the purpose of the research a multiple linear regression model was used. Regression analysis indicated that both hip and knee ROM asymmetries were significant in predicting the lumbar-pelvic flexion.

The research concerning the establishment of strength, power and muscular endurance exercises for weight room training (which are strong determinants of success in specific performance measures used to assess elite rowers) is presented in [18]. Two-factor linear regression and Pearson correlation moments

were used to establish strong common variances between weight room exercises and rowing ergometer performance. The analysis confirmed the greater specificity of ergometer over weight room dynamometer data or free weight exercise in the determination of rowing peak stroke power in 500 m and 2000 m performance.

The mathematical models presenting the interaction of data obtained from rigid systems and their influence on special efficiency rowers are showed in [15]. In the study, aerobic-anaerobic capacity, mobility-stability and capacity-profitability were taken into consideration. The regression equations used allowed to carry out an estimation of the functional condition of the rowers, as well as modelling of its different variants to achieve a programmed result at the stage of maximum realisation of individual capabilities.

A one-dimensional mathematical model of rowing was implemented to analyse the single sculling concerning learning, improvement and motion techniques optimisation [30]. It describes the hydrodynamic and aerodynamic forces that affect the physical model of rowing. Furthermore, it takes into account wind and water currents on the regatta outcome. The best regatta result was obtained for the rotation range of the oars located maximally in front of the boat.

Work [2] verified whether a crew's rowing performance was predictable from the total propulsive power, synchrony and total drag contribution using retrogression analysis. The research showed, however, that a crew's performance cannot be predicted by the linear model presented in the paper.

The aim of the study is construction of a mathematical model to estimate the parameters of the rowers' movement. The proposed method is kernel regression estimator. The modelling was performed using a mathematical method applying the fitting of a nonparametric regression function for analysing the speed and accuracy of the rowing technique. The analysis was carried out on professional and non-professional rower motion 3D data.

The method presented here, an effective transparent tool for modelling motion tracking, is based on the theory of statistical kernel estimators. The results were compared with results obtained for another four parametric models. The proposed methodology can allow examination of the repeatability of the rowers' movements and determine their progress in training. Such an approach has not been found in the established literature by the authors of this study.

2. Mathematical concepts

Classical parametric methods of determining an appropriate functional relationship between two variables: a response variable Y and one or more predictor variables X, impose certain arbitrary assumptions with regard to the functional form of the regression function. The rigidity of these methods can, however, be overcome by using nonparametric regression methods. These will

allow the accommodation of more complex regression curves without specifying the relationship between Y and X by way of a predetermined regression function.

2.1. Nadaraya-Watson estimator

Let $m: R^d \to R$ be the regression function (for the simplicity let $d = 1$) to estimate i.e.

$$m(X) = E(Y|X). \tag{1}$$

Alternatively it can be written in the form

$$Y = m(X) + \varepsilon, \tag{2}$$

where $E(\varepsilon) = 0$. We usually assume that $Var(Y|X) = \sigma^2(X)$ where $\sigma(\cdot)$ is a continuous and bounded function. The regression function can be computed from the joint density f and the marginal f_X.

$$E(Y|X = x) = \int y f_{Y|X=x}(y)\mathrm{d}y = \int \frac{y f(x,y)}{f_X(x)}\mathrm{d}y \tag{3}$$

Given n independent observations $(x_i, y_i) \in R \times R$, $i = 1, 2, \ldots, n$, where values x_i may designate some non-random numbers or realisations of the one-dimensional random variable X, whereas y_i designates realisations of the one-dimensional random variable Y; nonparametric estimate of m may follow by replacing the previous densities by their kernel density estimators [27], [29]:

$$\widehat{f}(x,y) = \frac{1}{nh_1h_2}\sum\nolimits_{i=1}^{n} K_1\left(\frac{x-x_i}{h_1}\right)K_2\left(\frac{y-y_i}{h_2}\right) \tag{4}$$

$$\hat{f}(x) = \frac{1}{nh_1}\sum_{i=1}^{n} K_1\left(\frac{x-x_i}{h_1}\right) \tag{5}$$

where the positive coefficients h_1, h_2 are called bandwidths, while the measurable functions $K_1: R \to [0, \infty)$ and $K_2: R \to [0, \infty)$ of unit integrals, symmetrical with respect to zero and having weak global maxima in this place, take the name of kernels [27], [29]. Thus, we have

$$\hat{E}(Y|X = x) = \int y \frac{\frac{1}{nh_1h_2}\sum_{i=1}^{n} K_1\left(\frac{x-x_i}{h_1}\right)K_2\left(\frac{y-y_i}{h_2}\right)}{\frac{1}{nh_1}\sum_{i=1}^{n} K_1\left(\frac{x-x_i}{h_1}\right)}\mathrm{d}y \tag{6}$$

$$= \frac{\frac{1}{nh_1h_2}\sum_{i=1}^{n} K_1\left(\frac{x-x_i}{h_1}\right)\int y K_2\left(\frac{y-y_i}{h_2}\right)\mathrm{d}y}{\frac{1}{nh_1}\sum_{i=1}^{n} K_1\left(\frac{x-x_i}{h_1}\right)} = \frac{\sum_{i=1}^{n} K_1\left(\frac{x-x_i}{h_1}\right)y_i}{\sum_{i=1}^{n} K_1\left(\frac{x-x_i}{h_1}\right)}.$$

Finally, replacing K_1 and h_1 in (6) by K and h, the resulting estimator is defined as

$$\widehat{m}_h(x) = \frac{\sum_{i=1}^{n} K\left(\frac{x-x_i}{h}\right) y_i}{\sum_{i=1}^{n} K\left(\frac{x-x_i}{h}\right)} \tag{7}$$

and is called the Nadaraya-Watson estimator. Most often, a kernel function K is usually taken to be a symmetric probability density such as a normal density:

$$K(x) = \frac{1}{\sqrt{2\pi}} e^{-\frac{x^2}{2}}. \tag{8}$$

For the bandwidth selection problem, the averaged squared error

$$\mathrm{ASE}(h) = \sum_{i=1}^{n}\left(m(x_i) - \widehat{m}_h(x_i)\right)^2 \tag{9}$$

is used as the criterion for goodness of fit. The unknown function values $m(x_i)$ are replaced by the observations y_i which yields the residual sum of squares

$$\mathrm{RSS}(h) = \sum_{i=1}^{n}\left(y_i - \widehat{m}_h(x_i)\right)^2 \tag{10}$$

However, an appropriate estimation of ASE is obtained by the cross-validation criterion

$$\mathrm{CV}(h) = \sum_{i=1}^{n}\left(y_i - \widehat{m}_{h,-i}(x_i)\right)^2 \tag{11}$$

where $\widehat{m}_{h,-i}(\cdot)$ denotes the regression estimator (7) which is obtained without using the i-th observation (x_i, y_i). For further calculations, it can be shown in [12] that

$$\mathrm{CV}(h) = \sum_{i=1}^{n}\left(y_i - \widehat{m}_h(x_i)\right)^2 \aleph(W_{h,i}(x_i)) \tag{12}$$

where $\aleph(u) = (1-u)^{-2}$ and $W_{h,i}(x_i) = K(0)/\sum_{j=1}^{n} K\left(\frac{x_j-x_i}{h}\right)$.

2.2. Local polynomial kernel density estimators

The Nadaraya-Watson estimator described in Section 2.1 is a local constant estimator, which minimises

$$\min_{\beta_0} \sum_{i=1}^{n} (y_i - \beta_0)^2 K\left(\frac{x_i - x}{h}\right) \tag{13}$$

Replacing β_0 by a p-th order polynomial in $x_i - x$ yields the local polynomial kernel regression estimator. If we let $p \in N$ be the degree of the polynomial's fit, the minimalisation problem is:

$$\min_{\beta} \sum_{i=1}^{n} \left(y_i - \beta_0 - \beta_1 (x_i - x) - \cdots - \beta_p (x_i - x)^p\right)^2 K\left(\frac{x_i - x}{h}\right) \tag{14}$$

where $\beta = [\beta_0, \beta_1, \ldots, \beta_p]^{\mathrm{T}}$. This leads to the solution:

$$\hat{\beta} = \left(X^{\mathrm{T}} W X\right)^{-1} X^{\mathrm{T}} W Y, \tag{15}$$

where $Y = [y_1, y_2, \ldots, y_n]^{\mathrm{T}}$ is the vector of responses,

$$X = \begin{bmatrix} 1 & x_1 - x & (x_1 - x)^2 & \cdots & (x_1 - x)^p \\ 1 & x_2 - x & (x_2 - x)^2 & \cdots & (x_2 - x)^p \\ \vdots & \vdots & \vdots & \ddots & \vdots \\ 1 & x_n - x & (x_n - x)^2 & \cdots & (x_n - x)^p \end{bmatrix}, \tag{16}$$

and is a $n \times (p + 1)$ design matrix, and

$$W = diag\left(K\left(\frac{x_1 - x}{h}\right), K\left(\frac{x_2 - x}{h}\right), \ldots, K\left(\frac{x_n - x}{h}\right)\right). \tag{17}$$

is a $n \times n$ diagonal matrix of kernel weights. Since the estimator of $m(x)$ is computed as:

$$\hat{m}_{h,p}(x) = e_1^{\mathrm{T}} \left(X^{\mathrm{T}} W X\right)^{-1} X^{\mathrm{T}} W Y, \tag{18}$$

here, e_1 is the $(p + 1) \times 1$ vector having 1 in the first entry and zero elsewhere, i.e. $e_1 = [1, 0, \ldots, 0]^{\mathrm{T}}$.

For sufficiently smooth regression functions, the asymptotic performance of $\hat{m}_{h,p}(\cdot)$ improves for higher values of p. However, for higher p, the variance of the estimator becomes larger, and in practice, a very large sample may be required. Therefore, two cases deserve special attention: $p = 0$ and $p = 1$. For

$p = 0$, the Nadaraya-Watson estimator (7) is obtained, and for $p = 1$, the convenient explicit formula for the local linear estimator exists as:

$$\hat{m}_{h,1}(x) = \frac{1}{nh}\sum_{i=1}^{n} \frac{(\hat{s}_2(x;h) - \hat{s}_1(x;h)(x_i - x))y_i K\left(\frac{x_i - x}{h}\right)}{\hat{s}_2(x;h)\hat{s}_0(x;h) - (\hat{s}_1(x;h))^2}, \tag{19}$$

where

$$\hat{s}_r(x;h) = \frac{1}{nh}\sum_{i=1}^{n}(x_i - x)^r K\left(\frac{x_i - x}{h}\right) \quad \text{for} \quad r = 0, 1, 2. \tag{20}$$

Because the kernel K is symmetric, we could write $K\left(\frac{x - x_i}{h}\right)$ rather than $K\left(\frac{x_i - x}{h}\right)$ for the kernel density estimator.

The tasks concerning the choice of the kernel and the bandwidth, as well as additional procedures improving the quality of the estimator obtained, can be found in [27, 29]. Examples of practical applications are described in [5, 6], [16, 17]. The computational aspects are considered in [11].

3. Material and methods

Regression analysis seems to be an important tool for testing the rowing technique. The validation of the efficiency and accuracy of regression methods for characterising the drive phase velocity of rowers was explored by comparing the results on a variety of rower movement data. Both the presented nonparametric kernel regression and several parametric regression models [9] were examined as far as the velocity of drive phases of rowers was concerned.

3.1. Participants

In our study, the sample population involved ten male non-professional rowers (age 39.36±11.12, BMI 24.72±1.91) (NR) and one professional (master) rower (MR) (age 29, BMI 24.2) belonging to the Academic Sports Association (AZS) at the Lublin University of Technology (LUT). The non-professional rowers were employees of LUT. All participants in the experiment were briefed about the study and signed the consent form.

3.2. Motion capture system

The participants' movement were recorded using a passive optical motion capture system (Vicon, Oxford Metrics Ltd., UK), which consisted of eight T40S near infrared cameras. Additionally, two Bonita video cameras were used. The reference video may be used both for data post-processing and for generating video files with a biomechanical model overlay. All cameras were

connected to a Giganet hub that collected all the data and transferred this into a computer. The frequency of the system was set to 100 Hz. The research was conducted in a shaded room (without windows) so that no additional reflections appeared, which might affect the quality of the data obtained.

The equipment was supplied with Vicon Nexus 2.0 software, used for system calibration, data recording and data processing. The system recorded the positions of the markers placed on the subject's body (each marker must be seen by at least two cameras).

The obtained three-dimensional data were post-processed in Vicon Nexus 2.0 using the implemented interpolation methods embedded into the software. Each marker was properly labelled, the trajectory gaps were filled-in, the redundant markers were deleted and the biomechanical model was applied. These data were read by the piece of software written in the C++ language with the use of the Eigen library and the biomechanical toolkit, b-tk 0.3.0. The GCC 4.8.5 suite was used for building executables from the source code. For each of the two phases of stroke: drive and recovery, the program computed values such as the number of strokes, duration of stroke, speed, angle of inclination in two planes (transversal and frontal) and angle of the participant's back – also in two planes (frontal and sagittal).

3.3. Methods

Each participant was prepared for the examination. Thirty-nine 14-milimeter-retroreflective markers were attached directly to the skin using double-sided hypoallergenic tape according to the Plug-in Gait biomechanical model. This model, properly applied, can calculate a number of different measures of a biomechanical model, including angles, moments and forces in the joints of a subject. All markers and their descriptions are presented in Table 1. Additionally, two more markers (named S1, S2) were put on the spine in order to better examine the subject's posture (Figure 1). The participant was measured for the purpose of creating and scaling a new subject in the Vicon Nexus software. The measured dimensions were: height, weight, leg length, arm offset, knee, ankle, elbow and the thickness of both hands. The subject's calibration was performed as the next step of the preparation. The participant stood in a "motorbike" pose that was then captured. Apart from calibration, this procedure is important because it verifies the markers' visibility and placement. The model of each participant was created and calibrated. Three retroreflective markers for indicating the handle trajectory were placed on the handle. They are marked MR1, MR2 and MR3 in Figure 2.

Table 1. Markers and their positions on the subject's body [10]

Marker name	Position	Description
Upper body		
LFHD	Left front head	Left temple
RFHD	Right front head	Right temple
LBHD	Left back head	Left back of head (defines the transverse plane of the head, together with the frontal markers)
RBHD	Right back head	Right back of head (defines the transverse plane of the head, together with the frontal markers)
C7	7th cervical vertebra	On the spinous process of the 7th cervical vertebra
T10	10th thoracic vertebra	On the spinous process of the 10th thoracic vertebra
CLAV	Clavicle	On the jugular notch where the clavicles meet the sternum
STRN	Sternum	On the xiphoid process of the sternum
RBAK	Right back	Anywhere over the right scapula (This marker has no equivalent marker on the left side. This asymmetry helps the autolabelling routine determine right from left on the subject. Placement is not critical as it is not included in the Plug-in Gait model calculations.)
LSHO	Left shoulder	On the acromio-clavicular joint
LUPA	Left upper arm	On the upper lateral 1/3 surface of the left arm (Place asymmetrically with RUPA)
LELB	Left elbow	On the lateral epicondyle
LFRM	Left forearm	On the lower lateral 1/3 surface of the left forearm (Place asymmetrically with RFRM)
LWRA	Left wrist marker A	At the thumb side of a bar attached to a wristband on the posterior of the left wrist, as close to the wrist joint centre as possible. Loose markers can be used, but for better tracking of the axial rotations, a bar is recommended.
LWRB	Left wrist marker B	At the little finger side of a bar attached to a wristband on the posterior of the left wrist, as close to the wrist joint centre as possible. Loose markers can be used, but for better tracking of the axial rotations, a bar is recommended.
LFIN	Left finger	Just proximal to the middle knuckle on the left hand
RSHO	Right shoulder	On the acromio-clavicular joint
RUPA	Right upper arm	On the lower lateral 1/3 surface of the right arm (Place asymmetrically with LUPA)
RELB	Right elbow	On the lateral epicondyle approximating the elbow joint axis
RFRM	Right forearm	On the lower lateral 1/3 surface of the right forearm (Place asymmetrically with LFRM)

RWRA	Right wrist marker A	At the thumb side of a bar attached symmetrically with a wristband on the posterior of the right wrist, as close to the wrist joint centre as possible
RWRB	Right wrist marker B	At the little finger side of a bar attached symmetrically with a wristband on the posterior of the right wrist, as close to the wrist joint centre as possible
RFIN	Right finger	Just below the middle knuckle on the right hand
Lower body		
LASI	Left ASIS	Left anterior superior iliac spine
RASI	Right ASIS	Right anterior superior iliac spine
LPSI	Left PSIS	Left posterior superior iliac spine (immediately below the sacro-iliac joints, at the point where the spine joins the pelvis) This marker is used with the RPSI marker as an alternative to the single SACR marker
RPSI	Right PSIS	Right posterior superior iliac spine (immediately below the sacro-iliac joints, at the point where the spine joins the pelvis) This marker is used with the LPSI marker as an alternative to the single SACR marker
LTHI	Left thigh	Over the lower lateral 1/3 surface of the left thigh
LKNE	Left knee	On the flexion-extension axis of the left knee
LTIB	Left tibia	Over the lower 1/3 surface of the left shank
LANK	Left ankle	On the lateral malleolus along an imaginary line that passes through the transmalleolar axis
LHEE	Left heel	On the calcaneous at the same height above the plantar surface of the foot as the toe marker
LTOE	Left toe	Over the second metatarsal head, on the mid-foot side of the equinus break between fore-foot and mid-foot
RTHI	Right thigh	Over the upper lateral 1/3 surface of the right thigh
RKNE	Right knee	On the flexion-extension axis of the right knee.
RTIB	Right tibia	Over the upper 1/3 surface of the right shank
RANK	Right ankle	On the lateral malleolus along an imaginary line that passes through the transmalleolar axis
RHEE	Right heel	On the calcaneous at the same height above the plantar surface of the foot as the toe marker
RTOE	Right toe	Over the second metatarsal head, on the mid-foot side of the equinus break between fore-foot and mid-foot

Fig. 1. Distribution of markers on the rower's back [28]

Fig. 2. Three markers placed on the ergometer's handle [28]

First, the participants had a 10-minute warm up on the ergometer. Second, they were asked to row for 500 meters on the Concept II Indoor Rower ergometer at maximal speed. The built-in microprocessor system and Performance Monitor 4 (PM 4) allowed to control the effects of rowing in real time.

4. Results and discussion

In our research, various regression models were applied to characterise 500 meter rowing ergometer performance. The relationship of the drive phase number to the drive phase velocity of the stroke of the professional rower and ten non-professional rowers, identified by labels from 1 to 10, were considered. For the needs of the kernel regression, the Nadaraya-Watson kernel density estimator (7) with standard normal kernel (8) was used. The bandwidth was determined using the cross-validation method (11). The results were compared with results obtained for classical parametric models: linear, exponential, logarithmic and second degree polynomial [13]. The reliability of the regression models was expressed by the coefficient of determination R^2, which is defined as follows [28]:

$$R^2 = \frac{\left(\sum_{i=1}^{n}(y_i-\bar{y})(\hat{y}_i-\bar{y})\right)^2}{\sum_{i=1}^{n}(y_i-\bar{y})^2 \sum_{i=1}^{n}(\hat{y}_i-\bar{y})^2} \ , \tag{21}$$

where n is the sample size, y_i for $i = 1,2,\dots,n$ denote the outcomes and $\hat{y}_i$ represent the fitted values for observation i. This measure lies in the range [0, 1], with the value 1 denoting a perfect fit to the sample data and 0 denoting no predictive power above that given by the unconditional mean of the outcome.

Table 2 shows minimum and maximum values of drive phase velocity of the professional rower (Master) and ten non-professional rowers measured in their drive phases. In general, the drive phase velocity values of non-professional rowers are lower than that for the Master. The differences that exist between professional rowers and non-professional rowers in terms of rowing speed are obvious. In almost all cases, except Rower 7, the maximum values of non-professional rowers are lower than or comparable with the minimum value of the Master. For further analysis, it seems important to examine the rowing technique. Hence, regression analyses were employed to constitute prediction models describing the rowers' drive phase velocity individually.

Table 2. Minimum and maximum values of drive phase velocity of the professional rower and ten non-professional rowers.

Rower ID	Minimum [mm/s]	Maximum [mm/s]
Master	1841.60	2074.19
Rower 1	1378.58	1722.15
Rower 2	1327.08	1712.69
Rower 3	1215.66	1672.64
Rower 4	1295.60	1784.30
Rower 5	1480.40	1857.43
Rower 6	1260.42	1670.03
Rower 7	1382.12	1966.75
Rower 8	1427.96	1852.72
Rower 9	1372.31	1541.57
Rower 10	1143.00	1896.14

Table 3 shows the regression equations and coefficients of determination for regression functions describing the relationship of drive phase number to drive phase velocity of the professional rower and ten non-professional rowers. The first column contains the Rower ID instead of the regression equations. For all rowers, the model which resulted in the highest coefficient of determination R^2 is the nonparametric Nadaraya-Watson regression. This provides a more accurate estimation. Herein, R^2 varies from 0.70 to 0.96.

Table 3. The regression equations and coefficients of determination for regression functions describing the relationship of drive phase number x to drive phase velocity y of the examined rowers. The first column contains the Rower ID instead of the regression equations.

Regression model				
Nadaraya-Watson	linear	exponential	logarithmic	a second degree polynomial
Master $R^2 = 0.89$	$y = -1.94x + 2061.5$ $R^2 = 0.46$	$y = 2062.91\ \mathrm{e}^{-1\mathrm{E}-03x}$ $R^2 = 0.46$	$y = -21.82\ln x + 2066.4$ R^2 =0.13	$y = -1.11x^2 + 5.45x + 1976.5$ R^2 =0.88
Rower 1 $R^2 = 0.95$	$y = -5.47x + 1742.6$ $R^2 = 0.87$	$y = 1750.8\ \mathrm{e}^{-0.004x}$ R^2 =0.86	$y = -95.22\ln x + 1868.9$ R^2 =0.60	$y = -0.04x^2 - 2.71x + 1711.8$ R^2 =0.88
Rower 2 $R^2 = 0.88$	$y = -2.63x + 1598.8$ $R^2 = 0.50$	$y = 1598.1\ \mathrm{e}^{-0.002x}$ $R^2 = 0.49$	$y = -50.12\ln x + 1662.9$ R^2 =0.27	$y = 0.02x^2 - 4.37x + 1622.9$ R^2 =0.51
Rower 3 $R^2 = 0.95$	$y = -6.41x + 1686.7$ $R^2 = 0.81$	$y = 1701.1\ \mathrm{e}^{-0.004x}$ R^2 =0.81	$y = -120.7\ln x + 1850.3$ R^2 =0.52	$y = -0.03x^2 - 3.97x + 1655.8$ R^2 =0.82
Rower 4 $R^2 = 0.96$	$y = -5.03x + 1772.1$ $R^2 = 0.91$	$y = 1784.3\ \mathrm{e}^{-0.003x}$ R^2 =0.91	$y = -125.9\ln x + 1988.3$ R^2 =0.71	$y = -0.01x^2 - 4.38x + 1762.1$ R^2 =0.91
Rower 5 $R^2 = 0.71$	$y = -2.36x + 1804.4$ $R^2 = 0.45$	$y = 1807.1\ \mathrm{e}^{-0.001x}$ $R^2 = 0.45$	$y = -40.77\ln x + 1842.7$ $R^2 = 0.17$	$y = -0.59x^2 + 2.89x + 1725.7$ $R^2 = 0.59$
Rower 6 $R^2 = 0.95$	$y = -3.657x + 1636.1$ R^2 =0.51	$y = 1638.0\ \mathrm{e}^{-0.002x}$ R^2 =0.49	$y = -84.62\ln x + 1780.6$ R^2 =0.47	$y = 0.09x^2 - 10.79x + 1728.8$ R^2 =0.64
Rower 7 $R^2 = 0.93$	$y = -7.10x + 1948.2$ R^2 =0.89	$y = 1966.1\ \mathrm{e}^{-0.004x}$ R^2 =0.88	$y = -133.8\ln x + 2134.9$ R^2 =0.62	$y = -0.08x^2 - 1.50x + 1880.1$ R^2 =0.92
Rower 8 $R^2 = 0.79$	$y = -3.99x + 1822.3$ R^2 =0.40	$y = 1827.0\ \mathrm{e}^{-0.002x}$ R^2 =0.40	$y = -61.04\ln x + 1887.1$ R^2 =0.22	$y = -0.04x^2 - 1.28x + 1792.0$ R^2 =0.41
Rower 9 $R^2 = 0.70$	$y = -1.34x + 1515.5$ $R^2 = 0.43$	$y = 1516.1\ \mathrm{e}^{-9\mathrm{E}-04x}$ R^2 =0.43	$y = -18.07\ln x + 1524.5$ R^2 =0.13	$y = -0.05x^2 + 2.55x + 1464.4$ R^2 =0.67
Rower 10 $R^2 = 0.93$	$y = -7.43x + 1803.1$ $R^2 = 0.77$	$y = 1817.1\ \mathrm{e}^{-0.005x}$ R^2 =0.76	$y = -155.1\ln x + 2045.1$ R^2 =0.62	$y = 0.06x^2 - 12.17x + 1862.3$ R^2 =0.79

It is worth noting that in the case of the parametric models, the coefficient of determination R^2 varies from 0.41 to 0.92. Moreover, this is less than 0.70 for more than half of all examined regression equations. Here, the best fit into the regression model is that of a second degree polynomial for which R^2 varies from 0.41 to 0.92.

Further analysis of rower technique in relation to drive phase velocity was performed using nonparametric regression. Figure 3 and Figure 4 present the Nadaraya-Watson estimator of drive phase number to drive phase velocity for each rower. Observations are represented by circles

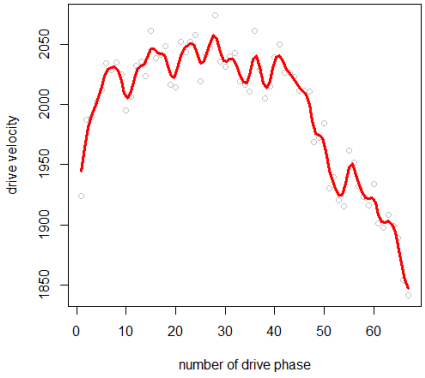

Fig. 3. The Nadaraya-Watson estimator of drive phase number to drive phase velocity of the professional rower. Observations are represented by circles

A relatively high level of drive phase velocity persistence over a longer period of examination is noticeable as far as the professional rower is concerned. After this, a gradual decrease of the drive phase velocity occurs. In the case of non-professional rowers, the number of drive phases with high drive phase velocity levels seems to be lower. For some rowers, an increase of the drive phase velocity is noticeable in the final phases of the experiment (see Rowers 6, 8, 10).

(1)

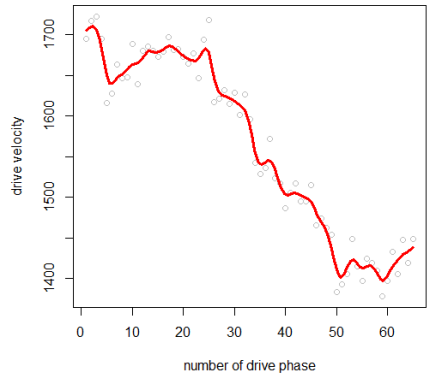
drive velocity
1400
1500
1600
1700
0
10
20
30
40
50
60
number of drive phase

(2)

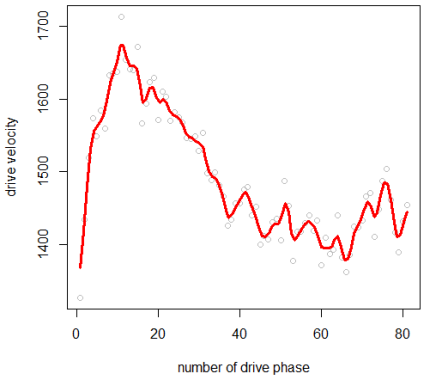
drive velocity
1400
1500
1600
1700
0
20
40
60
80
number of drive phase

(3)

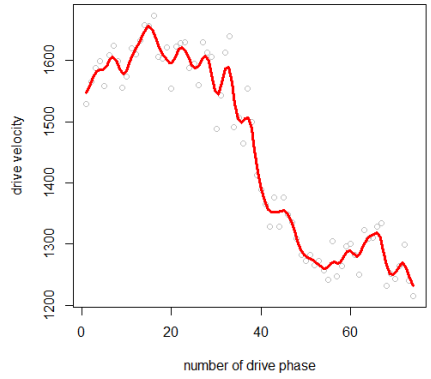
drive velocity
1200
1300
1400
1500
1600
0
20
40
60
number of drive phase

(4)

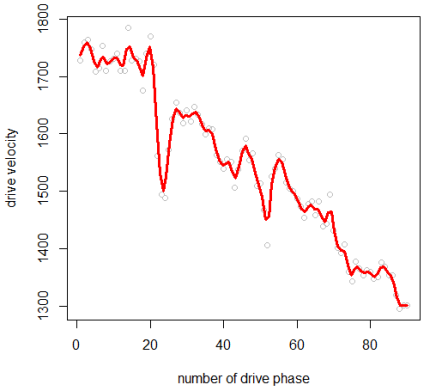
drive velocity
1300
1400
1500
1600
1700
1800
0
20
40
60
80
number of drive phase

(5)

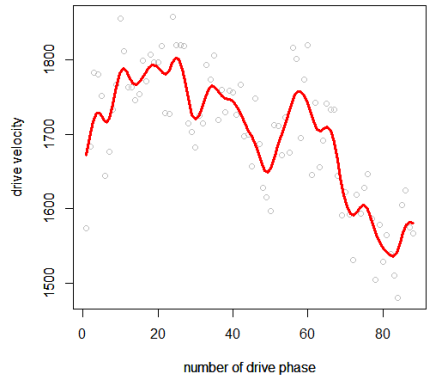
drive velocity
1500
1600
1700
1800
0
20
40
60
80
number of drive phase

(6)

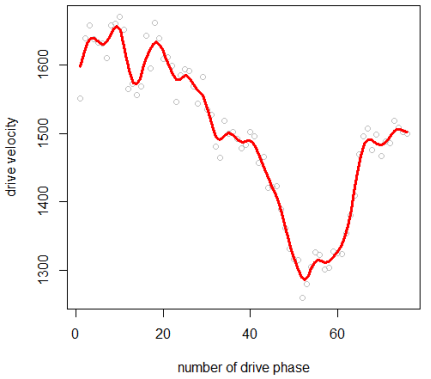
drive velocity
1300
1400
1500
1600
0
20
40
60
number of drive phase

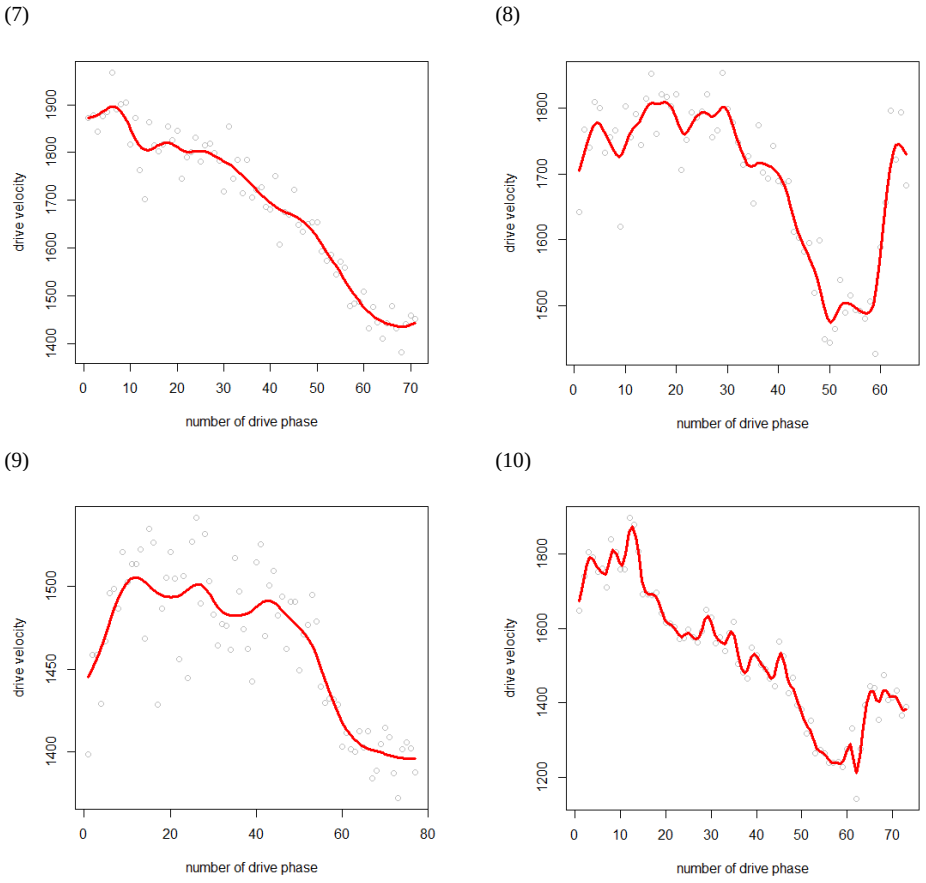

Fig. 4. The Nadaraya-Watson estimator of drive phase number to drive phase velocity of ten non-professional rowers identified by labels (1)-(10). Observations are represented by circles

The Nadaraya-Watson estimator was used to determine the point in which the decreasing of drive phase velocity begins. For this purpose, the differences between each pair of two subsequent extremes (maximum and minimum) of the Nadaraya-Watson estimator were calculated. The starting point of the drive phase velocity decrease (called herein the decline point) is taken as the phase number corresponding to the local maximum for which the difference is the largest.

The total number of drive phases n with relatively high drive phase velocity and the total number of drive phases N during the whole examination, together with the fraction n/N of the rowers, are shown in Table 4.

Table 4. The total number of drive phases n with a relatively high drive phase velocity and the total number of drive phases N during the examination, together with the fraction n/N of the rowers

Rower ID	n	N	n/N
Master	41	67	0.61
Rower 1	25	65	0.38
Rower 2	22	81	0.27
Rower 3	38	74	0.51
Rower 4	20	90	0.22
Rower 5	35	88	0.40
Rower 6	41	76	0.54
Rower 7	27	71	0.38
Rower 8	36	65	0.55
Rower 9	44	77	0.57
Rower 10	13	73	0.18

For the Master, the decrease in drive phase velocity occurred in the 41st phase, while the total number of phases was equal to 67. Thus the fraction n/N is equal to 0.61. This means that more than 60% of the total number of strokes correspond to the high velocity of the drive phase. In the case of non-professional rowers, the decline point occurred earlier and the fraction of strokes corresponding to the high velocity of the drive phase varies from 0.18 to 0.57, despite the much lower drive phase velocity when compared to the Master. These results can be seen by comparing Figure 3 and Figure 4.

5. Conclusions

The modelling proposed in the article for analysing the speed of rowing was performed using the Nadaraya-Wastson regression estimator. The method is based on the theory of statistical kernel estimators. The present method is an effective transparent tool for modelling motion tracking.

An average of 70 strokes for each rower while rowing over a distance of 500 meters were analysed. In each stroke, the two most important phases: drive and recovery were separated and analysed. The results, presented in Table 3 and Table 4, show that the proposed model, based on kernel regression, is the most effective of all five. The error of this method is also the smallest – as indicated by the value of the determination coefficient.

The computed functions allow an accurate determination of the level of the rowing technique of individual rowers. Moreover, their shape can be useful to compare the repetition of the moves in successive runs. This testifies to the level of individual training and degree of fitness. The obtained values provide the basis for trainers to quantify the technique level, examine the progress of the players and capture the technical deficiencies of the rower. As a side note, it may be possible to apply the technique to assess the quality of stroke of historical rowing greats.

Acknowledgments. The research program titled “Optimisation of training ergometer rowers based on the analysis of 3D motion data, EMG, ergometer and heart rate”, carried out in the Laboratory of Motion Analysis and Interface Ergonomics, was approved by the Commission for Research Ethics at the Lublin University of Technology, No. 7/2015 dated 12.11.2015.

Bibliography

[1] Akça F., 2004. Prediction of Rowing Ergometer Performance from Functional Anaerobic Power, Strength and Anthropometric Components. Journal of Human Kinetics 41: 133–142. DOI: 10.2478/hukin-2014-0041.

[2] Baudouin A., Hawkins D., 204. Investigation of biomechanical factors affecting rowing performance. Journal of Biomechanics 37: 969–976.

[3] Buckeridge E., Hislop S., Bull A., McGregor A., 2012. Kinematic asymmetries of the lower limbs during ergometer rowing. Med Sci Sports Exerc. 44 (11): 2147-53. DOI: 10.1249/MSS.0b013e3182625231.

[4] Charytanowicz M., Kulczycki P., 2008. Nonparametric Regression for Analyzing Correlation between Medical Parameters, [in:] Pietka E., Kawa J. (eds), Advances in Soft Computing – Information Technologies in Biomedicine, Information Technologies in Biomedicine, Springer-Verlag, Berlin, Heidelberg, 437–444.

[5] Charytanowicz M., Czachor H., Niewczas J., 2013. Nonparametric regression approach applications in agricultural science. Technical Transactions, series Automatic Control (Czasopismo Techniczne, seria Automatyka) 1-AC/2013: 17-27.

[6] Cerne T., Kamnik R., and Munih M., The measurement setup for real-time biomechanical analysis of rowing on an ergometer. Measurement, 2011, 44(10): 1819–1827.

[7] Cerne, T., Kamnik, R., Vesnicer, B., Gros, J.Z., Munih, M., 2013. Differences between elite, junior and non-rowers in kinematic and kinetic parameters during ergometer rowing, Human Movement Science 32: 691–707.

[8] Choszcz D., Podstawski R., Wysocka-Welanc M., 2009. Measurement of motor fitness of students using the rowing ergometer. Human Movement 10(1): 46–52.

[9] Draper N.R., Smith, H., 1981. Applied regression analysis. John Wiley and Sons, New York.

[10] Full body modeling with Plug in Gait, Vicon Documentation, https://docs.vicon.com/pages/viewpage.action?pageId=50888852#FullbodyFullbodymodeling?inGait-MarkersetsforPlug-inGaitfullbodymodeling.

[11] Gramacki A., 2018. Nonparametric Kernel Density Estimation and Its Computational Aspects, Springer.

[12] Hardle W., Marron J.S., 1985. Optimal bandwidth selection in nonparametric regression function estimation. The Annals of Statistics, 13: 1465–1481.
[13] Hayfield T., Racine J.S., 2008. Nonparametric econometrics: The np Package. Journal of statistical software 27(5): 1–32.
[14] Ingham S.A., Whyte G.P., Jones K., Nevill A.M., 2002. Determinants of 2,000 m rowing ergometer performance in elite rowers. European Journal of Applied Physiology 88: 243–246.
[15] Kropta R., Hruzevych I., Bohuslavska V., Galan Y., Nakonechnyi I., Pityn M., 2017. Correction of Functional Preparedness of Rowers at the Stage of Maximal Realization of Individual Capabilities. Journal of Physical Education and Sport 17(3): 1985–1991.
[16] Kulczycki P., 2005. Estymatory jądrowe w analizie systemowej. WNT, Warszawa.
[17] Kulczycki P., 2008. Kernel estimators in industrial applications, [in:] Prasad B. (ed) Soft Computing Applications in Industry, Springer-Verlag, Berlin.
[18] Lawton TW., Cronin J.B., McGuigan M.R., 2013. Strength, power, and muscular endurance exercise and elite rowing ergometer performance. Journal of Strength & Conditioning Research 27(7): 1928–1935. doi: 10.1519/JSC.0b013e3182772f 27.
[19] McGregor A.H., Bull A.M., Byng-Maddick R., 2004. A comparison of rowing technique at different stroke rates: A description of sequencing, force production and kinematics. International Journal of Sports Medicine 25: 465–470.
[20] Nolte V., 2005. Rowing faster. Champaign, USA: Human Kinetics Publishers.
[21] O'Sullivan F., O'Sullivan J., Bull A.M., 2003. Modelling multivariate biomechanical measurements of the spine during a rowing exercise. Clinical Biomechanics. 18: 488–493.
[22] Panjkota A., Stancic I., Supuk T., 2009. Outline of a qualitative analysis for the human motion in case of ergometer rowing, WSEAS International Conference. Proceedings. Mathematics and Computers in Science and Engineering. Rudas I., Demiralp M., Mastorakis N. (eds.) 5. WSEAS.
[23] Podstawski R., Choszcz D., Konopka S., 2011. The Impact of Training on the 500 M Rowing Ergometer Time and an Assessment of the Applied Test's Relevancy. Human Movement, 12(3): 264–272. doi: 10.2478/ v10038-011-0029-3.
[24] Podstawski R., Choszcz D., Konopka S., Klimczak J., Starczewski M., 2014. Anthropometric determinants of rowing ergometer performance in physically inactive collegiate females. Biol Sport. 31(4): 315–321. doi: 10.5604/20831862.1133936.

[25] Riechman S.E., Zoeller R.F., Balasekaran G, Goss FL, Robertson R.J., 2002. Prediction of 2000 m indoor rowing performance using a 30 s sprint and maximal oxygen uptake. J Sports Sci 20(9): 681–687.
[26] Sforza C., Casiraghi E., Lovecchio N., Galante D., Ferrario V.F., 2012. A three-dimensional study of body motion during ergometer rowing, The Open Sports Medicine Journal, 6: 22–28.
[27] Silverman B.W., 1986. Density Estimation for Statistics and Data Analysis, Chapman and Hall, London.
[28] Skublewska-Paszkowska M., Łukasik E., Montusiewicz J., 2016. Analysis of rowing based on handle trajectory, 9th International Conference on Human System Interactions (HSI) Communications in Computer and Information Science 639: 62–68.
[29] Wand M.P., Jones M.C., 1994. Kernel Smoothing. Chapman and Hall, London.
[30] Wychowanski M., Slugocki G., Orzechowski G., Staniak Z., Radomski D., 2018. Results of Single Sculling Technique Analysis Using 1D Mathematical Model. Elsevier. IFAC-PapersOnLine 51(2): 879–883.

Małgorzata Plechawska-Wójcik[1], Mikhail Tokovarov[2],
Mateusz Mitaszka[3], Przemysław Pudło[4]

Analysis of human brain responses to visual and audio stimuli based on EEG evoked potentials

Abstract: The aim of the paper is to perform comparative analysis of the human responses to visual and auditory stimuli. The human brain response latencies were measured and compared. The analysis was based on nineteen EEG electrodes. The presented case study is a preliminary study conducted to assess the measurement and analysis procedure, perform a preliminary selection of parameters and verify the hardware configuration. The paper verifies the hypothesis that the human response to visual stimuli is faster than to audio stimuli. The experiment was divided into two parts examining, correspondingly, the reaction to two types of stimuli: visual and auditory. The tool, called PsyTask was used in the experiment. Both parts included the following stages: pictorial description of the task to be solved by an examined person and the sequence of unordered trials. As for the visual part, a single trial included the demonstration of white background with one of five birds, whereas a single trial of the auditory part contained a record of separate birdsong. The trials were assessed in accordance with the Go/Nogo paradigm. Regarding the first part of the experiment, the following situation was concerned as a Go trial: the examined person clicked a left mouse button after the recognition of an owl in the presented picture, whereas a trial was considered as Nogo in case when the examined person did not click the left mouse button upon recognition of the demonstrated picture or when the left mouse button was clicked after false recognition. During the data acquisition it was observed that multiple factors, e.g. eye-blinking, eyeball movement, etc., can cause artefacts in the EEG record. As a result of the experiment, the numbers of correct and false reactions to stimuli were collected, the reaction times were measured as well. Another result was the observation that the said stimuli caused the activation of occipital and parietal lobes. The answer to the question placed in the abstract was obtained: shorter reaction times correspond to visual stimuli.

Keywords: electroencephalography, EEG, evoked potentials

1. Introduction

Electroencephalography (EEG) is a non-invasive method of measurement of spontaneous bioelectrical brain activity [16]. This measurement is performed with a dedicated amplifier and electrodes placed on the scalp using a special cap. The purpose of this recording is to measure changes in electrical potential from the neuronal brain activity [10]. The brain activity obtained after recorded

[1] Małgorzata Plechawska-Wójcik, Institute of Computer Science, Lublin University of Technology, Poland
[2] Mikhail Tokovarov, Institute of Computer Science, Lublin University of Technology, Poland
[3] Mateusz Mitaszka, Comarch, Poland
[4] Przemysław Pudło, Transition Technologies, Poland

potentials strengthening is called an electroencephalogram, whereas an electroencephalograph is a special type of amplifier, dedicated to small amplitude signals, such as EEG signals.

EEG is a relatively inexpensive technique which has a wide range of applications [22]. Typical EEG monitoring is applied in medicine for monitoring and diagnosing patients suffering from coma, epilepsy or sleep disorders [5]. Other applications of EEG are related to functional brain activity analysis [3]. EEG signal is different for every person. It also depends on the age of the patient, the actually performed activity and psychophysical aspects [7, 10].

In addition, EEG is an excellent tool to perform research in such fields as biofeedback (ensuring feedback about changes in the physiological condition of the body), neuroimaging (function analysis and imaging of the brain structure consisting in locating the functional areas of the brain during the test activities). Nowadays EEG analyses are also adapted in construction of brain-computer interfaces (BCI) [6] to provide a direct communication pathway between brain and an external device (such as robotic electric wheelchair navigation, computer or video game controlled) without using physical capabilities of the body [1, 8, 13, 17].

In the standard EEG recording 10–20 system is applied. It covers nineteen electrodes placed on the scalp (eight over each hemisphere and 3 in the centre line). However, due to better EEG equipment accessibility, more and more frequently researchers use systems with more electrodes, such as 128 or even 512.

EEG signals are varied. In particular, the characteristics of these signals differ from each other, depending on the state of the examined person. For example, another signal will be visible in the case of relaxation, another during dream and another during normal daily activity.

Single EEG test usually takes from several minutes to several hours and may serve as diagnostics (coma, epilepsy, sleep disorders, monitoring the patient during the operation), the study of neurological and functional properties of the brain as well as the construction of brain-computer interfaces and support for computer games. An additional advantage of EEG is high time resolution, especially compared to such imaging techniques as MRI and CT.

The aim of this paper is to present a comparative analysis of human reaction times to visual and auditory stimuli using electroencephalography. The scope of the work is based on two experiments. The first one was dedicated to gathering the reaction times to visual stimuli, and the second – to sound stimuli. The case study has the form of a preliminary study and was performed on five test users of different sex and age.

The research presented in the paper considers the possible future of EEG brain measurement applications. EEG measurement is a relatively inexpensive examination characterised by high time resolution. It is widely applied in medical neurological diagnosing. Moreover, EEG measurements are useful in

analysing brain reaction to applied stimuli (visual, auditory or tactile). This phenomenon might be further applied in research on such processes as cognitive workload or motor imagery, regarding additionally activities of specific EEG waves and their location over the brain lobes. These processes might be applied in practice to develop brain-computer interfaces which allow to control a computer (or other devices connected to a computer) with only a brain signal, without any external devices or muscle intervention.

2. Characteristic of EEG signal

The structures visible in the EEG signal might be, and often still are, analysed visually. A serious disadvantage of visual analysis is the limited repeatability and a relatively high cost as well as the ambiguity of standardisation. Ambiguous criteria of the analysis of visual difficulties are the reason for implementing the methods of computer analysis of EEG signals.

Five basic types of brain waves are defined with different characteristics and frequency ranges: alpha waves (in the range of 8–12 Hz), beta waves (12–30 Hz), delta waves (0–4 Hz), theta waves (3–7 Hz) and gamma waves (30–80 Hz).

EEG signal analysis might be carried out using a computer in both time and frequency domain. The analysis in the time domain is often associated with evoked potentials (EP), which represent the response of the brain to stimuli. Interpretation of this reaction usually requires averaging of signals aligned according responses to a specific stimulus. Properly realised averaging allows for analysis of the signal received in response to a stimulus.

Another way to work with EEG signals is spectral analysis, which involves analysing signal properties in the frequency domain. These analyses apply non-parametric methods, consisting of calculating spectra directly from the signal using non-parametric methods (such as Fourier transform or Z Transform) and parametric data models (such as autoregressive model).

3. Literature overview

Examination of reactions to stimuli is primarily based on the analysis of event-related potentials (ERP) or evoked potentials. Various forms of ERP and their brief analysis were addressed in [19]. The authors describe changing results depending on the components applied (e.g. P50, P300) and diseases affecting examined persons. Paper [8] focuses on user reactions to sound stimuli including music. It has been shown that changes in the rhythm of music caused the subject to feel changes in their mood. In [2] a study was performed of visual stimuli. The authors focused on a comparison of user responses to human live and drawn faces. The subjects were asked to count face occurrences. The authors therefore wanted to prove that an artificial (drawn) face can arouse strong reaction of the human brain.

Event-related potentials and the P300 paradigm are also widely applied in brain-computer interfaces (BCI). At the University of Arkansas, Yueqing Li and colleagues [11] tested different interfaces and screen sizes on a group of test users (10 healthy donors and 10 patients). The subjects had to count a specified stimulus displayed on the screen. The research allowed to evaluate perceptiveness and the users' ability to focus on the task. Paper [14] focused on the study of ADHD using ERP. The GO/NOGO study was conducted on a group of 148 subjects (74 patients and 74 healthy donors). The authors found that people suffering from ADHD make more errors than healthy individuals in both the test consisting in giving the response to a particular stimulus, and the task of not responding to it.

4. EEG evoked potentials

Evoked potentials are traces of the electrical brain responses to an applied stimulus. It was proven that it might be a visual, auditory or sensory stimulus [5]. Due to small EEG signal amplitudes (range 0 to 100 μV) and the many processes occurring simultaneously in the human brain, evoked potential analysis is based on the averaged signal responses. In an averaged signal one can notice potential changes in the form of increasing and decreasing waves. They are marked with the letter "P" for the positive deflection, and "N" for the negative one. The number (300) represents so-called latency – the time from the stimulus appearance (in milliseconds). What is more, it is possible to distinguish exogenous and endogenous potentials. Exogenous potentials are those arising in the early stages of communication, which is independent of the attention of the examined person. On the other hand, endogenous potentials represent more complex responses to stimuli, such as a conscious response to a stimulus or an emotional stimulation [20]. A common phenomenon accompanying evoked potentials is so-called habituation – a decline in activity accompanying the repeated stimuli.

P300 is a positive potential having a latency between 250 and 500ms [4]. It depends on the individual user characteristics, the level of user concentration and other issues related to both the performed experiment and individual user variation. The greatest strength of this signal is usually recorded in the parietal lobe of the brain. The paradigm is one of the basic EEG phenomenon and BCI paradigms. Such a stimulus needs to be presented to a user repeatedly in a sequence. However, such a sequence is optimal only if the target stimulus is rare and occurs among other, non-target stimuli. The target stimulus might be detected if it is presented among a series of multiple various non-target stimuli [11]. The P300 potential understood in this way, as an example of event-related potential, is elicited in the process of concentration and decision making based on the concentration level. Among other evoked potentials this is the strongest potential indicating a conscious conditional response. In the averaged signal [21]

it should be detected as a peak received as a brain response to the previously expected stimulus [1].

Evoked Potentials were applied in an ERP-based study of auditory stimuli in analysing ear-EEG signals [9]. Auditory evoked potential responses were also applied in hearing loss research and determination of the hearing threshold level [15, 17].

Visual and auditory stimuli were also applied in [12], where event related potentials in terms of different stimuli were analysed. The results proved that the amplitude of visual stimuli was smaller and with longer latency compared to the data obtained for auditory stimuli.

5. The experiment case study

5.1. Equipment

The signal was gathered with a 21 channel Mitsar 201 amplifier using cup-shaped electrodes attached to the cap located on the head. An EEG amplifier transmitted the data to a computer with the native software (EEG Studio) installed.

The program used to create the experiment was PsyTask. This is an application that allows both to create and present visual and auditory stimuli, and register user response times. PsyTask also allows to define a way of processing response to a stimulus, for example recognition of pressing the left mouse button as the GO reaction, and omitting to press it as a NoGo reaction. The project of the experiment also contains a list of all stimuli with defined parameters such as delay between successive stimulations and the time of particular stimuli exposure.

The application used for EEG signals recording was EEG Studio. This tool allows to import and perform experiments created in the PsyTask program. It controls the EEG recording, including adjusting filters and montages. What is more, EEG Studio controls parameters of the connected amplifier (for example impedance of each electrode) and ERP calibration options. Figure 1 presents electrodes applied in the experiment.

The WinEEG application was used for the collected data analysis. This program provides a range of functionalities allowing for EEG signal preprocessing, such as frequency filtration or artifact detection and correction. In addition, the program allows to calculate ERP and export the resulting values to text files. What is more, it generates spectra from selected portions of the signal.

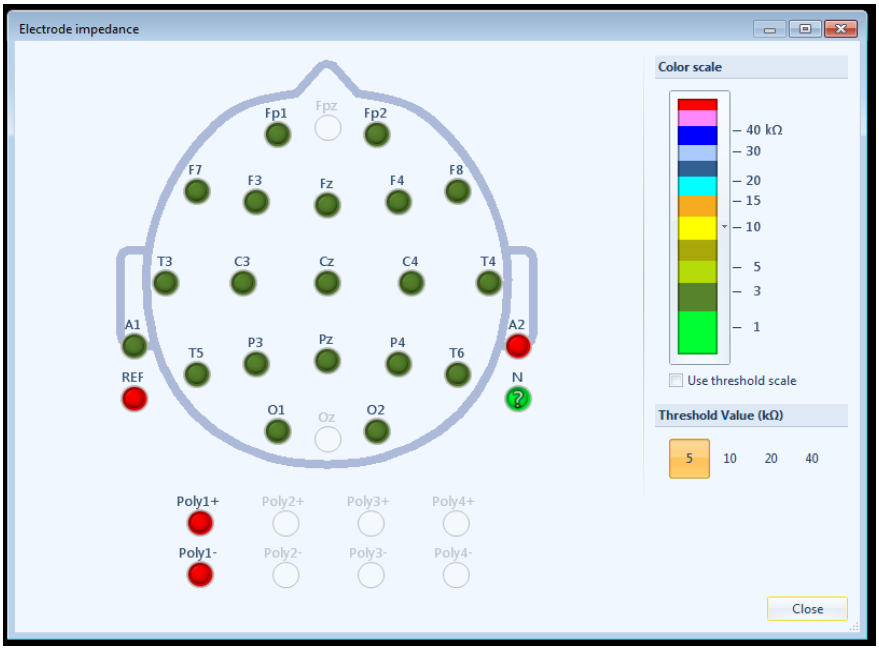

Fig. 1. Impedance of EEG electrodes applied in the experiment (EEG studio)

5.2. Experiment scenario

The experiment was divided into two parts examining, correspondingly, the reaction to two types of stimuli: visual and auditory. The tool used in the experiment was PsyTask. Both parts included the following stages: pictorial description of the task to be solved by a person examined and the sequence of unordered trials. As for the visual part, a single trial included the demonstration of white background with one of five birds, whereas a single trial of the auditory part contained a record of a separate birdsong. The number of trials was set to 828 repetitions for both parts. As for the first part, the break between the trials was 100 ms long, while for the second part the break was 1000 ms long. The trials were assessed in accordance with the Go/Nogo paradigm.

Regarding the first part of the experiment, the following situation was considered as a Go trial: the subject clicked a left mouse button after the recognition of an owl in the presented picture (see Figure 2), whereas a trial was considered as Nogo either when the subject did not click the left mouse button upon recognition of the demonstrated picture or when the left mouse button was clicked after false recognition.

Fig. 2. Pictures used in the visual part of the experiment

5.3. Experiment procedure

Five persons of different sex of an age from 17 to 35 years took part in the experiment. Prior to examination every participant expressed in written form his/her consent to take part, along with that he/she gave permission for processing the signal registered during the examination. Afterwards every participant underwent the same preparation procedure. A special cap for EEG examination was put on the head of the participant and his head skin was cleaned and deprived of fat with the use of ethanol, after which the hair in the electrode positions were removed. When the subject was prepared, the electrodes were attached to the cap, and ensuring sufficient conductivity through the use of special conductive gel was the final stage of preparation. The conductivity value of every electrode was checked and corrected if the initial amount of gel was insufficient for maintaining high conductivity.

Every participant sat in an armchair in front of an LCD screen with the resolution of 1280x1024 and frame rate of 60 Hz. Afterwards the participant was asked to relax and avoid unnecessary movements, during that stage the plan of the experiment was presented to the participant. Previous to the start of the experiment itself the registration of relaxed state was conducted: 1 minute for eyes-open and 1 minute for eyes-closed. The next step was carrying out of the first stage of the experiment (visual stimuli). After this stage the conductivity values were check and eventual corrections were performed. Upon that the second stage (auditory stimuli) was performed. The first stage covering the reaction to visual stimuli was 16 minute long, while the second part lasted for 27 minutes.

6. Data analysis

6.1. Data description

As the result of the experiment two datasets per user were gathered: visual stimuli related and auditory stimuli related. The moments of demonstration of

a stimulus as well as the moments of a patient's reaction to the demonstrated stimulus were marked in the signal records. In addition to the said values, the following data were recorded in the coma-separated text files: time of the experiment, stimulus number, time after stimulus demonstration, time of reaction to the stimulus. The recorder data were used in further statistical analysis. Table 1 contains an example of results obtained in the visual stage of the experiment.

Table 1. Part of data gathered during the visual stage of the experiment

Time [s]	GO-1/NOGO-2	Reaction time	Reaction
0	2	0	NO
1.098	2	0	NO
2.196	2	0	NO
3.298	2	0	NO
4.398	1	304	YES
5.496	2	0	NO
6.598	2	0	NO
7.696	2	0	NO
8.796	1	0	NO
9.896	2	0	NO
10.996	1	282	YES
12.094	2	0	NO
13.194	2	0	NO
14.294	2	0	NO
15.394	2	0	NO
16.494	1	0	NO
17.594	2	0	NO
18.694	2	0	NO
19.794	2	0	NO
20.894	2	0	NO
21.994	2	0	NO
23.092	2	0	NO
24.192	2	0	NO
25.292	2	0	NO
26.394	1	220	YES
27.492	1	496	YES
28.592	2	0	NO
29.69	2	0	NO
30.79	1	344	YES
31.89	2	0	NO
32.99	2	0	NO
34.09	1	258	YES
35.188	2	0	NO

36.288	2	0	NO
37.39	2	0	NO
38.488	2	0	NO
39.588	2	0	NO
40.688	1	262	YES
41.788	2	0	NO

6.2. Data analysis procedure

The registration of EEG data is only the first step in the process of the experiment. Upon the signal registration the data preprocessing should be carried out. The software called WinEEG was applied in the present study. The complete data processing procedure can be divided in the following stages:

1. Applying corresponding montage;
2. Definition of high- and low-pass filters;
3. Artifact detection;
4. Artifact elimination;
5. Export of the ERP data to a text file.

Stage 1

A montage is called the configuration of electrodes placed on the head of the examined person ensuring required registration of brain electrical activity. In the present study the Monopolar 1 [A1/A2] montage was applied for data analysis. In this montage the voltage in microvolts is measured between every electrode and the referential point, in the present case A1 and A2, i.e. ear lobes. An additional feature of this montage is the fact that the scull is divided into two hemispheres.

Stage 2

A filter is called an algorithm or electronic scheme applied in order to limit an input signal. Low pass and high pass filters were used in the present study. The high pass filter was set to 3 Hz, while the low pass one to 50 Hz. The said values ensured the best possible quality of the output signal. Kaiser function was used as the window.

Stage 3

The noises appearing in an EEG signal during registration are called artifacts. They appear in many forms and can be caused by various reasons. One of the main problems is the use of significant signal amplification for registration of brain activity. This significant amplification can cause appearance of voltage drops and peaks originating from some other source. The artifacts can be caused by the following reasons:

- muscular potentials;
- blinking and eyeball moving;
- body movement;

- external electric fields.
  The software WInEEG was used for artifact detection in the present study.

Stage 4

Two main methods were used for artifact correction:

- ICA – Independent Component Analysis. This method is based on decomposing the signal into independent components assuming that they are statistically independent and are not normally distributed.
- PCA – Principal Component Analysis. This method transforms data in such a way, that the obtained components are arranged in accordance with their variance.

Stage 5

The last stage included counting correct and incorrect answers during the ERP analysis as well as exporting the data to a .csv file.

7. Results

Figures 3-6 present the maps of EEG spectral power in various areas of the brain. Figure 3 presents an example of conducted examination of open eyes relaxed state before visual part of the experiment. The increase of signal power in the areas of parietal and occipital lobes is noticeable especially for alpha component. High activity of the said lobes may be evidence of the relaxed state of the participant as well as carrying out the analysis of visual stimuli. In addition to the said area, high activity can be observed in the right hemicerebrum, which is known to be responsible for spatial orientation.

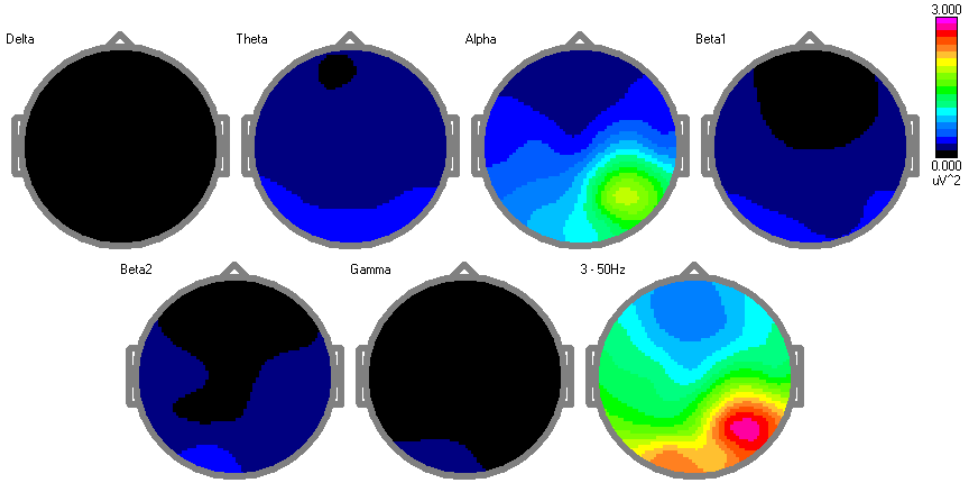

Fig. 3. Relaxed state – eyes open 14:32:09, length: 20.67 s

Upon the end of the open eyes relaxed state part of the examination the participant was asked to close the eyes. The spectral power map is presented on the Figure 4. An increase of EEG signal power in the area of left parietal and occipital lobes along with a decrease of power in the area of temporal lobe are clearly seen in Figure 4. This effect can be explained by increased attention paid to auditory stimuli.

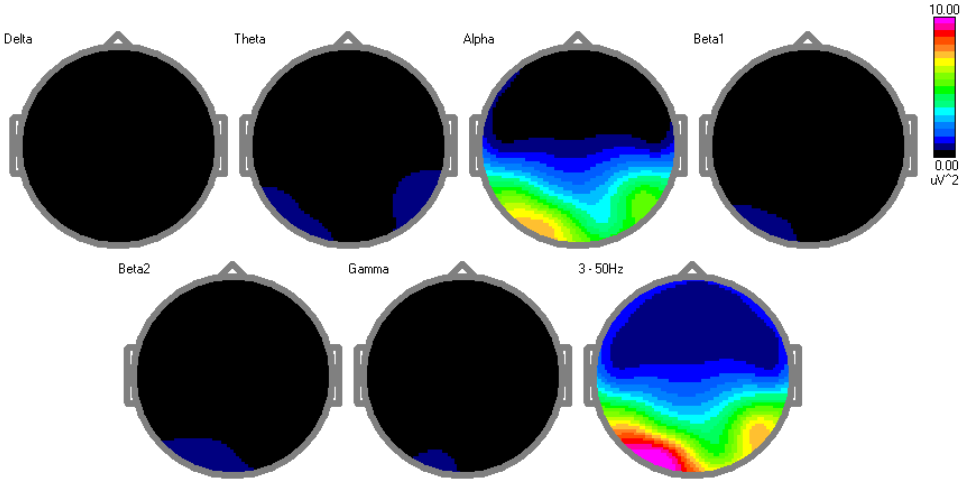

Fig. 4. Relaxed state – eyes closed 14:34:03, length: 20.26 s

Figures 5 and 6 presents a map of spectral power of an EEG signal registered during visual part of the experiment. Increased activity was registered in the area of frontal and occipital lobes. This activity can be evidence of intensive analysis of visual stimulus.

The map of spectral power of the signal registered during the second stage of the experiment (auditory) presents intensive activity both in the area of parietal and occipital lobes. Most possibly it may be evidence of intensive analysis of auditory stimuli being received by the participant.

Figures 7 and 8 present the results of ERP analysis of the signal averaged across several hundreds of stimuli. Two parallel dashed lines show, correspondingly, beginning and end of stimulus demonstration.

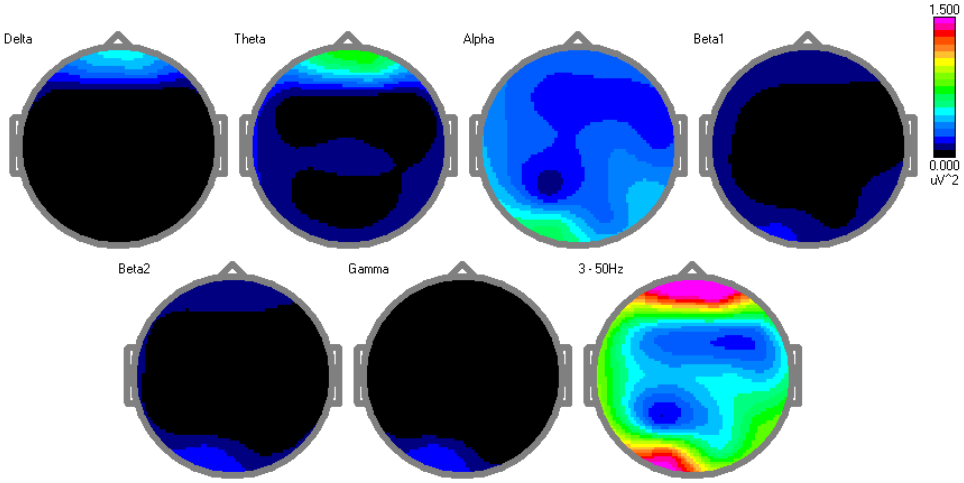

Fig. 5. The experiment – visual stimulus 14:35:40, length: 20.37 s

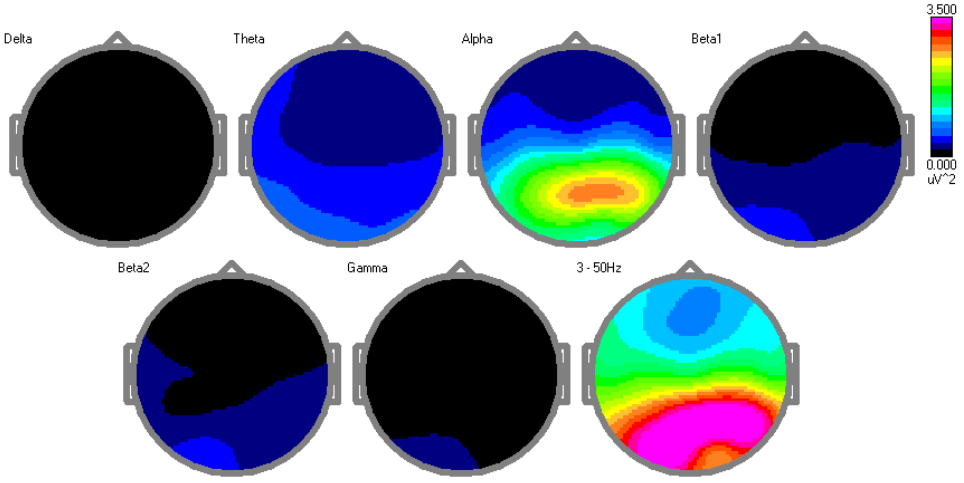

Fig. 6. The experiment – auditory stimulus 16:05:10, length: 20.50 s

Figure 7 contains the averaged signal of the visual part of the experiment. The figure clearly shows that most electrodes registered higher potential values for Go stimuli compared to Nogo. Moreover, a significant increase of potentials can be observed in about 350 ms after stimulus demonstration, which can be evidence of P300 potential.

The ERP graphs originating from the auditory part of the experiment are presented in the Figure 8. As for this part, both positive and negative potentials can be observed. This part contains a significant increase of potentials near 350-450 ms, which corresponds to recognition of the stimulus.

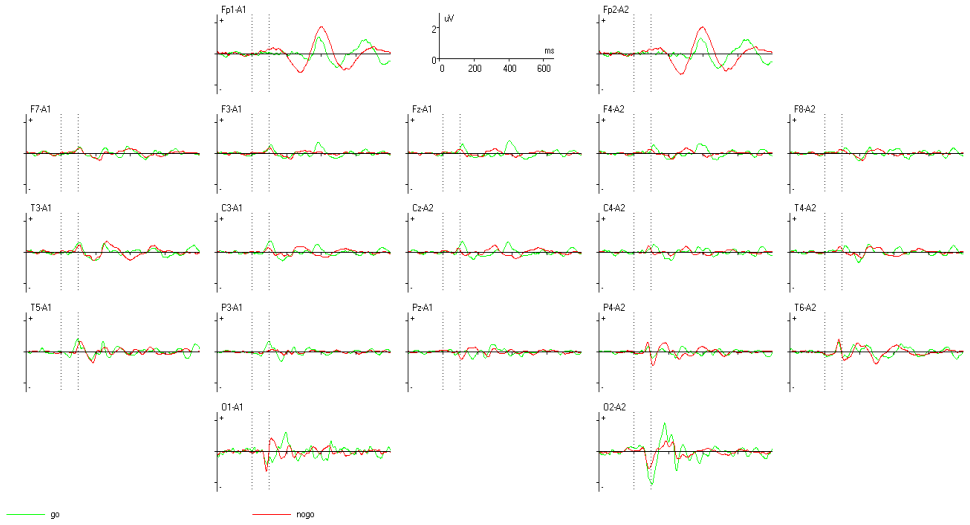

Fig. 7. ERP – visual stimulus

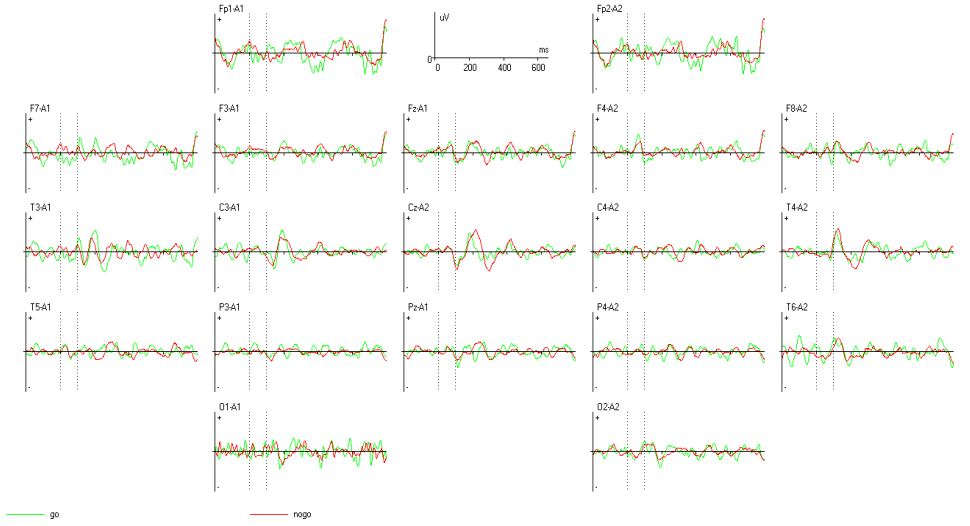

Fig. 8. ERP – auditory stimulus

Table 2 contains the results of both parts of the experiment. The total number of stimuli was equal to 828, including 184 Go stimuli and 644 NoGo stimuli. Clicking the left mouse button in an inappropriate moment during the Go stimulus demonstration was considered as incorrect answer. As can be seen from the table, the maximum number of incorrect answers in the visual part of the experiment was 4. The mean number of incorrect answers was 2.4 for the said part of the experiment. As for the auditory part, the maximum number of incorrect answers equalled 11, while the mean incorrect answer number was as high as 4.8. On the basis of these observations it may be noticed that the number of incorrect answers in the visual part is twice lower compared to the auditory part. It may be evidence of the fact that the participants focused at the demonstrated pictures more intensively or that, compared to sound, pictures are easier to recognise.

Table 3 contains the mean values and the standard deviations of reaction time for both visual and auditory stimuli. The lowest mean value for the visual part was obtained during the registration of signal of participant No. 3, whereas the longest mean time was demonstrated by participant No. 5. As for the auditory part, participant No. 4 was the fastest and participant No. 1 was the slowest. On the basis of the obtained results it may be stated that the time of reaction to visual stimuli is shorter by 100 ms compared to auditory stimuli.

Table 2. The number of correct/incorrect answers

		Visual		Auditory	
Participant No.	Stimulus	Number of correct answers	Number of incorrect answers	Number of correct answers	Number of incorrect answers
1.	GO	183	1	173	11
	NOGO	644	0	644	0
2.	GO	183	1	180	4
	NOGO	644	0	644	0
3.	GO	180	4	183	1
	NOGO	644	0	644	0
4.	GO	181	3	183	1
	NOGO	644	0	644	0
5.	GO	181	3	177	7
	NOGO	644	0	644	0

Table 3. Mean values of reaction time

	Visual part		Auditory part	
Participant No.	Mean value [ms]	Standard deviation [ms]	Mean value [ms]	Standard deviation [ms]
1.	356.65	45.90	512.38	91.91
2.	367.17	51.70	461.16	117.62
3.	290.27	44.58	455.42	106.92
4.	299.26	48.40	427.17	115.87
5.	374.64	57.81	451.27	118.01

8. Conclusions

The aim of the present paper was to conduct a comparative analysis of human reaction times to visual and auditory stimuli. The initial assumption was that reaction time to a visual stimulus is shorter.

The experiment was organised into two parts: visual and auditory. In accordance with that structure the examination of five persons was conducted, upon which the data were analysed with the hardware and software described in the present paper. During the data acquisition it was noticed that multiple factors may cause the appearance of artifacts in the electroencephalogram, e.g.: eye-blinking, eye-movement, etc. The times of reaction to the stimuli as well as correct/incorrect reactions (Go/Nogo) were obtained. It was observed that parietal and occipital lobes underwent higher or lower degree of activation during reaction to the said stimuli were observed.

On the basis of the experiment results it may be clearly concluded that the reaction to visual stimuli is faster compared to that to auditory.

Unfortunately, the experiment did not completely cover the subject of the paper as additional examination of the group separated on the basis of sex or age is still possible.

Bibliography

[1] Beverina F., Palmas G., Silvoni S., Piccione F., Giove S., 2003. User adaptive BCIs: SSVEP and P300 based interfaces. PsychNology Journal, 1(4): 331–354.

[2] Chena L., Jina J., Zhanga Y., Wanga X., Cichocki A., 2015. A survey of the dummy face and human face stimuli used in BCI paradigm. Journal of Neuroscience Methods, 239: 18–27.

[3] Coenen A., Fine E., Zayachkivska O., 2014. Adolf Beck: A forgotten pioneer in electroencephalography. Journal of the History of the Neurosciences, 23(3): 276–286.

[4] Corralejo R., Nicolás-Alonso L.F., Álvarez D., Hornero R., 2014. A P300-based brain-computer interface aimed at operating electronic devices at

home for severely disabled people. Medical & Biological Engineering & Computing, 52(10): 861–872.
[5] Cunnington R., Iansek R., Bradshaw J.L., Phillips, J.G., 1996. Movement-related potentials associated with movement preparation and motor imagery. Experimental Brain Research, 111(3): 429–436.
[6] Gross R.E., 1992. Psychology: the science of mind and behaviour. Hodder Education Publishers, London.
[7] Haas, L.F., 2003. Hans Berger (1873–1941), Richard Caton (1842–1926), and electroencephalography. Journal of Neurology, Neurosurgery & Psychiatry, 74(1): 9.
[8] Huisheng L., Mingshi W., Hongqiang Y., 2005. EEG model and location in brain when enjoying music. In: Proceedings of the 2005 IEEE Engineering in Medicine and Biology 27th Annual Conference Shanghai, China, 2005, 2695–2698.
[9] Kidmose P., Looney D., Ungstrup M., Rank M.L., Mandic, D.P., 2013. A study of evoked potentials from ear-EEG. IEEE Transactions on Biomedical Engineering, 60 (10): 2824–2830.
[10] Kooi K.A., 1971. Fundamentals of electroencephalography. Harper & Row, New York.
[11] [11] Li Y., Nam C.S., Shadden B.B., Johnson S.L., 2011. A P300-based brain–computer interface: Effects of interface type and screen size, Int. Journal of Human–Computer Interaction, 27(1): 52–68.
[12] Lim S., Sim K., Shin D., Yoon G., 2016. Event related potentials in terms of visual and auditory stimuli. World Academy of Science, Engineering and Technology, International Journal of Biological, Biomolecular, Agricultural, Food and Biotechnological Engineering, 10(12): 859–864.
[13] Longstaff A., Neurobiology, 2006. PWN, Warsaw.
[14] Mueller A., Candrian G., Kropotov J.D., Ponomarev V.A., Baschera G.M. 2010. Classification of ADHD patients on the basis of independent ERP components using a machine learning system. In: Mueller, A. et al., eds., Nonlinear Biomedical Physics, 4 (Suppl 1): S1.
[15] Paulraj M.P., Subramaniam K., Yaccob S.B., Adom, A.H.B., Hema C.R., 2015. Auditory evoked potential response and hearing loss: a review. The Open Biomedical Engineering Journal, 9: 17–24.
[16] Pfurtscheller G., Neuper C., 2001. Motor imagery and direct brain-computer communication, 2001. Proceedings of the IEEE, 89(7): 1123–1134.
[17] Regan D., Human brain electrophysiology: Evoked potentials and evoked magnetic fields in science and medicine, 1989. Elsevier, New York, NY, USA.
[18] Sriraam N., 2012. EEG based automated detection of auditory loss: A pilot study. Expert Syst. Appl., 39: 723–731.

[19] Sur S., Sinha V.K., 2009. Event related potential: An overview. Ind. Psychiatry J., 18(1): 70–73.
[20] Swartz B.E., 1998. The advantages of digital over analog recording techniques. Electroencephalography and Clinical Neurophysiology, 106(2): 113–117.
[21] Szelenberger W., 2000. Potencjały wywołane. Wydawnictwo Elmiko, Warszawa.
[22] Wolpaw J.R., Birbaumer N., Heetderks W.J., McFarland D.J., Peckham P.H., Schalk G., Vaughan T., 2000. Brain-computer interface technology: a review of the first international meeting. IEEE Transactions on Rehabilitation Engineering, 8(2): 164–173.

Maria Skublewska-Paszkowska[1], Paweł Powroźnik[2], Edyta Łukasik[3], Jakub Smołka[4], Marek Miłosz[5], Jolanta Taczała[6], Agnieszka Zdzienicka-Chyła[7], Anna Kosiecz[8]

Adjusting the type of neural networks to evaluate children's gait

Abstract: Artificial neural networks are an excellent tool to classify patterns. Depending on the knowledge about dependencies between input and output data, different neural structures are used. The aim of the paper is to select the neural network structure, parameters and learning method to distinguish the gait of healthy children and those with disorders. The input vector to the neural network is: step length, step velocity, step duration, step width, step cadence, the maximal height of heel and toe during the step and average ankle angle. These items were generated from three-dimensional data recorded using a motion capture system (Vicon, Oxford Metrics Ltd., UK) and the biomechanical model Plug-in Gait. The children were walking along a straight 2.5 m path. Possessing the data describing the children's walk is a condition insufficient to be able to clearly assign a specific patient to groups of people characterised by a correct or incorrect walk. It is also desirable to separate individual groups. In other words, it should be shown that it is possible to extract a set of parameters from the data sets that will allow for an unambiguous classification of the children's gait. During the research, 1608 sets of samples suitable for classification and derived from both children with walking defects and healthy children were obtained. One way neural networks as well as the Support Vector Machine were tested as a classifier. The separability of the collected data using the tSNE method was also shown.

Keywords: children’s gait analysis, one way neural network, data classification, motion capture, support vector machine

[1] Maria Skublewska-Paszkowska, Electrical Engineering and Computer Science Faculty, Lublin University of Technology, Poland
[2] Paweł Powroźnik, Electrical Engineering and Computer Science Faculty, Lublin University of Technology, Poland
[3] Edyta Łukasik, Electrical Engineering and Computer Science Faculty, Lublin University of Technology, Poland
[4] Jakub Smołka, Electrical Engineering and Computer Science Faculty, Lublin University of Technology, Poland
[5] Marek Miłosz, Electrical Engineering and Computer Science Faculty, Lublin University of Technology, Poland
[6] Jolanta Taczała, Department of Rehabilitation, Physiotherapy and Balneotherapy, Faculty of Health Sciences, Medical University in Lublin, Poland
[7] Agnieszka Zdzienicka-Chyła, Department of Rehabilitation, Physiotherapy and Balneotherapy, Faculty of Health Sciences, Medical University in Lublin, Poland
[8] M. Anna Kosiecz, Department of Physiotherapy, University Children's Hospital in Lublin, Poland

1. Introduction

Gait assessment is very important for children with Cerebral Palsy (CP). Qualitative ways of classifying the abilities of CP children in their gait performance has limited significance. Therefore, there is a need to quantify their gait so that their overall performance can be quantified and monitored as a result of treatment. Automated recognition and classification of the CP gait characteristics could offer many potential benefits for the evaluation of the treatment outcomes and set a diagnosis.

Gait quality assessment methods can be divided into: observational (subjective, burdened with a large measurement error), laboratory gait analysis (objective, precise) and indirect – "semi-quantitative" (gait assessment protocols, camera recording). One of the uses of motion capture technology is assessment of the progress in the rehabilitation of patients with neuromuscular disorders (e.g. Cerebral Palsy) after the use of soft orthoses.

Soft orthopedic equipment has in recent years been an increasingly popular therapeutic agent for children with cerebral palsy. The main purpose of using soft orthosis is to improve the patient's functioning.

The aim of this study is to select the neural network structure, parameters and learning method to distinguish the gait of healthy children and those with cerebral palsy. The parameters were computed on the basis of three-dimensional data gathered during motion capture sessions. The participants were under treatment with soft orthoses.

2. Review

Hahn et al. [4] have shown that neural networks can be used to quantify the extent of abnormality in the balance impairments in older adults. Classification of normal and pathological gait functions with the aid of neural networks [26, 11, 27] and fuzzy logic classifiers have been used on numerous occasions [18, 21].

O'Malley et al. [18], using the fuzzy clustering technique, have demonstrated that a membership function, derived from basic gait features, can be used to differentiate between normal and CP patients. Using gait data from 88 spastic diplegia CP children and from 68 normal children, their technique assigned each child's gait data a membership function related to one of the five different clusters. The authors provided four feature values: stride length, cadence, leg length and age.

A support vector machine (SVM) was used for automated detection and classification of children with CP using two basic temporal-spatial gait parameters: stride length and cadence as input features [9]. These two features are particularly significant as they are considered to be the fundamental gait parameters [7]. The SVM classification outcomes are compared with multilayer

perceptron (MLP) and linear discriminant analysis (LDA) classifiers. In this study an SVM with four kernel functions was used. The paper describes the CP and normal gait data acquisition and normalisation techniques described in [17]. The SVM method was applied to a set of data provided by [17]. Three measures: accuracy, sensitivity and specificity were used to assess the performance of the classifier. SVM accuracy in identifying children with CP and healthy ones was 96,8% using only two temporal distance gait parameters. Previously, gait pattern analysis using neural networks reported close to 95% accuracy, but it was obtained using kinetic features measured by two ground reaction force platforms [6].

In [28] the gait analysis was based on the Bayesian approach. The proposed approach was compared with five other popular classification methods such as: SVM, LDA, k-nearest neighbour classifier (k-NN), artificial neural networks, and random forest. Three different kinds of input features have been experimented with and the best model turned out to be the expectation-maximisation (EM) algorithm with one Gaussian component which had 94% accuracy.

Electrical stimulation (ES) was investigated as a means of correcting the motor deficits associated with CP. One source for gait event detection is electromyographic (EMG) signals in combination with gait patterns recorded with a motion capture system. The use of EMG as a switch to either initiate or end an action for the control of limb ES systems was studied in [5, 15]. Time-delayed adaptive neural network was used to predict movements about the shoulder and elbow [1]. Neural networks with the EMG signals recorded from the trunk musculature were applied to control an ES system for the lower extremity [3, 12]. An adaptive neuro-fuzzy inference system (ANFIS) [8] with a supervisory control system (SCS) was used to predict the occurrence of gait events using the EMG activity of lower extremity muscles in a child with CP in [13].

3. Material and methods

3.1. Participants

Four healthy 4-year-olds and four 3-5-year-olds with CP took part in the study. Their height was between 0.925 m and 1.14 m, their weight between 13.5 kg and 21.8 kg. They suffered from spastic paresis related to lower limbs, nevertheless walked alone (according to the Gross Motor Function Classiffication System I). They wore soft trunk orthoses for four hours a day. The children's parents signed the consent for participation in the study.

3.2. Method

There are three stages of the method presented in Figure 1. The first one, qualifications of the patients for the study, is performed by doctors and physiotherapists. The second one concerns recording three-dimensional motion data using a motion capture system. The final stage is the most time-consuming, because the post-processing of data must be performed as well as data analysis. Based on the 3D data obtained, the proper calculations are performed using the author's own software written in the C++ language using Eigen and b-tk libraries. As a result, the input vector for the neural network is computed.

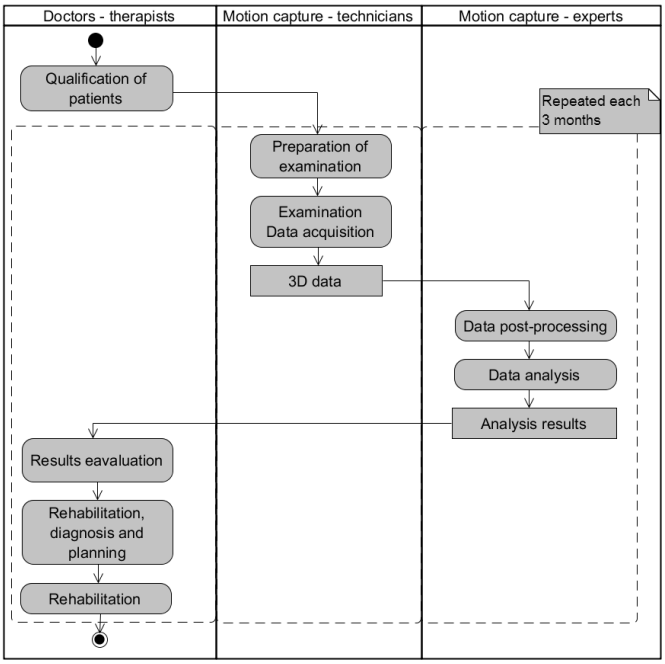

Fig. 1. Three stages of the study [20]

3.3. Motion data acquisition

The participants are prepared for the examinations. They should wear a body or a T-shirt and tight trousers. The clothes should be close-fitting. On the clothes and the skin 39 markers according the Plug-in Gait model [20] are attached, using hypoallergenic double-sided tape. The measurements of the child's body parameters are performed and entered into the motion capture system. The body mass and height, as well as for both sides of the body: leg length, shoulder offset, ankle width, knee width, elbow width, wrist width and hand thickness are measured.

The study is performed in two stages: with and without soft orthosis. The dynamic exercises concern walking along a straight distance of 2.5 meters. The participant should walk slowly, and try not to run. This exercise is repeated four times, so the child is walking in two directions. Each participant is examined every three months in order to verify the improvement of a child's gait (four examinations).

The Vicon passive optical motion capture system was used to track the participant's movements at the Laboratory of Motion Analysis and Interface Ergonomics at the Lublin University of Technology in Poland. The research was conducted in a shaded room (without windows) so that no additional reflections appeared, which might affect the quality of the data obtained. The motion capture system consisted of: eight T40S cameras operating in near infrared, two reference video Bonita cameras, a Giganet hub collecting data, a desktop computer and a set of accessories (e.g. markers, a calibration wand, double-sided tape). The system recorded the positions of the markers placed on the subject's body. The reference video may be used both for data post-processing and for generating video files with a biomechanical model overlay.

Each 3D recording was post-processed using the above-mentioned Vicon Nexus software. The process consisted of four main steps: marker labelling, gap filling using interpolation methods, data cleaning (e.g. deleting all unlabelled markers) and applying the Plug-in Gait model for the human subject. The post-processed recordings were exported as C3D files. These files were used for further analysis and creation the input vector.

3.4. Data characterising children's gait

The research carried out with the use of motion capture technology allowed the registration of parameters participating in the classification process. The following data characterising the children's gait were extracted:

- time of the step,
- step length,
- step velocity,
- step width,
- maximum height of the toe,
- maximum height of the heel,
- cadence,
- average ankle angle computed by the Plug-in Gait model.

However, processing the data describing the children's walk is a condition insufficient to be able to clearly assign a specific patient to groups of people characterised by correct or incorrect walk. It is also desirable to separate individual groups. In other words, it should be shown that it is possible to extract a set of parameters from the data sets that will allow for an unambiguous classification of the children's gait. During the research, 1608 sets of samples

suitable for classification and derived from both children with walking defects and healthy children were obtained.

3.5. Pre-processing of data characterising children's gait

The set of registered data was characterised by a different number of values for each of the tests. Due to the rather static and predetermined structure of classifiers, the input parameter vector had to be prepared in such a way that the number of input data was constant regardless of the number of registered samples. Preparing data in the first step consisted in removing evidently incorrect values (e.g. step length or step speed equal to zero). Then, the various data recorded during the tests were transformed into an input vector consisting of eight values, each of which characterised one of the parameters. Two methods of data transformation were investigated: the first using the arithmetic mean, the second – the median. Due to the different ranges of values adopted and the problems associated with this in the visualisation, the values assumed by all parameters were normalised to the range [0,1].

3.6. Visualisation of input parameters

Visualisation of multidimensional data is a significant problem in many science issues, in which it is necessary to present them in two- or three-dimensional space. Many techniques have been developed for the above issue. It is worth mentioning the methods proposed by Chernoff [3], Keim [10] and Weinberger, together with the band [24]. However, due to the ease of implementation, data visualisation in the conducted research was based on the t-Distributed Stochastic Neighbour Embedding method developed by Geoffrey Hinton and Laurens van der Maaten [22]. The basis of the proposed method is an algorithm allowing for the conversion of the Euclidean distance, in a multidimensional space, between two points in a condition of likelihood to represent their similarity. The way the tSNE method works is as follows [22]:

- calculate the distance between points in a multidimensional space,
- determine the standard deviation σi for each multidimensional point so that the uncertainty of each point is at a predetermined level,
- calculate the similarity matrix (probability distribution of distances between points),
- create an initial set of small-scale points,
- iteratively update small-scale points to minimise the Kullback-Leibler discrepancy between the Gaussian distribution in the quantum space and the t-distribution in the small-dimensional space.

Based on the above algorithm and the parameters described, the data sets were visualised, the results of which are presented in Figure 2.

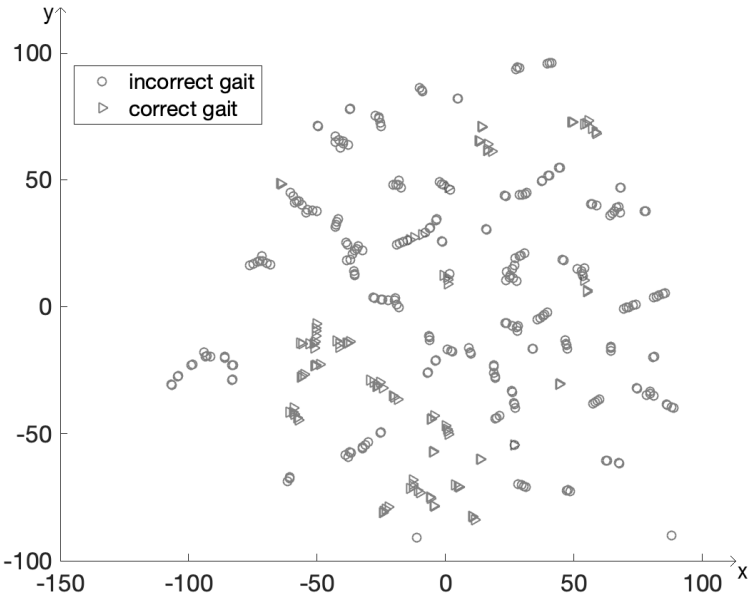

Fig. 2. Visualisation of parameters registered during the tests

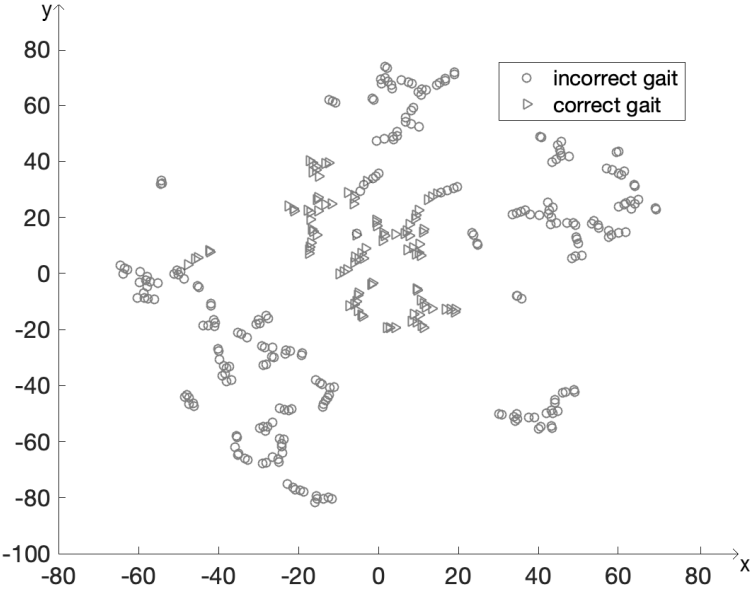

Fig. 3. Visualisation of the second set of parameters

The data presented in Figure 2 may suggest some problems with unambiguous classification due to its "mixing". The ideal situation would be if the samples formed two disjoint, compact sets located in two areas of space. The reason for this situation may be the negative impact of one or more factors or their insufficient number. Since the recorded data are directly related to the reasonable dimensions, it seemed to be using the patient's height as the next input parameter. The obtained visualisation results are presented in Figure 3.

Apart from a few samples, both considered groups form quite compact sets, so it can be assumed that automatic classification can provide the desired results.

4. Classification

The last stage of data processing is classification. All classification work was carried out in the Matlab 2018 environment. Four classifiers were tested in the study:

- support vector machine (SVM) algorithm,
- artificial neural networks (ANN) with various activation functions.

Due to the arrangement of samples on the plane (Figure 3), the SVM algorithm seems to be a natural classifier. It is based on the concept of decision space, which is divided, building boundaries separating objects of different class affiliation with the maximum margin of trust (margin of separation). Through the margin of trust, we will understand the distance of the hyperplane from the nearest points on which the supporting vectors will be formed. In the analysed case, the plane defined by the ellipse equation was used. The non-linear network SVM is designed to determine the values of the weight vector w in order to determine the optimal hyperplane for linearly non-verse data, which minimises the probability of making a classification error while maintaining the condition of maximising the margin of separation. The dataset was divided into subsets: learner, validation and testing respectively in relation: 50%–30%–20%. The division was made randomly. The classification efficiency using the support vector method is shown in Figure 5 and Figure 6.

The second tested classifier was artificial neural networks. The structure of it was shown in Figure 4.

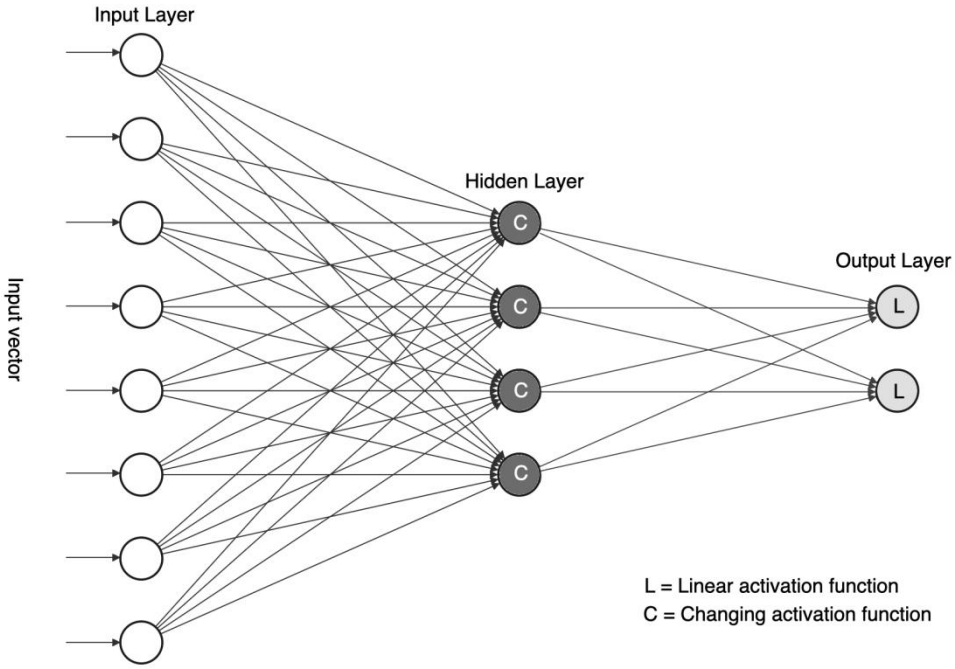

Fig. 4. The structure of the neural network used (changing the activation function depended on the experiment)

The input layer consisted of 8 neurons corresponding to the registered parameters. The network had one hidden layer. The number of neurons in this layer was 4 and was determined on the basis of the geometric mean of the number of inputs and outputs. During the study, the activation function of hidden layer neurons changed and is described below The output layer consisted of 2 neurons, represented considered two gait classes.

The influence of the activation function on the effectiveness of classification was examined. In the research carried out the cells in the hidden layer were activated using the following functions:

- linear,
- sigmoidal,
- hyperbolic tangent.

The network constructed in this way was taught using the backwards error propagation algorithm. The learning process ended when 1000 epochs were reached or when the learning error was less than 0.01 As in the case of the SVM classifier, the dataset was divided into subsets: training, validation and testing, respectively, in relation: 50%–30%–20%. The division was made randomly. The learning process was interrupted at 483, because the validation error reached achieved its lowest value. The initial learning error is large – it is related to the

random initialisation of the weights. During the learning process, the error systematically decreases. Moreover, the error value determined on the basis of data from the validation set is usually higher than the value of this error determined on the basis of the training file [25]. The effectiveness of classification using the ANN method is presented in Figure 5 and Figure 6 – true positive results.

The Matlab environment provides several methods to initiate the weights of the constructed artificial neural network. Among the most frequently used, it is necessary to replace the RAND function that allows to generate random values and the RANDN function enabling the generation of normalised random values. In addition, it is possible to generate a normalised value up to 1 using the RANDNC function. In all the tests carried out, the INITNW method (Nguyen-Widrow [16]) was chosen as a function of the initialisation of weights, due to the small learning error [19].

The classification results (true positive) for the median value and for the average value are presented in the successive Figure 5 and Figure 6.

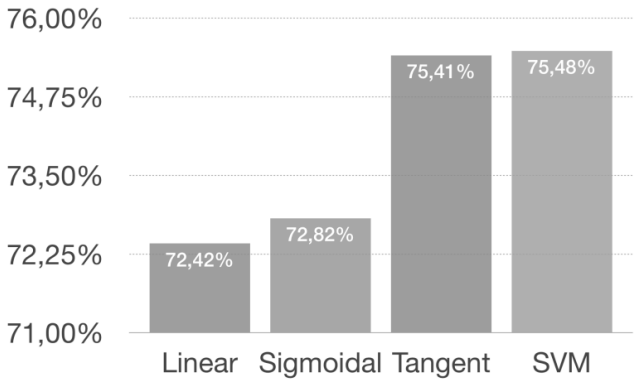

Fig. 5. Classification results using the median value

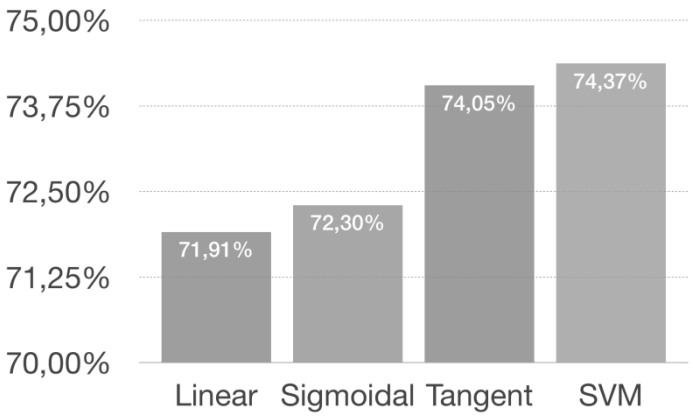

Fig. 6. Classification results using the average value

5. Conclusions

The aim of the study was to select the neural network structure, parameters and learning method to distinguish the gait of healthy children and those with cerebral palsy (CP). Based on the obtained results (Figure 5 and Figure 6), it can be stated that the correctness of children's gait (both of healthy children and those with CP) can be distinguished through the average or median of the succesive steps using the input vector created with: time of the step, step length, step velocity, step width, maximal height of the toe, maximal height of the heel, cadence and average ankle angle. The best results were obtained for two neural networks: Support Vector Machines and one way artificial neural network with hyperbolic tangent as a hidden layer activation function. It can be concluded that a much higher effectiveness of the gait correctness classification has been obtained compared to the results presented in [11, 18] or [6]. Slightly better results were presented in articles [9] and [28]; however, the number of the parameters used was higher in comparison to the parameters proposed in this study. In the future, the authors will increase the input data samples by performing motion capture examinations. They would like to apply other classifiers, such as Kohonen network, convolutional neural networks (CNN) or Learning Vector Quantisation Networks, which are common in gait features analysis [14, 23] and investigate their results.

Bibliography

[1] Au A. T., Kirsch R. F., 2000. EMG-based prediction of shoulder and elbow kinematics in able-bodied and spinal cord injured individuals. IEEE Trans. Rehabil. Eng., 8(4): 471–480.

[2] Charnoff H., 1973. The use of faces to represent points in k-dimensional space graphically. Journal of the American Statistical Association, 68: 361–368.
[3] Graupe D., Kordylewski H., 1995. Artificial neural network control of FES in paraplegics for patient responsive ambulation. IEEE Trans. Biomed. Eng., 42(7): 699–707.
[4] Hahn M. E., Chou L. S., 2005. A model for detecting balance impairment and estimating falls risk in the elderly. Ann. Biomed. Eng., 33 (6), 811–820.
[5] [5] Hart R., Kilgore K. L., Peckham P. H., 1998. A comparison between control methods for implanted FES hand-grasp systems. IEEE Trans. Rehabil. Eng., 6(2): 1–11.
[6] Holzreiter S. H., Kohle M. E., 1993. Assessment of gait pattern using neural networks. J. Biomech., 26(6): 645–651.
[7] Inman V. T., Ralston H. J., Todd F., 1981. Human Walking. Williams & Wilkins.
[8] Jang J. S., 1993. ANFIS: Adaptive-network-based fuzzy inference system. IEEE Trans. Syst., Man, Cybern., 23(3): 665–685.
[9] Kamruzzaman J., Begg R. K., 2006. Support vector machines and other pattern recognition approaches to the diagnosis of cerebral palsy gait. IEEE Trans. Biomed. Eng., 53(12): 2479–2490.
[10] Keim D. A., 2000. Designing pixel-oriented visualization techniques: Theory and applications. IEEE Transactions on Visualization and Computer Graphics, 6: 59–78.
[11] Kohle M., Merkl D., Kastner J., 1997. Clinical gait analysis by neural networks: issues and experience. Proceedings of 10th IEEE Symposium on Computer-based Medical Systems, Maribor, Slovenia, 138–143.
[12] Kordylewski H., Graupe D., 2001. Control of neuromuscular stimulation for ambulation by complete paraplegics via artificial neural networks, Neurol. Res., 23: 472–481.
[13] Lauer R., Smith B., Coiro D., Betz R., McCarthy J., 2005. Application of a neuro-fuzzy network for gait event detection using electromyography in the child with cerebral palsy. IEEE Transactions on Biomedical Engineering, 52(9): 1532–1540.
[14] Lee S., Choi S. T., Choi S., 2019. Classification of Gait Type Based on Deep Learning Using Various Sensors with Smart Insole. Sensors, 19 (8).
[15] Nathan R., 1993. Control strategies in FNS systems for the upper extremities. Crit. Rev. Biomed. Eng., 21: 485–568.
[16] Nguyen D., Widrow B., 1990. Improving the learning speed of 2-layer neural networks by choosing initial values of the adaptive weights, Proceedings of the International Joint Conference on Neural Networks, 21–26.

[17] O'Malley M. J., 1996. Normalization of temporal-distance parameters in paediatric gait. J. Biomech., 29(5): 619–625.
[18] O'Malley M. J., Abel M. F., Damiano D. L., Vaughan C. L., 1997. Fuzzy clustering of children with cerebral palsy based on temporal-distance gait parameters. IEEE Trans. Rehab. Eng., 5(4): 300–309.
[19] Pavelka A., Prochazka A., 2004. Algorithms for initialization of neural network weights. In: Proceedings of the Conference Technical Computing.
[20] Skublewska-Paszkowska M., Łukasik E., Miłosz M., Smołka J., Taczała J., Zdzienicka-Chyła A., Napiórkowski J., Kosiecz A., 2018. Motion Capture Technology as a Tool for Quantitative Assessment of the Rehabilitation Progress of Gait by Using Soft Orthoses. In: IEEE 11th International Conference on Human System Interaction (HSI), 384–390.
[21] Su F. C., Wu W. L., Cheng Y. M.,Chou Y. L., 2001. Fuzzy clustering of gait patterns of patients after ankle arthrodesis based on kinematic parameters. Med. Eng. Phys., 23(2): 83–90.
[22] Van der Maaten L., Hinton G., 2008. Visualizing high-dimensional data using t-sne. Journal of Machine Learning Research, 9: 2579–2605.
[23] Wang J., Zielińska T., 2017. Gait features analysis using artificial neural networks – testing the footwear effect. Acta of Bioengineering and Biomechanics, 19(1).
[24] Weinberger K., Sha F., Saul L., 2004. Learning a kernel matrix for nonlinear dimensionality reduction. In: Proceedings of the 21st International Conference on Machine Learning.
[25] Wieczorek T., 2008. Neuronowe modelowanie procesów technologicznych. Wydawnictwo Politechniki Śląskiej, Gliwice.
[26] Wolf S., Loose T., Schablowski M., Doderlein L., Rupp R., Gerner H., Bretthauer G., Mikut R., 2006. Automated feature assessment in instrumented gait analysis. Gait Posture, 23(3): 331–338.
[27] Wu W. L., Su F. C., Chou C. K., 1998. Potential of the back propagation neural networks in the assessment of gait patterns in ankle arthrodesis. Neural Networks and Expert Systems in Medicine and Health Care, Ifeachor E. C., Sperduti A., and Starita A., eds., 92–100.
[28] Zhang B., Zhang Y., Begg R. K., 2009. Gait classification in children with cerebral palsy by Bayesian approach. Pattern Recognition, 42: 581–586.

Stanisław Skulimowski[1], Jerzy Montusiewicz[2], Marcin Badurowicz[3], Marcin Barszcz[4]

Virtual reality for cross cultural education: a case study

Abstract: In the modern world, through the intensification of migration phenomena related to economic factors, security and education, we are dealing with the development of multicultural and multinational environments. In such societies, cross-cultural competence turn out to be very useful. A better understanding of a foreign culture allows faster assimilation in business structures as well as during tourist stays. Researchers are still looking for ways to improve education in this area. The authors describe the idea of using virtual reality technologies for this purpose. In their opinion, the immersive nature of this technology can be used to strengthen the educational process.The article describes the process of creating a virtual reality cultural game. The authors also present the results of pilot studies, conducted on a group of students of different nationalities: Poles, Turks, Georgians, Slovenians, Slovaks, and Ukrainians.

Keywords: cross-cultural competence, Unity, virtual reality, virtual environments, pairwise testing

1. Introduction

There is a rising group of students taking part in various international projects at the Polish universities. There is a group of over 400 foreign students from the Erasmus programme at the Lublin University of Technology every year. These students are coming from various countries on different continents. There may be people from 6 different countries of origin meeting in a single laboratory group – representing different traditions and cultures, mostly Muslim and different variants of Christianity (Catholic, Orthodox, Greek Catholic) or people declaring no affiliation to any of these cultures. In this situation, the research on cross-cultural competence of these students, cooperating for at least one term, may be an interesting goal. An appropriate level of cross-cultural competence may be a foundation for building tolerance and respect for others.

The authors believe that an interesting method for cross-cultural competence research for young adults may be the use of the virtual reality (VR) environment. Virtual reality is a created digital world which may be experienced, usually by

[1] Stanisław Skulimowski, Electrical Engineering and Computer Science Faculty, Lublin University of Technology, Poland
[2] Jerzy Montusiewicz, Electrical Engineering and Computer Science Faculty, Lublin University of Technology, Poland,
[3] Marcin Badurowicz, Electrical Engineering and Computer Science Faculty, Lublin University of Technology, Poland
[4] Marcin Barszcz, Electrical Engineering and Computer Science Faculty, Lublin University of Technology, Poland

using specialised equipment, e.g. VR goggles. In this digital world there is a possibility of digital 3D model recognition, acquisition of detailed information and mutual interaction with virtually present participants.

The VR technology is currently used in various areas, ranging from interactive reportage [18], phobia treatment [6, 17], cultural heritage and museums [1, 4, 5, 10], serious games for anti-stress therapy development [8] or exposure treatments [16] to learning new skills – from specialist ones [12, 15] in the healthcare industry, to regular social skills [8]. The technical aspects of required software and hardware, as well as methods of development of photorealistic virtual reality environments for healthcare and phobia treatment were discussed in [7]. In [14] the low-cost virtual reality environment development showing the hudjra of madrasah's student in Samarkand was presented.

An interesting usage of VR techniques may be situations of teaching cross-cultural competence [9, 21], and its evaluation [2, 19]. Such solutions were proposed both for soldiers [13] as well as volunteers taking part in the international missions, especially in the aspect of healthcare [11, 16] and its influence on cross-cultural contacts.

The goal of this work was to prepare an effective research system in virtual reality for conducting a pilot experiment in the area of cross-cultural competence in a group of Lublin student participants of the Erasmus programme. The experiment was performed for verification of the created software for such research. In the paper there is also a description of building a photorealistic interactive VR environment with 3D models, using 3ds max modelling software, 3D scanning with Artec Eva 3D scanner and Unity software development engine.

2. Research methodology

The research methodology included the following components: construction of the research stand (2.1), preparation of 3D models and a VR world (2.2), development of research scenarios (2.3) and the method of performance evaluation (2.4).

2.1. Research stand

The research stand consisted of BlackBerry Priv and Samsung S8 devices for launching the designed virtual reality environment placed in the Vrizzmo VR goggles, allowing them to match individual user characteristics. In order to navigate in the virtual world, the subjects used the Mocute gamepad connected to the phone via Bluetooth. During the experiments (up to 10 minutes each), the image from the phone was recorded and simultaneously streamed to the experiment computer using the Vysor program, which allowed to control the participants' actions. The layout of the station is shown in Figure 1.

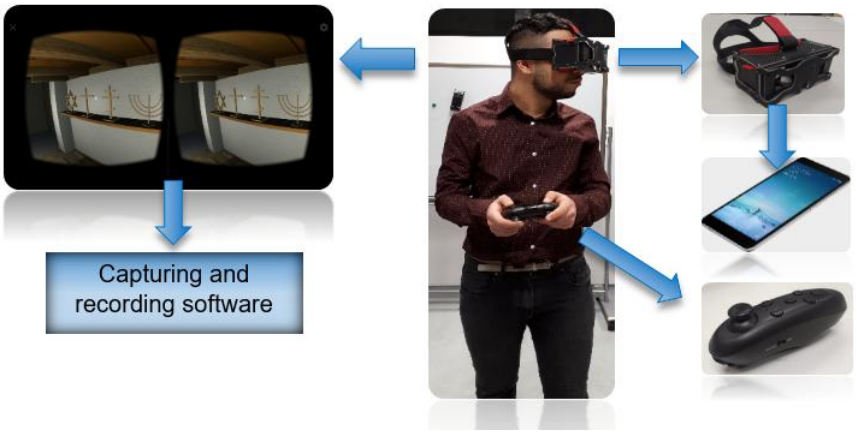

Fig. 1. Outline of the test stand

Source: own elaboration

2.2. Preparation of 3D models and VR stage

2.2.1. Preparation of 3D scene

As a base of a virtual reality environment, the application prepared in Unity development environment in [14] was used. The objects in the scene were enriched with text descriptions as part of the interaction (Figure 2). Moreover, the outline shader was replaced by brightness modifier shader.

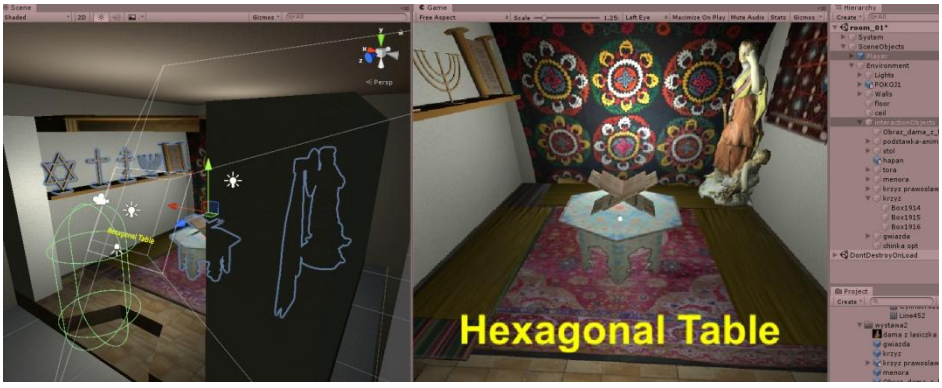

Fig. 2. The Unity software scene design

Source: own elaboration

The application was modified to include a set of new objects for the experiment. Apart from the previously implemented Islamic-style models, new ones were added, representing Christian and Judaic culture.

2.2.2. 3D model preparation

The current VR mobile application, being a student's room from the medresa (hudjra) along with its equipment, has been enriched with additional models of objects representing selected cultural circles. Objects representing Christian culture were added to the application (Roman and Orthodox cross), the well-known painting "Lady with an Ermine" by Leonardo da Vinci, a porcelain sculpture depicting a Chinese woman with Cupid, as well as Judaic culture (Star of David, menorah and the Torah – a hand-written scroll of the Pentateuch on two rollers).

In the process of classical modelling using 3ds Max, 3D models were made: Menorah, Star of David, Torah, Roman and Orthodox cross and a picture on the wall, as well as a shelf on which the models were placed. In the modelling process, two different technologies for creating 3D objects were used:

- volumetric primitives, tools to change them by using Boolean algebra operations and modification tools,
- previously defined 2D objects and their subsequent transformation into 3D objects.

The reverse engineering technique of 3D scanning was used to obtain a digital model of the Chinese sculpture located in the Zamoyski Museum in Kozłówka. The scanning was carried out *in situ* using the Artec Eva mobile scanner working in structured light technology. This scanner captures surface points with an accuracy of 0.05 mm at a speed of 2 million points per second and the texture at 1.3 Mpx resolution, with a scanning speed of 16 frames per second, which ensures a fast scanning process. The Artec Studio version 12 Professional software was used to operate the scanner and perform the post-processing of data. The resulting 3D mesh model with superimposed texture contained too many edges (vertices: 37041, faces: 73914) and was therefore not suitable for use in VR, because it would slow down the mobile application (in terms of responsiveness and refresh rate). For this reason, it was exported to a file in STL format, and then imported into 3ds Max where the mesh optimisation was performed using the Optimise tool. Finally, a mesh model was obtained, described by the following values – vertices: 15048, faces: 29927, Figure 3. Simplification of the model had a direct impact on the increase of VR application performance (plus 25% frames per second) without any noticeable deterioration in the visual quality of the model.

Fig. 3. 3D model of Chinese woman with Cupid

Source: own elaboration

The 3D models made were arranged in such a way as to fill the free spaces of the room and were clearly visible to the participants of the experiment. The image model was hung at the top of the left wall. The remaining objects, in addition to the sculpture, were placed on a modelled shelf attached to the wall under the image model (Figure 2). Then the sculpture model was placed on the floor in the corner of the room.

The 3D models that made up earlier room equipment belong to Muslim culture. These were the following models: a lauch – a folding wooden bookcase cut from one piece of wood without the use of nails, glue or hinges (an object made only in Uzbekistan), a hexagonal table meticulously decorated with paintings, a turban – a traditional headgear in Central Asia, a chapan – a caftan worn by men and women, rugs – decorative fabrics placed on the walls, and a carpet.

2.3. Developing research scenarios and conducting research

2.3.1. Research scenarios

Three tasks were prepared for the study, each necessitating VR interaction with objects from one of the cultures:

- Z1 – identifying objects connected with Christian culture,

- Z2 – identifying objects connected with Judaic culture,
- Z3 – identifying objects connected with Muslim culture.

Interaction involved approaching the object in VR until it was highlighted and pressing the button on the controller. Participants were asked to read the item's name, which appeared after interacting with it. The participant who thought to have already interacted with all the objects from the task was to signal that the task had been carried out. By enabling the image streaming from the VR world to an external computer, it was possible to observe the presence of the participant in it.

Three research scenarios were prepared using the tasks described:

- S1_CJ – including tasks Z1 and Z2,
- S2_CI – including tasks Z1 and Z3,
- S3_IJ – including tasks Z2 and Z3.

The research scenarios were assigned to the respondents to account for their country of residence and declared affiliation to a specific cultural background:

- KC – an affiliation to Christian culture,
- KJ – an affiliation to Judaic culture,
- KI – an affiliation to Muslim culture,
- KX – a different cultural affiliation or no affiliation declared.

The experiment was carried out using the pairwise testing method with base choosing, in accordance with Table 1. In addition, participants did not know or influence the type of test that was assigned to them.

Table 1. Matrix of research scenarios

Base chosen	S1_CJ = Z1 + Z2	S2_CI = Z1 + Z3	S3_IJ = Z2 + Z3
KC	KC S1_CJ	KC S2_CI	KC S3_IJ
KJ	KJ S1_CJ	KJ S2_CI	KJ S3_IJ
KI	KI S1_CJ	KI S2_CI	KI S3_IJ
KX	KX S1_CJ	KX S2_CI	KX S3_IJ

Source: own elaboration

2.3.2. Performing the research

The experiment was conducted by two people, one of whom took the position of controlling the experiment, while the other was responsible for the transmission of the content of tasks by voice, recording of audiovisual material and possible care for the participant (e.g. corrections in the arrangement of VR goggles). Participants were not informed in any way whether they marked items correctly. The information obtained was only saved by the person at the experimental control station.

In the first step, participants of the research were familiarised with the purpose and research methods used in the experiment, and then on the appropriate form confirmed their consent to their participation in the study and being recorded. Then they declared their country of origin and the cultural background with which they felt connected.

In the second step, the participants took their seats in the swivel chair, set up VR goggles and received a gamepad to navigate them through the application. They had their ears exposed so that no audio experience could be used in the study. In this way, voice communication was possible with the people conducting the experiment.

In the third step participants were asked to familiarise themselves with the application and its control through a virtual walk in the virtual environment presented and to use the button on the pad to activate the information function about the currently observed object in order to learn the methods of interaction inside the application.

In the fourth step, the participants, according to the scenario to which they were assigned based on the interview, received tasks to be carried out. The transition to the second task was immediate after completing the first task; the information was provided by voice.

In the fifth step, after completing both tasks, the participants were asked to remove the VR goggles, followed by a brief interview about the application and the possibilities of its improvement, the content of the experiment, the methods of control and interaction used, and the experience of being in virtual reality.

2.4. Evaluating the results

While collecting data from the participants, the authors took into account the possibility of the participants not noticing some objects, or the unwillingness to give an uncertain answer. The answers obtained were divided in such a way that it was possible to distinguish the results within the sum of responses given by the participants (relative correct diagnoses and relative incorrect diagnoses) and the results in relation to the expected ones (absolute correct answers in relation to all the participants should post, absolute incorrect answers in relation to all errors that a participant could have made).

The development of the results consisted in the aggregation of the results by means of the selection function, selection and summation of the values obtained and the preparation of the graphs. Preparation of the procedures for the analysis of the results included the preparation of formulas for determining correct, erroneous and missing diagnoses, including the answers that the participants would provide and the answers they should give. The whole was implemented by preparing an interactive spreadsheet in the Google Sheets software.

3. Conducting the experiment and obtaining the results

3.1. Description of the test group

The pilot experiment was carried out on a group of 17 people studying at the Lublin University of Technology as part of the Erasmus programme and at the Maria Curie-Skłodowska University in Lublin (2 women and 15 men) from 8 countries (Poland, Ukraine, Turkey, Georgia, Kyrgyzstan, Slovenia, Slovakia and Spain), representing various declared cultural backgrounds (Figure 4). None of the participants identified themselves as coming from the Judaic culture (KJ), four of them declared affinity with Muslim culture (KI), three did not declare belonging to the anticipated cultural environments. The rest determined their affiliation to Christian culture (KC).

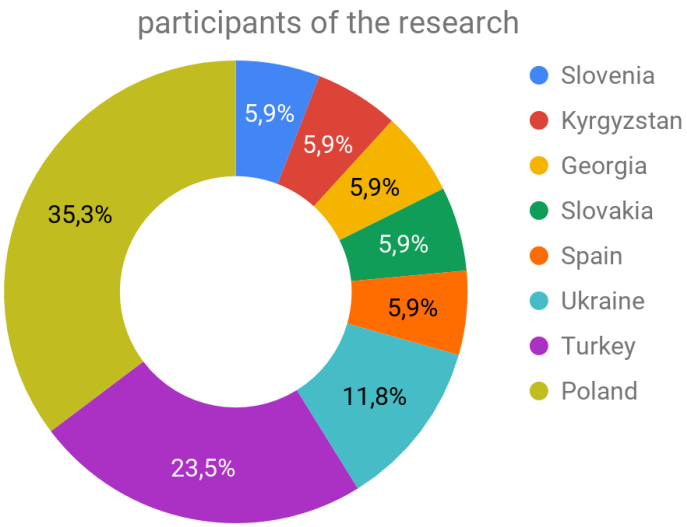

Fig. 4. Diagram of participants' distribution by country of origin

Source: own elaboration

Most of the pilot experiment tests were conducted in the premises of the Laboratory of Intelligent Systems Programming and Computer 3D Technology, "Lab 3D", of the Institute of Computer Science of the Lublin University of Technology. During the session in VR, the comments of the participants and the content of the tasks to be carried out were passed orally by the persons conducting the experiment. In addition, they were recorded in audio form, and pictures and video recordings were also taken, Figure 5 and Figure 6.

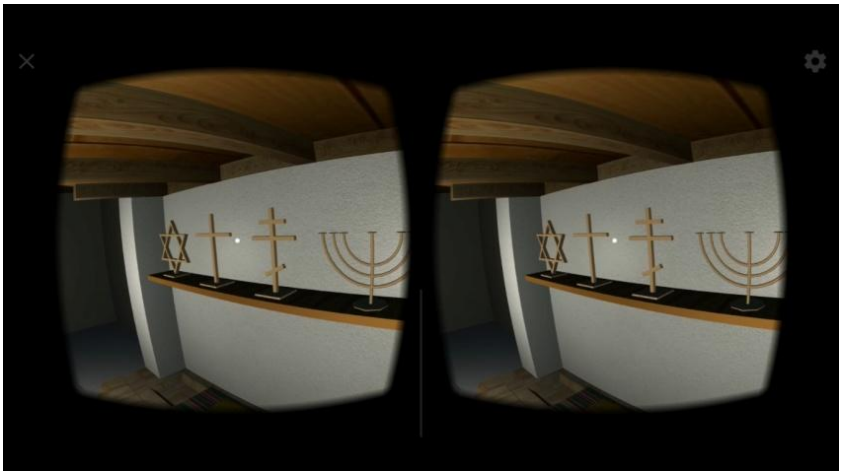

Fig. 5. Registered view of the scene from the VR session

Source: own elaboration

Fig. 6. Participants during the experiment session

Source: own elaboration

3.2. Developing research scenarios and conducting research

The statistics presenting the indicators of recognisability of objects in relation to all participants of the study are presented in Figure 7. The list includes:

- percentage of correct diagnoses – DC*100/ APCD,
- percentage of the lack of diagnoses – (APCD-DC)*100/ APCD,
- percentage of incorrect diagnoses – DE*100/APD,

where APCD stands for total number of all possible correct diagnoses or number of participants that should recognise the objects, APD – number of all possible incorrect diagnoses or number of all participants, DC – number of correct diagnoses, DE – number of erroneous diagnoses.

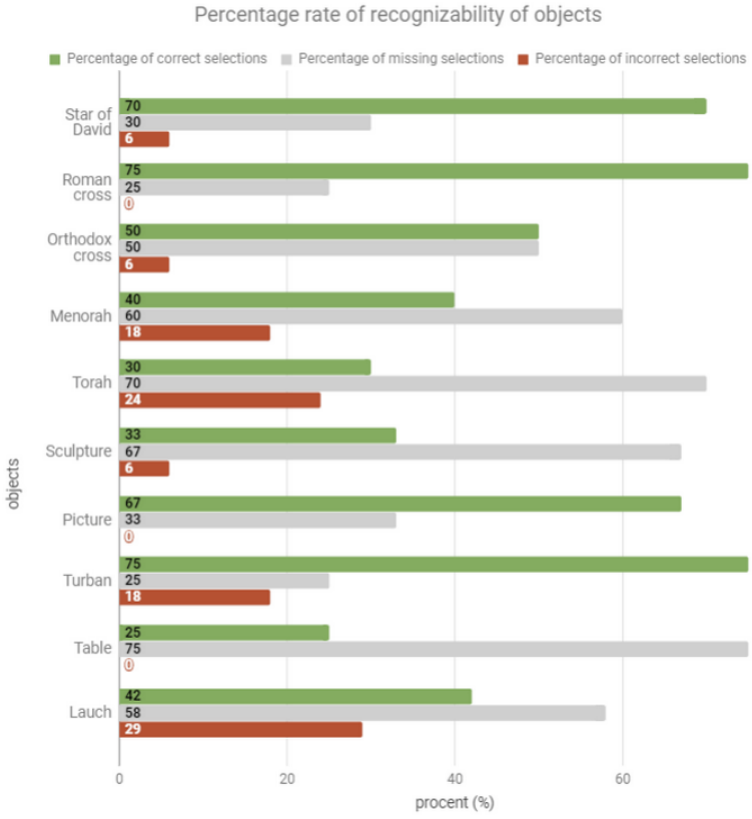

Fig. 7. Diagram of object recognition indicators

Source: own elaboration

Based on the collected data, it was found that the most frequently correctly indicated objects were: Roman cross (75% of correct diagnoses), turban (75% of correct diagnoses) and Star of David (70% of correct diagnoses). Therefore, the most often incorrectly indicated objects were the lauch (29% of incorrect diagnoses), the Torah (24% of incorrect diagnoses), and the menorah (18% of incorrect diagnoses). On the contrary, subjects most often overlooked by the study participants were: the hexagonal table (75% of the lack of diagnoses), the Torah (70% of the lack of diagnoses) and the sculpture (67% of the lack of diagnoses).

Furthermore, based on the data collected, it was possible to determine the quality of responses for types of questions (questions about objects from the Christian, Judaic and Muslim culture), depending on the participant's country of origin (division between Poles and persons from abroad) and declared belonging to the cultural affiliation. The results from Table 2 include:

- average percentage of correct answers in relation to all possible correct answers (PP),
- average percentage of incorrect recognition of objects to all answers given (PNP),
- average percentage of missing answers in relation to those that should be granted (PB).

Table 2. List of percent results of types of object diagnoses in the group of Poles and foreigners, divided into declared cultural affiliation and types of objects recognised

Declared membership of cultural circle	Objects	Poles			Foreigners		
		PP	PNP	PB	PP	PNP	PB
KC	Christian (Z1)	50	33,3	50	68,75	6,25	31,25
	Judaic (Z2)	66,6	16,67	33,3	22,2	16,67	77,7
	Muslim (Z3)	55,5	47,78	44,4	44,4	50	55,5
KI	Christian (Z1)	none	none	none	66,6	0	33,3
	Judaic (Z2)	none	none	none	66,6	16,67	33,3
	Muslim (Z3)	none	none	none	77,7	11,11	22,2
KX	Christian (Z1)	0	100	100	50	0	50
	Judaic (Z2)	33,3	50	66,6	33,3	0	66,6
	Muslim (Z3)	33,3	50	66,6	33,3	0	66,6

In the group of Poles, only identification with Christian culture (KC) or with none was declared (KX). Poles from the KC group more often correctly recognised objects from each of the cultures provided for in the study. In addition, this group completed sessions with fewer markups than the group declaring that they did not belong to the culture. In the case of making incorrect

markings, a group of Poles from the KC group more often misidentified the KI objects. In other cases, incorrect markings were more often made by Poles who did not belong to any of the cultures in question.

In the group of foreigners, no one has declared identification with the Judaic cultural background. On average, the most correct answers were given by people declaring affiliation with Muslim culture.

A comparison of the results of groups declaring a relationship with specific cultural environments clearly shows that those who declared a lack of connection with the cultures identified objects located in the VR scene the worst – average 22% PP among Poles from KX and average 39% PP among foreigners from KX – against average 57% PP for Poles from KC group and average 70% PP of foreigners from KI group. The KX group also most often refused to answer (average 61% PB).

Furthermore, the participants of the study pointed to the fact that not all objects on the stage could be interacted with. This was particularly true of objects such as the carpet and rugs, which were characteristic of Muslim culture for some participants. This is an indication of the possibility of adding such an option to supplement the experience.

4. Conclusions and further plans

The results from the conducted research show that the overall level of cross-cultural knowledge among the surveyed participants is not, in the authors' belief, sufficient and satisfactory. This may come as a surprise in a situation where almost unlimited knowledge resources are currently available in the Internet using mobile technologies. The results obtained may indicate that cultural issues are not in the mainstream of the interests of modern students.

The average value of well-recognised objects among all study participants was only 51%, the percentage of badly recognised objects reached the value of about 17%, and the percentage of unrecognised objects was nearly 49%. These results show, among other things, that many of the research participants preferred to opt out of searching for more objects related to the indicated cultural area than to give a wrong answer. This may indicate a certain responsibility of the respondents and their sensitivity, as well as a desire to avoid failure.

Most of the participants admitted that the tool presented in the form of interactive VR sessions is a very attractive, fast and interesting form of initial education in the field of knowledge of different cultures. Preparation of research on the so-called cross-cultural competition in the form of creating an environment operating in the virtual world is an effective and relatively cheap solution that allows quick exchange of objects and their adaptation to the current needs and subjects.

Building an interactive virtual environment is possible in a low-cost version using mobile devices, but with high computing power and cheap glasses in the

form of frames for placing a smartphone in them. The advantage of such a solution is the lack of connection of VR goggles using cables for stationary computers, which allows greater freedom of movement for participants of the research. The problem is, however, the fast overheating of the device and depletion of the battery due to the handling of numerous 3D objects placed in the VR scene.

Preparing the stage and 3D objects to the VR world depending on the specificity of the problem being solved requires acquisition of many skills in 3D modelling in various programs, 3D scanning and post-processing, optimisation of generated 3D objects, creation of photorealistic copies of real objects, as well as programming skills in environments that create VR worlds, e.g. Unity. It turns out that importing and exporting objects between programs is not always a compatible process and sometimes you lose some of features of the object, e.g. texture.

Further use of VR environments to conduct research related to cross-cultural competition requires the preparation of a VR stage not related to the subject of research to allow carrying out preliminary virtual walks, so that participants can get acquainted with ways of moving around in the virtual world and interacting with digital objects, and feel the phenomenon of immersion in the VR environment.

Acknowledgments. The research program titled "Study of human behaviour induced by visual stimuli originating from the virtual reality environment", realised in the Laboratory of Intelligent Systems Programming and Computer 3D Technology ‘Lab 3D’, was approved by the Commission for Research Ethics, No. 7/2016 dated 19.12.2016.

Bibliography

[1] Barbieri L., Bruno F., Muzzupappa M., 2018. User-centered design of a virtual reality exhibit for archaeological museums. International Journal on Interactive Design and Manufacturing (IJIDeM), 12(2): 561–571.

[2] Bayer Ch., Jellá J., Kapoor A., Matts R., Murdoch H., Woodruff H., An B., Guerlain S., Brown D., 2017. The Simple Methodology for Developing and Evaluating Cross-Cultural Virtual Training Systems SIEDS 2017. In: 2017 Systems and Information Engineering Design Symposium (SIEDS), 289–293.

[3] Beig M., Mayer A., Chan Ch., Kapralos B., Dubrowski A., 2014. A Serious Game for Medical-Based Cultural Competence Education and Training. In: 2014 IEEE 14th International Conference on Advanced Learning, 211–212.

[4] Bruno F., Bruno S., De Sensi G., Luchi M. L., Mancuso S., Muzzupappa M., 2010. From 3D reconstruction to virtual reality: A complete

methodology for digital archaeological exhibition. Journal of Cultural Heritage, 11(1): 42–49.
[5] Drosos V., Alexandri A., Tsolis D., Alexakos C., 2017. A 3D serious game for cultural education. In: 2017 8th International Conference on Information, Intelligence, Systems & Applications (IISA), 1–5.
[6] Eichenberg C., Wolters C., 2012. Virtual Realities in the Treatment of Mental Disorders: A Review of the Current State of Research. Intech, 35–64.
[7] Horváthová D., Siládi V., Lacková E., 2015. Phobia treatment with the help of virtual reality. In: 2015 IEEE 13th International Scientific Conference on Informatics, Poprad. 114–119.
[8] Kandalaft M. R., Didehbani N., Krawczyk D. C., Allen T. T., Chapman S. B., 2013. Virtual Reality Social Cognition Training for Young Adults with High-Functioning Autism. Journal of Autism and Developmental Disorders, 43(1): 34–44.
[9] Khan Z., Kapralos B., 2015. A Scenario and Dialogue Editor for a Cultural Competence Serious Game. 2014 IEEE Games Media Entertainment.
[10] Liu S., Jia J., 2009. Design and implementation of virtual culture museum. In: 2009 4th International Conference on Computer Science & Education, 686–689.
[11] Mayr S., Schneider S., Ledit L., Bock S., Zahradnicek D., Prochaka S., 2017. Game-based Cultural Competence Training in Healthcare. In: 2017 IEEE 5th International Conference on Serious Games and Applications for Health (SeGAH), 1–5.
[12] McGrath J. L., Taekman J. M., Dev P., Danforth D. R., Mohan D., Kman N., Crichlow A., Bond W. F., 2018. Using Virtual Reality Simulation Environments to Assess Competence for Emergency Medicine Learners. Academic Emergency Medicine Journal, 25(2): 186–195.
[13] Moenning A., Turnbull B., Abel D., Meyer Ch., Hale M., Guerlain S., Brown D., 2016. Developing avatars to improve cultural competence in US soldiers. In: 2016 IEEE Systems and Information Engineering Design Symposium (SIEDS), 148–152.
[14] Montusiewicz J., Barszcz M., Skulimowski S., Kayumov R., Buzrukov M., 2018. The concept of low-cost interactive and gamified virtual exposition. In: INTED 2018: 12th International Technology, Education and Development Conference, 353–363.
[15] Ota D., Loftin B., Saito T., Lea R., Keller J., 1995. Virtual reality in surgical education. Computers in Biology and Medicine, 25(2): 127–137.
[16] Pallavicini F., Cipresso P., Raspelli S., Grassi A., Serino S., Vigna C., Triberti S., Villamira M., Gaggioli A., Riva G., 2013. Is virtual reality always an effective stressors for exposure treatments? Some insights from a controlled trial. BMC Psychiatry, 13(1): 52.

[17] Parab T., Pawar D., Chaudhari A., 2016. A Cost Effective Approach towards Virtual Reality: Phobia Exposure Therapy. IJARCCE, 5: 670–674.
[18] Pena N., Weil P., Llobera J., Giannopoulos E., Pomes A., Spanlang B., Friedman D., Sanchez-Vives M., Slater M., 2010. Immersive Journalism: Immersive Virtual Reality for the First-Person Experience of News. Presence: Teleoperators and Virtual Environments, 19(4).
[19] Sheridan M., An B., Brown D., Bolger M., Epstein M., Matteo F., Semunegus R., Daniel J., Clarkin Ch., Gringley G., Roberts J., Schafer T., 2018. Investigating the effectiveness of virtual reality for cross-cultural competency training SIEDS 2018. In: 2018 Systems and Information Engineering Design Symposium (SIEDS), 53–57.
[20] Skulimowski S., Badurowicz M., 2017. Wearable Sensors as Feedback Method in Virtual Reality Anti-Stress Therapy. In: 2017 International Conference on Electromagnetic Devices and Processes in Environment Protection with Seminar Applications of Superconductors (ELMECO & AoS), 1–4.
[21] Zhang B., Benton S., Pearson W., LeMoine J., Herbertson N., Williams H., Goodman L., 2017. Playing 3D: Digital technologies and novel 3d virtual environments to support the needs of Chinese learners in western education: Cross-cultural collaboration, gamification, well-being and social inclusion. In: 2016 22nd International Conference on Virtual System & Multimedia (VSMM).

Waldemar Suszyński[1], Rafał Stęgierski[2], Karol Kuczyński[3]

Remote access to a hardware and software teaching laboratory: a case study

Abstract: The article provides firstly a discussion of the major challenges related to the widely understood notion of remote education. This provides the framework for the presentation of an integrated remote access system for university teaching resources. Through this means, access can be provided to hardware laboratories, purely virtual labs or mixed environments (with both physical and virtual components) for training, scientific or engineering purposes. While some of the solutions of the proposed functionality are complementary to functionality of the products available on the market, most have already been implemented and tested.

Keywords: remote access, remote learning, virtualization, computer networking, remote access to resources

1. Introduction

Advanced systems for integrated network management, remote learning and access to university resources are becoming more popular and commercially available [1, 2, 3]. Especially recently, the e-learning laboratory has been gaining popularity and many programming, hardware and network laboratories exist in the virtual space – they are accessible from anywhere, not only directly on the training site.

Such laboratories are used mainly for:

- teaching and learning [4],
- test environments for engineers,
- numerous scientific purposes.

In each case there are special needs that are difficult to address with ready-made systems. That is why in most of networking and hardware laboratories no special management system is used or their use is limited. Users have direct, physical access to the hardware (routers, switches, controllers, IoT systems etc.), so that they can freely connect intermediary or end devices, using all ports (including console and power outlets).

This approach only seems to be good for teaching the basics, as beginner students can concentrate on actual devices and cabling, without being distracted by any additional higher-level mechanisms and features. For all other user

[1] Waldemar Suszyński, Institute of Computer Science, Lublin University of Technology, Poland
[2] Rafał Stęgierski, Institute of Computer Science, Maria Curie-Skłodowska University, Poland
[3] Karol Kuczyński, Institute of Mathematics and Information Technology, State School of Higher Education in Chełm, Poland

categories, physical access to devices is only necessary to perform cabling, hardware repair or hardware hacking. However, being located within immediate distance to such devices is inconvenient due to the generated heat and noise, as well as possibly many other factors. Thus, remote access would be preferred so that users can either be located a room or even a world away (students of remote studies, teleworkers or telecommuters [5]). In such cases, physical lab infrastructure is also simplified, because students can use their own virtual machines instead of a common physical computer.

Laboratory remote access systems are expected to have the following attributes:

- allow web-based client or client software installation with neither administrator privileges nor special non-standard libraries;
- provide simultaneous access to multiple console (out-of-band) ports of the devices, out of band access to graphical consoles of remote PCs;
- enable support for both physical and virtual devices;
- have high responsiveness, no noticeable lags;
- allow the possibility to reset, turn on and off the devices and virtual machine on demand;
- include support for wireless solutions;
- provide support for full 802.1x protocol in the lab network;
- support multi-vendor environments;
- support group work;
- incorporate precise, centrally controlled user rights, comprehensive system administrator consoles;
- enable the sharing of lab resources located in multiple localizations;
- provide possibilities to reserve access to lab bundles in advance, and to create configuration snapshots to be used later;
- demonstrate high configurability, customizability and security;
- incorporate simple licensing models.

Commercial network remote access system for e-learning do exist. However, in the authors' opinion, none of currently available systems meets all or at least most of the aspects listed above.

The main building box of the proposed solution have been already implemented and described in [6, 7, 8]. The system is currently used to provide Cisco NetAcad (CCNA, CCNA Security, CCNP), Extreme Networks (routing, switching, access control, wireless) courses (locally and remotely) and to access the same lab for scientific purposes.

The laboratory can also be used for typically programming or software-based classes (for example various cybersecurity courses). The appropriate technology makes it possible to provide remote access to both physical computers in a university lab and virtual machines.

This paper is focused upon the system's further development (clientless access) and performance tests.

2. Materials and methods

2.1. The hardware

The main server runs under VMware ESXi™ (either free or paid version, depending on requirements), thus, any VMware-compatible machine with enough resources is suitable. Other popular solutions (Hyper-V, Virtual Box, etc.) are also supported. In the approach put forward, 802.11 wireless network USB NICs (network interface cards) are used to connect virtual PCs to wireless lab networks (assuming that wireless solutions are to be explored). Similarly, USB Ethernet NICs are mapped to virtual PCs, so that, for example, full 802.1x authentication can be implemented through lab switches. In the created environment, the terminal server provides network access to the console ports of the network devices that are to be managed. This can be a separate device or a multi-port RS-232 PCI card, attached to the server (Figure 1).

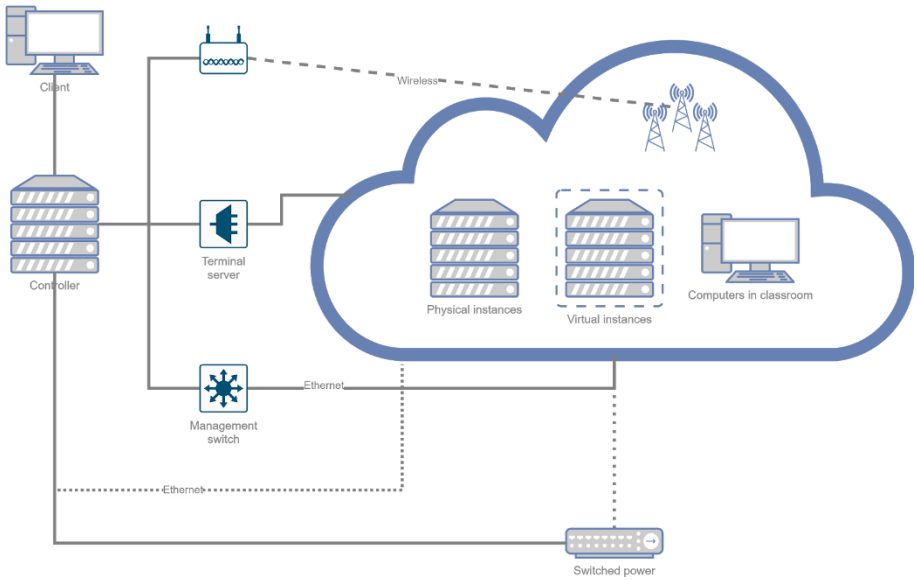

Fig. 1. General topology of the proposed environment

Similar access methods can be used to connect other devices like USB IoT appliances or scientific equipment.

2.2. Software components

The main server is used to run both the access environment management software (virtual Management server) and virtual machines (PCs, servers, virtual appliances, etc.) for the laboratory network (Figure 2).

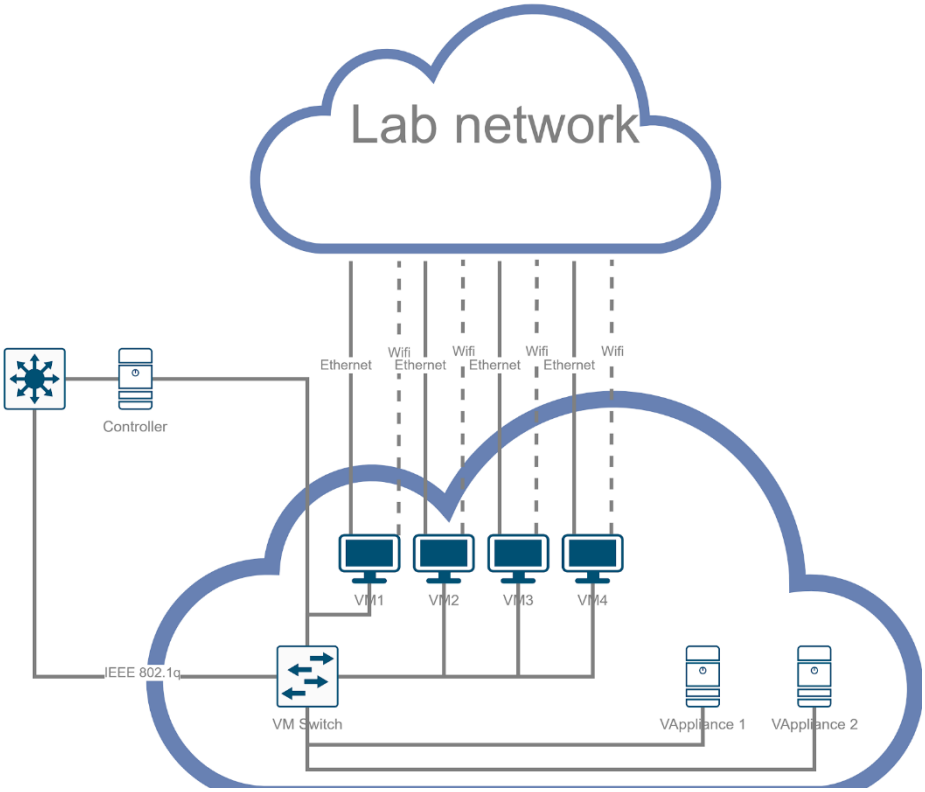

Fig. 2. The virtual part of the environment

Virtual and physical devices are grouped into bundles. Users are authorized to access only the bundles assigned to them by the administrator. Additionally, a bundle is visible for a user in slot time reserved in advance, because some bundles are available only in on specific dates. This comes about as a result of the fact that hardware could be bonded in different bundles, according to current hardware configuration (Figure 3).

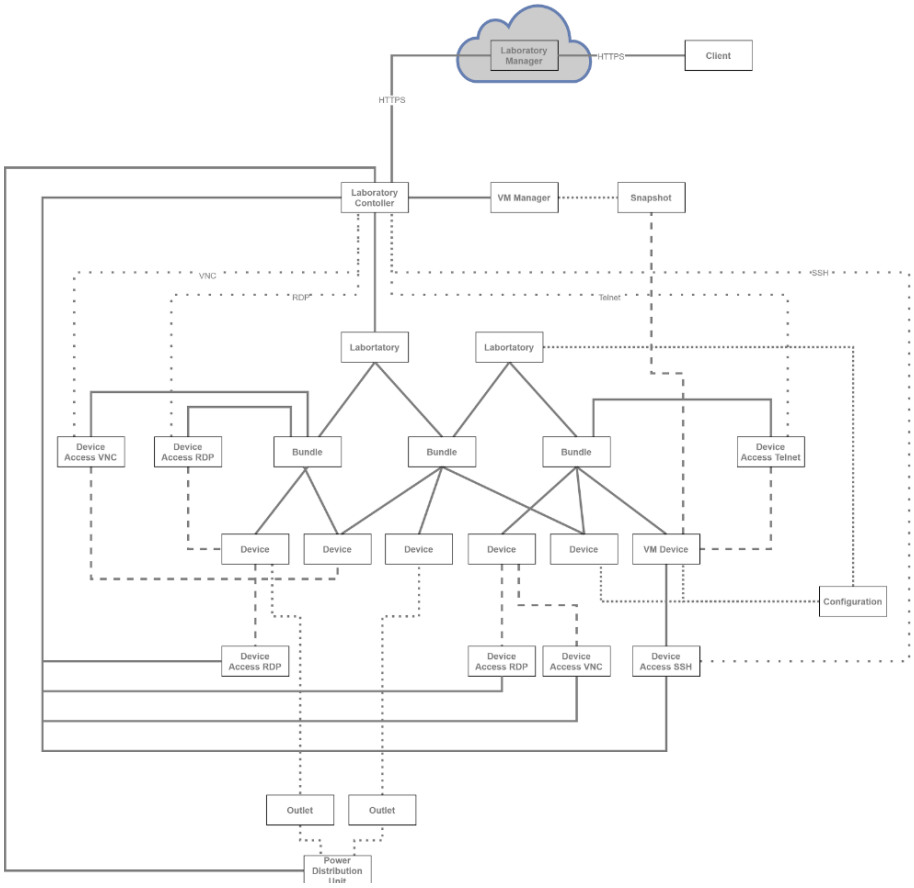

Fig. 3. Management software architecture diagram

In the solution put forward, all configuration files and virtual machine snapshots are centrally managed and stored. Hence, user sessions can be automatically saved and restored later. VLAN configuration of the management switch and the VM switch is also performed automatically for the bundles that are to be used. Each laboratory could have stages defined by administrator with proper configuration and/or VM snapshot. Such a stage could be restored by a user who wants to have a faultless environment for a subsequent part of an exercise. Web access is built within a Symfony framework with Twig templates and Doctrine as the O/RM database access engine. Application is based on a MVC software pattern, while PHP code execution is accelerated with APC. All devices can have defined multiple access types, both on and out-of-band. In addition, initial configuration of each device is performed via SNMP communication and/or Telnet/SSH parsed access. Furthermore, the built-in

VNC, RDP and Telnet/SSH are the HTML5 clients and could be, in some cases, configured with tunneled connection to restrict Web Service to act as the only public address of the whole laboratory.

An example user web-based interface is presented in Figure 4. Buttons at the right hand side provide access to the lab components.

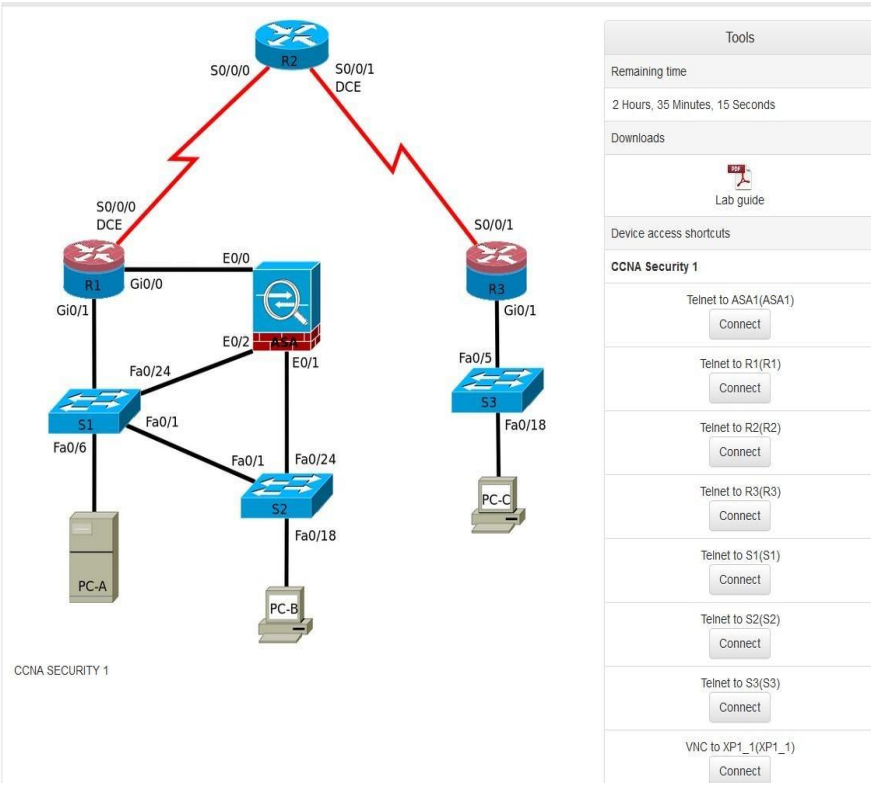

Fig. 4. Sample laboratory: a computer network with physical devices and virtual machines attached

3. Results

It is important to know the resource requirements (CPU, memory, network bandwidth) of any proposed remote access system. This information is crucial for a system user to scale an implementation according to actual needs (number of users, devices, virtual machines, etc.). The testing procedure is described below. The other aspect is user satisfaction.

The remote access server was tested under VMware ESXi, Hyper-V and other supervisors, on a machine with Intel XEON E5-2640 processor and 32GB

RAM. The server has two virtual CPUs assigned. The test remote lab consisted of 16 virtual machines, running on the same physical computer as the remote access system. Six users were expected to perform the following procedures at the same time: log into the virtual PC, start Netsight client (Java-based application) on the virtual PC, perform a few simple tasks (restore Netsight database, search for available devices, use the help and close the Netsight client and use a web browser). According to a user satisfaction survey, the system is considered simple, intuitive and fast.

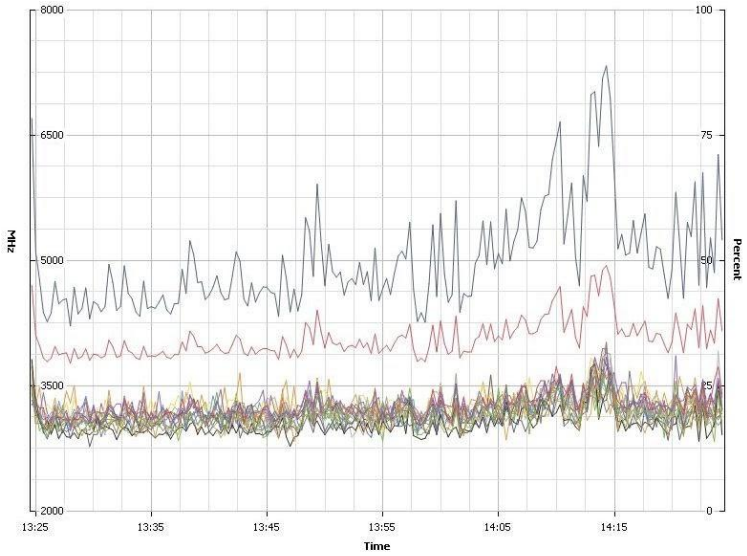

Performance Chart Legend

Key	Object	Measurement	Rollup	Units
	fujitsu	Usage in MHz	average	MHz
	fujitsu	Usage	average	Percent
	15	Usage	average	Percent
	10	Usage	average	Percent
	12	Usage	average	Percent
	11	Usage	average	Percent
	14	Usage	average	Percent
	13	Usage	average	Percent
	9	Usage	average	Percent
	2	Usage	average	Percent
	1	Usage	average	Percent
	4	Usage	average	Percent
	3	Usage	average	Percent
	6	Usage	average	Percent
	5	Usage	average	Percent
	8	Usage	average	Percent
	7	Usage	average	Percent
	0	Usage	average	Percent

Fig. 5. Server CPU utilization during the test

Users had their Browser clients to connect to the virtual lab. The remote access server was then responsible only for access control, network traffic translation and redirection (between the virtual PC and the remote user). Web-based (HTML5) access was also applied. The total access server CPU utilization (Figure 5), was up to 90% for the entire system. Network bandwidth utilization remained well below 1 MBps for each server NICs (Figure 6) during normal lab classes

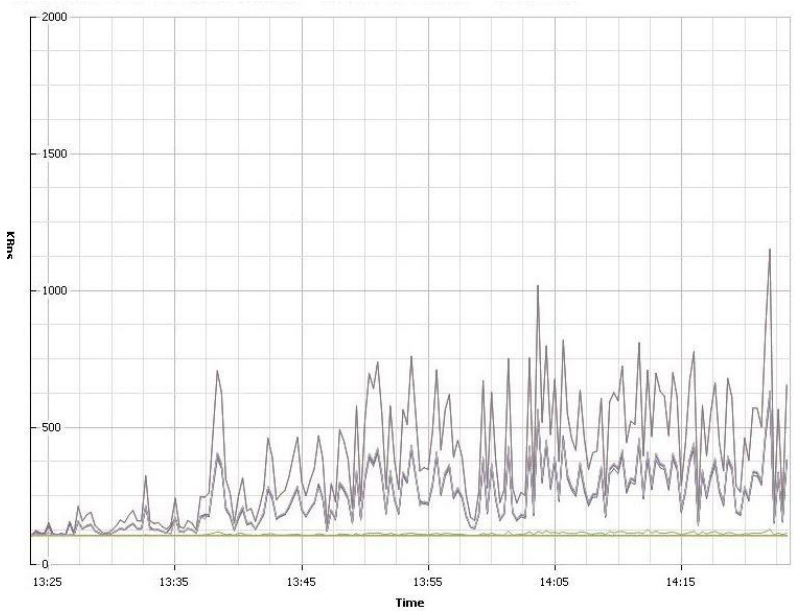

Performance Chart Legend

Key	Object	Measurement	Rollup	Units
	vmnic2	Data transmit rate	average	KBps
	vmnic3	Data transmit rate	average	KBps
	vmnic0	Data transmit rate	average	KBps
	vmnic1	Data transmit rate	average	KBps
	vmnic2	Data receive rate	average	KBps
	vmnic3	Data receive rate	average	KBps
	vmnic0	Data receive rate	average	KBps
	vmnic1	Data receive rate	average	KBps
	REMOTELAB	Data transmit rate	average	KBps
	4000	Data receive rate	average	KBps
	4001	Data transmit rate	average	KBps
	4001	Data receive rate	average	KBps
	4000	Data transmit rate	average	KBps
	REMOTELAB	Usage	average	KBps
	4001	Usage	average	KBps
	4000	Usage	average	KBps
	vmnic0	Usage	average	KBps
	vmnic2	Usage	average	KBps
	vmnic1	Usage	average	KBps
	vmnic3	Usage	average	KBps
	REMOTELAB	Data receive rate	average	KBps

Fig. 6. Server NICs bandwidth utilization during the test

According to the test user satisfaction survey and to opinions expressed after several months of system usage, the presented solution is simple, intuitive and fast. During local networking trainings (routing, switching, wireless courses, currently on Cisco), for beginners, the system enabled direct access to the lab network infrastructure. This was considered a positive aspect. The system allows advanced students a choice of connecting directly to the physical devices or using the access system. All our students chose the remote access system-based option. According to the advanced users, this has features that make the work more comfortable, without noticeable responsiveness degradation (compared to direct physical access), plus allows the possibility to remotely continue lab work after regular class hours.

A similar approach can be used for IoT classes. In such classes and through utilizing the system, an instructor can prepare the initial infrastructure and the student are tasked to program the components (LEDs, airflows, engines or more complicated elements, such as automatic booms and sticks). The results can be remotely observed in real time thanks to a webcam.

The same infrastructure is useful for scientific purposes (various kinds of computer networking research) and to test and refine network-based software in a controlled environment.

The presented solution is also used in typical software-based training. By means of the lab, each student receives their own, preconfigured virtual machine, which can be used according to policies set by the instructor, for the class period. Trainings can be related to software development, testing, cybersecurity and many other fields.

The implemented networking lab system has also significantly reduced the amount of lab administration work, as it provides a centralized management tool for both physical and virtual infrastructure. Its current form constitutes a solid and flexible framework for future extensions and development.

4. Conclusion

The presented system has been used for a few years and has proved its usability. Nowadays, in the pandemic world, remote education is the dominant and often the only possible teaching method. As there is more demand for remote access systems than ever, the presented solution needs, however, to evolve, to become more scalable, manageable and resource efficient.

Bibliography

[1] Cisco Systems, 2014. Cisco Prime Infrastructure 2.0 Data Sheet, http://www.cisco.com/c/en/us/products/collateral/cloud-systems-management/ prime-infrastructure/data_sheet_c78-729088.pdf

[2] Extreme Networks, 2014. NetSight Data Sheet, http://www.extremenetworks.com /product/netsight/
[3] Hewlett-Packard Development Company, 2014. Network Management, http://www8.hp.com/us/en/software-solutions/software.html?compURI= 1171412.
[4] Bastidas C.E.C., 2011. 41st Enabling Remote Access to Computer Networking Laboratories for Distance Education. In ASEE/IEEE Frontiers in Education Conference, Rapid City, SD.
[5] Ellison N.B, 2004. Telework and Social Change: how technology is reshaping the boundaries between home and work, Westport, Connecticut: Praeger, p. 18, ISBN 9780313051715, OCLC 57435712.
[6] Kuczyński K., Stęgierski R., Suszyński W., Królica D., 2017. Remote Access Environment for Computer Networking Laboratory: Challenges and Solutions, Annales Universitatis Mariae Curie-Skłodowska. Sectio AI, Informatica, 16(1): 21–29.
[7] Kuczyński K., Stęgierski R., Suszyński S., 2016. Optymalizacja systemu zdalnego dostępu do laboratorium sieciowego, Lubelskie Dni Nauki i Biznesu WD 2016.
[8] Kuczyński K., Stęgierski R., Suszyński S., Pellerin M., 2015. Versatile Remote Access Environment for Computer Networking Laboratory, Image Processing and Communications Challenges 6, Advances in Intelligent Systems and Computing, Springer-Verlag, Berlin Heidelberg, 313: 293–300.

Author Index